The Pennsylvania State University

The Graduate School

IMPACT OF PROTEIN O-GLCNACYLATION IN RETINA: MECHANISMS REGULATING MRNA TRANSLATION AND IDENTIFICATION OF NOVEL THERAPEUTIC TARGETS FOR DIABETIC RETINOPATHY

A Dissertation in

Biomedical Sciences and Clinical and Translational Sciences

by

Sadie K. Dierschke

Submitted in Partial Fulfillment
of the Requirements
for the Degree of

Doctor of Philosophy

May 2020

The dissertation of Sadie K. Dierschke was reviewed and approved by the following:

Michael D. Dennis
Assistant Professor, Department of Cellular & Molecular Physiology
Assistant Professor, Department of Ophthalmology
Dissertation Advisor
Co-Chair of Committee

Scot R. Kimball
Professor, Department of Cellular & Molecular Physiology

Amy C. Arnold
Assistant Professor, Department of Neural & Behavioral Sciences

Alistair J. Barber
Associate Research Director, Penn State Eye Center
Associate Professor, Department of Ophthalmology
Associate Professor, Department of Cellular & Molecular Physiology
Associate Professor, Department of Neural & Behavioral Sciences

David J. DeGraff
Assistant Professor, Department of Pathology & Laboratory Medicine
Assistant Professor, Department of Surgery
Co-Chair of Committee

Ralph L. Keil
Associate Professor, Department of Biochemistry and Molecular Biology
Chair of Biomedical Sciences Graduate Program

ABSTRACT

Diabetes promotes the post-translational modification of proteins by O-linked addition of N-acetylglucosamine (O-GlcNAcylation) to serine and threonine residues of proteins and thereby contributes to diabetic complications, including diabetic retinopathy (DR) which is the leading cause of blindness in working age adults. In the retina of diabetic mice, the repressor of mRNA translation eIF4E-binding protein 1 (4E-BP1) is O-GlcNAcylated and sequestration of the cap-binding protein eukaryotic translation initiation factor (eIF4E) by 4E-BP1 is enhanced. However, the functional consequence of this enhanced interaction in retina is unknown. The overarching goals of this dissertation were to determine if O-GlcNAc-mediated sequestration of eIF4E by 4E-BP1 affects gene expression in the retina and to identify the mechanism by which retinal protein O-GlcNAcylation is attenuated.

To achieve our goal, we assessed retinal gene expression in mice administered thiamet G (TMG), an inhibitor of O-GlcNAcase (OGA), via ribosome profiling. The principal effect of TMG on retinal gene expression was observed in mRNAs undergoing translation, as <1% of mRNAs were altered in total abundance. In retina, the effect of OGA inhibition on translation of specific mitochondrial proteins was dependent on 4E-BP1/2. The retina of diabetic wild-type mice exhibited increased reactive oxygen species levels, an effect not observed in diabetic 4E-BP1/2-deficient mice. From our ribosome profiling dataset, we identified CD40 as a gene candidate in rodent retina subject to enhanced translational efficiency upon TMG administration. Hyperglycemia increases CD40 expression in Müller glia, which drives expression of other inflammatory molecules. The mechanisms responsible for this increase are unknown. To test the hypothesis that diabetes promotes translation of the mRNA encoding CD40 in Müller glia, we assessed CD40 mRNA translation in whole retina, Müller cells *in situ*, and Müller cells *in vitro*. We found that O-GlcNAcase inhibition increases CD40 mRNA translation, and a similar effect

was observed in retina from diabetic mice. However, 4E-BP1/2 deletion prevented diabetes-induced translation of the CD40 mRNA. In cells in culture, 4E-BP1/2 deletion prevented O-GlcNAcylation-induced CD40 mRNA translation, and expression of a 4E-BP1 variant that constitutively binds eIF4E promoted cap-independent CD40 mRNA translation as assessed by a bicistronic reporter. Collectively, these findings provide evidence for a mechanism whereby diabetes-induced O-GlcNAcylation promotes oxidative stress and contributes to inflammation in the retina by altering the selection of mRNAs for translation.

Given the impact of enhanced retinal protein O-GlcNAcylation on oxidative stress and induction of inflammation, we wanted to understand how it may be attenuated. Pharmacological blockade of the renin angiotensin system (RAS) mediates beneficial outcomes in the retina of diabetic patients, likely through increased systemic production of the RAS effector peptide angiotensin-(1-7) (Ang1-7). Thus, we hypothesized Ang1-7 was capable of modulating protein O-GlcNAcylation. To test this hypothesis, mice fed a high fat diet were treated with the ACE inhibitor captopril or captopril plus an Ang1-7 Mas receptor antagonist. In the retina of mice fed a high fat diet, captopril attenuated protein O-GlcNAcylation in a manner dependent on Mas receptor activation. In Müller cells in culture, Ang1-7 or adenylate cyclase activation were sufficient to enhance cAMP levels and inhibit O-GlcNAcylation. The repressive effect of cAMP on O-GlcNAcylation was dependent on exchange protein activated by cAMP (EPAC), but not protein kinase A. We further provide evidence that Ang1-7 acts to suppress O-GlcNAcylation by inhibition of O-GlcNAc Transferase (OGT) activity. This dissertation thus provides evidence to support a model wherein stimulating cAMP production in Müller cells to attenuate retinal protein O-GlcNAcylation and its downstream negative consequences may represent a novel therapeutic strategy to preserve vision in diabetic individuals.

TABLE OF CONTENTS

LIST OF FIGURES

LIST OF TABLES

List of Abbreviations

4E-BP1	4E binding protein 1
ACE	Angiotensin converting enzyme
ACEi	Angiotensin converting enzyme inhibitor
AMPK	AMP-activated protein kinase
Ang1-7	Angiotensin-(1-7)
AT1R	Angiotensin II type 1 receptor
AT2R	Angiotensin II type 2 receptor
AQP4	Aquaporin 4
BRB	Blood retinal barrier
BSA	Bovine serum albumin
cAMP	Cyclic adenosine monophosphate
CD40	Cluster of Differentiation 40
CRALBP	Cellular retinaldehyde–binding protein
DCF	Dichlorofluorescein
DKO	Double knockout
DR	Diabetic retinopathy
eIF4E	Eukaryotic initiation factor 4E
Elmsan1	ELM2 and Myb/SANT Domain Containing 1
ER	Endoplasmic reticulum
EPAC	Exchange protein activated by cAMP
EV	Empty Vector
Fam122a	Family with sequence similarity 122A
FBS	Fetal bovine serum
FOXO1a	Forkhead box O1a
Fsk	Forskolin
GFAT	Glutamine:fructose-6-phosphate aminotransferase
GFAT2	Glutamine:fructose-6-phosphate aminotransferase 2
GlcN	Glucosamine
GO	Gene ontology
GS	Glutamine synthetase
GSK3	Glycogen synthase kinase 3
GTP	Guanosine triphosphate
HA	Hemagglutinin
HBP	Hexosamine biosynthetic pathway
HFD	High fat diet
HG	High glucose
ICAM-1	Intracellular cell adhesion molecule 1
IL1Rap	Interleukin 1 receptor accessory protein
INL	Inner nuclear layer
IP	Immunoprecipitation

IPA	Ingenuity pathway analysis
IRES	Internal ribosome entry site
IRS1	Insulin receptor substrate 1
JNK	c-Jun N-terminal kinase
LG	Low glucose
m6A	N6-methyladenosine
Man	Mannitol
MEFs	Mouse embryonic fibroblasts
METTL14	Methyltransferase like 14
MnSodBP	Manganese superoxide dismutase binding protein
MnSodRE	Manganese superoxide dismutase response element
Mrpl47	Mitochondrial ribosomal protein L47
mtDNA	Mitochondrial DNA
mTORC1	Mammalian target of rapamycin complex 1
Nat8l	N-acetyltransferase 8 like
NFL	Nerve fiber layer
NOS2	Nitric oxide synthase 2
NPDR	Nonproliferative diabetic retinopathy
Nr6a1	Nuclear receptor subfamily 6 group A member 1
NT	No treatment
OCR	Oxygen consumption rate
OGA	O-GlcNAcase
OGT	O-GlcNAc transferase
ONL	Outer nuclear layer
OXPhos	Oxidative phosphorylation
P	Polysomal
PABP	Poly A binding protein
PCR	Polymerase chain reaction
PDGFRa	Platelet derived growth factor receptor alpha
PDR	Proliferative diabetic retinopathy
PI3K	Phosphoinositide-3-kinase
PKA	Protein kinase A
RAS	Renin Angiotensin System
RFU	Relative fluorescent units
RGCs	Retinal ganglion cells
ROS	Reactive oxygen species
RPF	Ribosome protected Fragment
Rpl22	Ribosomal protein L22
RT-PCR	Reverse transcription polymerase chain reaction
SEM	Standard error of the mean
SHP-1	Src homology region 2 domain-containing phosphatase 1
SIRT3	Sirtuin 3

Sod2	Superoxide dismutase 2
SP	Subpolysomal
Sp1	Specificity protein 1
STAT3	Signal transducer and activator of transcription 3
STZ	Streptozotocin
TE	Translational Efficiency
TMG	Thiamet G
Tufm	Tu translation elongation factor
UPR	Unfolded protein response
UTR	Untranslated region
VEGF	Vascular endothelial growth factor
Veh	Vehicle
WT	Wild type

ACKNOWLEDGEMENTS

My first thanks goes to the eternal and everlasting Father, the Lord of heaven and earth, for which I have dedicated the past five years of study to uncover a deeper understanding of your natural creation. Though the darkness of both sin and ignorance cloud my understanding, I pray my efforts to reveal the natural wonders of your creation only serve to reflect more fully your glory.

I would also like to thank my mentor Dr. Michael Dennis, for training me to be an independent and well-rounded scientist capable of developing important research questions and assessing data critically. The opportunity provided by his resources, time, and support were invaluable in achieving the whole of this dissertation. In that vein, I would also like to thank past and fellow Dennis lab members, Dr. WeiWei Dai, William Miller, Dr. Siddharth Sunilkumar, and Joseph Giardano. I would also like to extend a special thanks to the Dennis lab technician Allyson Toro. Without her assistance in breeding mice for my animal studies as well as technical assistance throughout my time in the Dennis lab, I would not have been able to complete this work in the timeline that I have.

I would also like to extend gratitude toward members of my thesis committee: Alistair Barber, Scot Kimball, Amy Arnold, and Dave DeGraff. Without their support and guidance, it is unlikely this work would have come to fruition.

I am also very grateful for technical assistance from members of the Kimball laboratory: Holly Lacko and Jaclyn Welles. Without Jackie's assistance, I never would have obtained retinal polysomes.

Finally, I would like to thank my parents Monroe and Mollie whose tireless work ethic and devotion taught me that hard work pays off and that nothing worth having is ever generally very easy to obtain. I am especially grateful for my mother who should most likely be awarded an

honorary PhD for all the times she patiently listened to the highs and lows of graduate school over the phone, and for offering the sage, yet profound, advice: “They can kill you, but they can’t eat you.” It may be hard to believe, but such words were a comfort during difficult times. I would also like to thank my sisters Sarah and Sally for providing moral support, giving me life advice, and supplying me with a steady stream of pictures of their adorable children. A special thanks also goes out to my grandmother Patsy who always sent me a check in the winter to make sure I could pay my electric bill to keep warm. And finally, I would like to thank my fiancé Aaron for reminding me success is not defined by anyone’s standards but my own, for constantly telling me that I’m brilliant and can do anything, and for generally being the best person I know.

In the words of the von Trapp family: “So long, farewell, auf Wiedersehen, adieu. Adieu, adieu to yieu, and yieu, and yieu…Goodbye, goodbye, goodbye!

This work was supported by American Diabetes Association Pathway to Stop Diabetes Grant 1-14-INI-04; NEI, National Institutes of Health Grant EY023612 and the Penn State Eye Center Frontiers in Eye and Vision Research Award (to Michael D. Dennis); startup funds from the Human Genetics Institute of New Jersey and NIGMS, National Institutes of Health Grant GM124976 (to Premal Shah); and NIDDK, National Institute of Health Grants DK13499 and DK15658 (to Scot R. Kimball). Research reported in this publication was also supported by the National Center for Advancing Translational Sciences, NIH Grants TL1 TR002016 and UL1 TR002014 (Sadie Dierschke). The content is solely the responsibility of the authors and does not necessarily represent the official views of the National Institutes of Health.

Chapter 1

Literature Review

Introduction to the Pathogenesis of Diabetic Retinopathy

Retinal Anatomy & Physiology

The eye is the organ responsible for focusing light and generating an electrochemical signal to stimulate a hierarchy of retinal neurons to relay a visual scene to the brain. Much like on film in a camera, light will be focused onto the light-sensing retina. As the retina lines the back of the eye, light must pass through several layers before it is focused onto light-sensing photoreceptors. Light is first refracted through the cornea and then directed through the pupil, a small hole in the colored iris. Iris sphincter muscles regulate the size of the pupil to control the light that passes through the lens. Ciliary muscles then either contract or relax the lens to control the degree to which light rays are refracted onto the retina, which perceives an inverted image. When the visual signal is relayed to visual cortexes of the brain, the brain re-orients the image into a visually and behaviorally useful perception.

The retina contains an estimated 50 distinct cell types arranged into three layers of nerve cell bodies interspersed by two plexiform layers of synapses [1]. Light is absorbed by rod and cone photoreceptors located in the outermost layer of the retina. The massive image processing feat of visualizing the outside world is carried out by approximately 100 million photoreceptors, the second most numerous type of neuron found in the human body [2, 3]. This army of photoreceptors responds to light by hyperpolarizing and electrochemically stimulating second-

order neurons, primarily bipolar and amacrine cells. Second-order neurons synapse onto retinal ganglion cells (RGCs) located in the inner nuclear layer (INL) via either excitatory or inhibitory connections [4]. Approximately 1.2 million RGC axons will form the nerve fiber layer (NFL) that enters the optic nerve and ultimately synapses onto visual cortexes in the brain [5].

Three major classes of glial cell types are also found in the retina: astrocytes, microglia, and Müller cells. The stellate-shaped astrocytes are mostly confined to the NFL; however the presence and distribution of astrocytes is also correlated with the distribution of retinal blood vessels [6, 7]. This correlation reflects the close association astrocytes have with endothelial cells of the retinal vasculature. Astrocytes exert supportive functions for the retinal vasculature: ensheathing blood vessels, producing trophic factors (including vascular endothelial growth factor [VEGF]), and maintaining the integrity of the blood retinal barrier (BRB) [8, 9]. As an immune privileged site, the retina relies on microglia to respond to inflammatory insults. Microglia represent the retinal macrophage population; they will undergo rapid morphological and functional transformation into phagocytes upon activation by a stimulus. Additional roles for microglia in maintaining retinal homeostasis include: control of neuronal apoptosis, guidance of retinal vasculature growth, and aid in forming neuronal connections [10-12]. Microglial activation often occurs either prior to or concurrently with neuronal cell death, and therefore is thought to contribute to the pathogenesis of retinal degenerative diseases [13].

The most common glial cell type in the retina are Müller cells, which were first identified in 1850 by the German anatomist Heinrich Müller. Described by Müller as radial glial fibers, these cells are situated transversally to all nuclear and plexiform layers of the retina. Müller cells are the only glial cell to span all layers of the retina. Longitudinal cytoplasmic projections enable Müller cells to develop intimate contact with retinal blood vessels, neurons, and other glial cells.

Given their spanning dimension, Müller cells play a critical role in supporting and maintaining retinal homeostasis. The function of Müller cells can generally be grouped into three categories: *1*) metabolic support and nutrient synthesis, *2*) handling of neurotransmitters and ions, and *3*) maintenance of the BRB [14, 15]. Structurally, Müller cells help to minimize intraretinal light scatter by providing light a direct path to focus onto photoreceptors, thereby improving visual acuity [16]. Disturbances in the retinal environment can cause Müller cells to become dysfunctional as they try to counter-regulate an experienced insult. The first reaction to a deleterious stimulus is referred to as gliosis, which may be defined by the morphological and biochemical changes Müller cells undergo in response to an external signal. If the damage is particularly extensive or intense, Müller cells remain in reactive gliosis long after the stimulus has dissipated, which is an indicator of poor prognosis for the retina [15]. Given the intimate associations formed with other retinal cell types and their geographic domination, Müller cells are critical for maintaining healthy retinal function and homeostasis.

Clinical Manifestations and Molecular Pathophysiology of Diabetic Retinopathy

The intimate associations formed between glial, endothelial, and neuronal cells of the retina support a model wherein different retinal cell types cooperate together to form a neurovascular unit [17-19]. While diabetes has classically been thought to induce aberrant alterations in the retinal microvasculature, the concept has evolved to suggest a more accurate representation of diabetic pathophysiology in the retina encompasses disruption of the cooperativity and degeneration of the retinal neurovascular unit [20, 21]. This degeneration, culminating in a clinical diagnosis of diabetic retinopathy (DR), is, in part, a result of poor glycemic control [22, 23]. The Diabetes Control and Complications trial and UK Prospective Diabetes Study demonstrated that intensive glycemic control delays both the onset and

progression of DR [24, 25]. It is estimated 42% of Type 1 diabetics and 8% of Type 2 diabetics have a vision-threatening form of DR, which is the leading cause of blindness in working age adults [26, 27]. DR manifests clinically in the form of retinal hemorrhaging, neovascularization, leakage of fluid into the retina, and formation of cotton wool spots and hard exudates. Retinal function deteriorates progressively in DR patients. Within the first months of disease onset, adaptive biochemical changes made in the retina include a reduction in biosynthetic and electrical activity, likely to reset the normally high metabolic activity in the new diabetic milieu of the retina [18]. Clinically, altered electroretinograms, diminished color vision, and defects in contrast sensitivity are present before vascular manifestations of DR are visible via fundus examination [18]. After several years of uncontrolled diabetes duration, the adaptive changes begin to fail, and impairment of the retinal vasculature begins to manifest clinically in the form of non-proliferative DR (NPDR). Over time, the disintegration of the retinal neurovascular unit worsens, resulting in the most severe stage of the disease, proliferative DR (PDR), which is characterized by neovascularization, fibrosis, and loss of visual acuity [18]. Vision loss occurs from either unrestrained proliferation of new retinal blood vessels (PDR) or from leakage of fluid through the retinal vasculature (diabetic macular edema) [28].

VEGF plays a central role in mediating the breakdown of the BRB, and examination of vitreous fluid from the eyes of patients with PDR demonstrates an increase in VEGF [29, 30]. However, the molecular pathophysiology of DR likely encompasses a complex interaction between oxidative stress, pro-inflammatory, endoplasmic reticulum (ER) stress, and VEGF signaling pathways [31-33]. A major underlying factor of DR, however, is hyperglycemia [23]. The instigating factor of hyperglycemia-induced diabetic complications is hypothesized to be the overproduction of superoxide, a type of reactive oxygen species (ROS) produced by the electron transport chain of the mitochondria [34]. Although hyperglycemia systemically affects the body,

differential effects may be seen in specific cell types such as retinal endothelium or mesangial cells of the kidney because they lack the ability to regulate glucose transport into the cell in a hyperglycemic environment [35, 36]. Consequently, the large influx and subsequent oxidation of glucose increases the voltage gradient across the electron transport chain. Eventually, oxidative phosphorylation activity reaches a threshold, and the electron transport chain becomes bottlenecked, favoring the formation of superoxide [23, 37]. Downstream effects of ROS include activation of Protein Kinase C which has several purported mechanisms of influencing blood flow in the retina, including enhancing expression of VEGF [34, 38]. Additionally, downstream metabolites formed consequentially of ROS can be fed into the polyol pathway which oxidizes glucose into sorbitol (consuming NADH and contributing to ROS susceptibility in the process) [39]. Finally, aberrant ROS production resulting from hyperglycemia can increase flux through the hexosamine biosynthetic pathway (HBP), a pathway that produces the *O*-linked β-D-*N*-acetyl-glucosamine (O-GlcNAc) moiety necessary for the post-translational modification of the hydroxyl side chains of serine and threonine residues in a process referred to as protein O-GlcNAcylation [40].

O-GlcNAc Modifications in Diabetic Retinopathy

Protein O-GlcNAcylation and Nutrient Sensing

First described in 1984, O-GlcNAcylation is a post-translational modification that more closely mimics phosphorylation than other forms of traditional glycosylation [41]. The O-GlcNAc modification cycles dynamically (and reversibly) on serine and threonine residues of proteins in response to environmental stimuli, such as hyperglycemia. The rapid cycling of O-GlcNAc is regulated by only two proteins: O-GlcNAc transferase (OGT) and O-GlcNAcase

(OGA). OGT catalyzes the addition of the O-GlcNAc moiety while OGA catalyzes its removal. Traditional *N*-linked glycosylation occurs in the lumen of the ER and Golgi body [42]. However, proteins may be O-GlcNAc modified in either the cytoplasm or nucleus. The O-GlcNAc modification further differs from traditional glycosylation in that it is not modified by elongation or branching. O-GlcNAc modifications are abundant and critical for several fundamental cellular processes including gene expression, cell cycle control, apoptosis, inflammation, and nutrient sensing [43]. Global O-GlcNAcylation is highly sensitive to nutrient status within the cell as it requires input from nearly every major metabolic pathway—glucose, amino acid, nucleotide, and

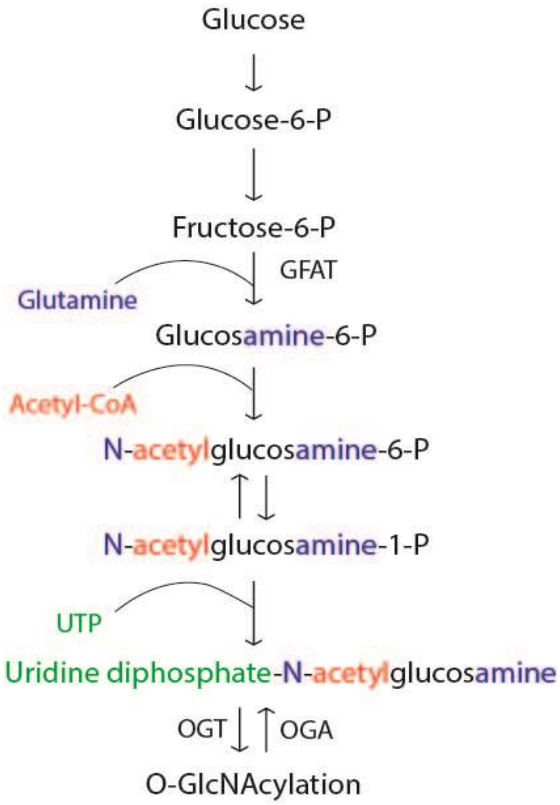

Figure 1-1. The Hexosamine Biosynthetic Pathway. Glucose is metabolized into Uridine diphosphate-N-acetylglucosamine (UDP-GlcNAc) which serves as the glycosyl donor for the post-translational modification of O-GlcNAcylation. Synthesis of UDP-GlcNAc requires input from several major metabolic pathways. Blue indicates input from amino acid metabolism. Orange indicates input from fatty acid metabolism. Green indicates input from nucleotide metabolism. Black indicates input from glucose metabolism.

fatty acid (Fig. 1-1). Therefore, overabundance of nutrients can drastically alter levels of protein O-GlcNAcylation via enhancing flux through the HBP.

The HBP is a nutrient sensing pathway that is linked to the development of glucose-induced insulin resistance characteristic of type 2 diabetes [42]. Under physiological conditions, the HBP is a minor metabolic pathway, accounting for 2-5% of glucose metabolism [44]. The HBP ultimately metabolizes the glycolytic intermediate fructose-6-phosphate into the O-GlcNAc donor uridine diphosphate *N*-acetylglucosamine (UDP-GlcNAc). The rate limiting enzyme for the entry of fructose-6-phosphate into the HBP is glutamine:fructose-6-phosphate aminotransferase (GFAT). GFAT isoform expression is distributed differentially across tissues. However, we recently reported the GFAT2 isoform (rather than GFAT1) is likely the primary isoform responsible for committing fructose-6-phosphate to the HBP in retina [45]. These results are consistent with other studies demonstrating GFAT2 is the predominant isoform in the central nervous system [46]. GFAT2 mRNA expression in retina is elevated in mice fed a high fat diet (HFD) [45]. However, regulation of GFAT expression and activity in the retina is not well understood.

Protein O-GlcNAcylation-induced Abnormalities in DR

Sustained hyperglycemia increases flux through the HBP. Given that the HBP is responsible for synthesizing UDP-GlcNAc, increased flux through the HBP results in increased levels of protein O-GlcNAcylation. Indeed, several studies have confirmed O-GlcNAcylation is abnormally elevated in both diabetic humans and animals [44, 47-49]. For example, retinal protein O-GlcNAcylation is increased in both streptozotocin (STZ)-induced diabetic mice [50] and mice fed a HFD [45]. These results are consistent with other reports indicating retinal protein

O-GlcNAcylation is elevated in 6-week-old diabetic Akita mice [51] and in a *db/db* type 2 diabetes mouse model, in which O-GlcNAcylated proteins localize to the ganglion cell layer, retinal pigmented epithelium, and inner plexiform layers [52]. OGT expression is also elevated in the vitreous humors of patients with PDR [53].

Abnormalities in O-GlcNAc cycling are associated with glucose toxicity in diabetic individuals [54]. Additionally, global elevation of O-GlcNAcylation, induced by inhibiting OGA in the absence of hyperglycemia, can cause insulin resistance, a hallmark of type 2 diabetes [55]. Impaired insulin signaling is a primary agent responsible for the development of DR, in addition to poor glycemic control. OGT binds the insulin receptor substrate 1 (IRS1) where it catalyzes addition of O-GlcNAc modifications on downstream effectors of the insulin signaling pathway. Enhanced O-GlcNAc modifications of IRS1 attenuate its ability to mediate the pro-survival effects of insulin by promoting phosphorylation at inhibitory serine residues and thereby dampening insulin-induced Akt activity [55-59]. Furthermore, enhancing intracellular O-GlcNAcylation via glucosamine (a metabolite that enters the HBP downstream of GFAT) impairs activation of critical pro-survival proteins downstream of IRS1, including phosphatidylinositol-4,5-bisphosphate-3-kinase (PI3K), Akt, glycogen synthase kinase 3 (GSK3), and the transcription factor forkhead box protein O1a (FOXO1a) [60]. Degeneration of the neuroretina is an early stage in the pathogenesis of DR. Altered electroretinograms, diminished color vision, and defects in contrast sensitivity are present before clinical manifestations of DR are visible via fundus examination [18]. Insulin administration reduces the rate of apoptosis in retinas of diabetic mice [61]. However, given the inhibitory effect of O-GlcNAcylation on the machinery of the insulin signaling pathway, insulin administration is likely not sufficient to overcome hyperglycemia-induced retinal protein O-GlcNAcylation.

Aside from the neuroretina, enhanced protein O-GlcNAcylation also causes deleterious consequences for retinal endothelial, epithelial, and glial cells. Abnormal O-GlcNAc cycling can induce early cell death of retinal pericytes, one of the earliest signs of DR [62]. Protein O-GlcNAcylation is elevated in both retinal endothelial cells and pericytes in Akita mice and in a model of oxygen-induced ischemic retinopathy during the neovascularization phase [51]. In cells exposed to hyperglycemic cell culture medium, protein O-GlcNAcylation is highest in retinal pericytes as compared to retinal endothelial cells or astrocytes [62]. Hyperglycemic cell culture conditions also induce proliferation and migration of retinal endothelial cells with minimal apoptotic effects [62, 63]. Furthermore, enhanced protein O-GlcNAcylation in retinal endothelial cells contributes to angiogenic factor release and enhanced proliferation and migration [51, 52]. Elevation of intracellular O-GlcNAc is sufficient to upregulate VEGF, a critical mediator of BRB permeability in DR, in multiple retinal epithelial cell lines [64]. In an astroglial cell line, O-GlcNAc modification of the cell cycle regulator p27 inhibited astrocyte migration while glucosamine-induced flux through the HBP caused acute activation of Akt and consequent increased ER stress [65, 66].

Retinal Müller cells are a particularly susceptible target of the glucotoxic effects of hyperglycemia, given they are the only cell type in the retina to express GLUT2 transporters, which possess a high capacity, yet low affinity, for glucose [67]. In other retinal cell types lacking GLUT2, glucose transporters become quickly saturated under hyperglycemic conditions. However, the high-capacity GLUT2-mediated glucose transport in Müller cells continues to increase under hyperglycemic conditions. Recent evidence suggests Müller cells are also susceptible to type 2 diabetes-associated dyslipidemia. O-GlcNAcylation is elevated in retinal Müller cells in culture exposed to the saturated fatty acid palmitate or the ceramide analog Cer6 [45]. Exposure of retinal Müller cells in culture to Cer6 resulted in suppression of Akt

phosphorylation, increased c-Jun N-terminal kinase (JNK) phosphorylation, and activation of caspase 3 [68]. Notably, inhibition of GFAT, the rate-limiting enzyme of the HBP, prevented Cer6-induced protein O-GlcNAcylation in Müller cells in culture [45].

Protein O-GlcNAcylation and Gene Expression

O-GlcNAcylation and Transcription

Protein O-GlcNAcylation plays a key role in nutrient regulation of gene expression. Many early studies investigating protein O-GlcNAcylation support a model wherein the O-GlcNAc modification alters the transcriptional activity, localization, and binding partners of multiple transcription factors [69-72]. Nearly all RNA polymerase II transcription factors are O-GlcNAc modified, and assembly of the pre-initiation complex necessary for transcription initiation requires O-GlcNAcylation of the C-terminal domain of RNA polymerase II [73-76]. OGA itself localizes to transcription start sites to catalyze the removal of the O-GlcNAc moiety from the C-terminal domain of RNA polymerase II in order for transcription elongation to proceed [77]. O-GlcNAc also plays an epigenetic role as it regulates both ubiquitination and methylation of histones [78-80]. A detailed overview of O-GlcNAc-mediated regulation of gene expression at the level of transcription has been reviewed in [74].

Several transcription factors that play a role in the pathogenesis of DR are subject to O-GlcNAc modification. Specificity protein 1 (Sp1) is a transcription factor that facilitates upregulation of the VEGF gene in response to hyperglycemia. In retinal endothelial and pigmented epithelial cells in culture, O-GlcNAcylation of Sp1 resulted in upregulation of VEGF mRNA and protein [64]. Notably, depletion of cellular OGT prevented glucose-induced changes

in levels of VEGF [64]. Similarly, O-GlcNAcylated Sp1 also mediates hyperglycemia-induced intracellular cell adhesion molecule 1 (ICAM-1), an important inflammatory molecule, expression in retinal endothelial cells [81]. Signal transducer and activator of transcription proteins 3 (STAT3) is a transcription factor that facilitates breakdown of the BRB via increased VEGF expression and downregulation of endothelial tight junction protein levels [82, 83]. STAT3 expression is elevated in retinas from diabetic rats and is O-GlcNAcylated in retinal endothelial cells exposed to high glucose cell culture medium [53]. NF-κB is a pleiotropic transcription factor with multiple roles in development, apoptosis, and inflammation [84]. Activation of NF-κB is associated with experimental and clinical diabetes [85]. After two months of streptozotocin-induced diabetes, O-GlcNAcylated NF- κB is enhanced in retinas from diabetic mice as compared to non-diabetic controls [50]. In fact, the level of O-GlcNAcylated NF-κB was elevated in apoptotic RGCs in retinas of diabetic mice [50]. These results indicate diabetes-induced O-GlcNAcylation of NF- κB induces activation of the transcription factor and contributes to RGC cell death that is associated with diabetes. Another important mediator of cell death is pro-apoptotic transcription factor p53. Primary cultures of retinal pericytes exposed to hyperglycemic cell culture conditions displayed elevated levels of O-GlcNAc modified and total p53. Pharmacological inhibition of both GFAT and OGT attenuated the hyperglycemia-induced increase in total p53. Given these results, it is plausible O-GlcNAcylation enhances the stability of p53, possibly by interfering with its proteasomal-mediated degradation [62].

While there are several descriptive studies interrogating the role of O-GlcNAc in transcription, the functional significance of O-GlcNAc modification in retinal gene transcription in the diabetic milieu remains to be fully elucidated. The limited studies mentioned herein suggest O-GlcNAcylation of certain transcription factors affects their transcriptional activity. Further detailed studies identifying a potential molecular mechanism by which this regulation happens are

needed to develop a more robust understanding of how nutrient sensing via HBP flux and subsequent protein O-GlcNAcylation control gene expression at the level of transcription.

O-GlcNAcylation and mRNA translation

Regulation of protein synthesis is critical in controlling cellular responses to biological cues such as nutrient status. Protein synthesis is one of the most energy-intensive processes in the cell, and therefore regulation of mRNA translation must be integrated with overall cellular metabolic status. O-GlcNAc cycling may be one mechanism by which control of protein synthesis is integrated with the nutritional state of the cell. In fact, recent data suggests the O-GlcNAc modification plays an underappreciated role in nutrient-mediated regulation of gene expression at the level of mRNA translation [86]. Over 20 core ribosomal proteins are O-GlcNAcylated, and both OGT and OGA are tightly bound to cytosolic ribosomes [87].

The rate of mRNA translation is limited by recruitment of ribosomal subunits during the initiation phase. The 5'-end of all eukaryotic mRNA is capped by an m^7GTP structure. The cap-binding complex eIF4F (a heterotrimer composed of a helicase [eIF4A], a scaffolding protein [eIF4G], and a cap-binding protein [eIF4E]) assembles at the 5'-cap structure, and the eIF4F·mRNA complex recruits the 40S ribosomal subunit [88]. Alternatively, ribosomes may also be recruited to the 5'-untranslated region (UTR) of mRNA by highly structured nucleotide sequences known as internal ribosomal entry sites (IRES). IRES elements enable a cap-independent mechanism of translation initiation [89].

Interaction between initiation factors eIF4E and eIF4G is critical for cap-dependent translation initiation, and is primarily regulated by the translational repressor 4E-BP1, a downstream target of the master kinase mammalian target of rapamycin complex 1 (mTORC1) and an eIF4E sequestering protein. eIF4E is the only canonical initiation factor differentially

utilized in cap-dependent translation, but not cap-independent translation [90]. Indeed, eIF4E negatively regulates cap-independent mechanisms of translation by enhancing competition with capped mRNAs for initiation factor binding [91]. eIF4E remains sequestered when 4E-BP1 is hypophosphorylated, thereby preventing the critical interaction of eIF4E with eIF4G which facilitates binding to the 5'-cap of mRNA. Therefore, control of eIF4E availability is critical in regulating the balance between cap-dependent and cap-independent mechanisms of mRNA translation.

Diabetes is associated with increased binding of 4E-BP1 to eIF4E, which is consistent with a diabetes-associated attenuation of mTORC1 signaling [92]. However, an O-GlcNAc-mediated mechanism could also account for the enhanced 4E-BP1-eIF4E interaction. Indeed, in hyperglycemic cell culture conditions, O-GlcNAcylation of 4E-BP results in an enhanced interaction with eIF4E, independent of phosphorylation status [93]. In a transgenic mouse model expressing a bicistronic mRNA containing two open reading frames that encoded two distinct luciferase enzymes (LucR driven by cap-dependent translation and LucF driven by the FGF-2 IRES), cap-dependent translation was attenuated over 2-fold in the liver of mice with STZ-induced diabetes compared to nondiabetic littermates [94]. In contrast, LucF activity was elevated almost 3-fold in the liver of diabetic mice compared to nondiabetic controls. Notably, ablation of 4E-BP prevented the hyperglycemia-mediated shift from cap-dependent to cap-independent translation in a cell culture system utilizing the same bicistronic reporter [94]. O-GlcNAc-mediated sequestering of eIF4E by way of 4E-BP thus facilitates a shift from cap-dependent to

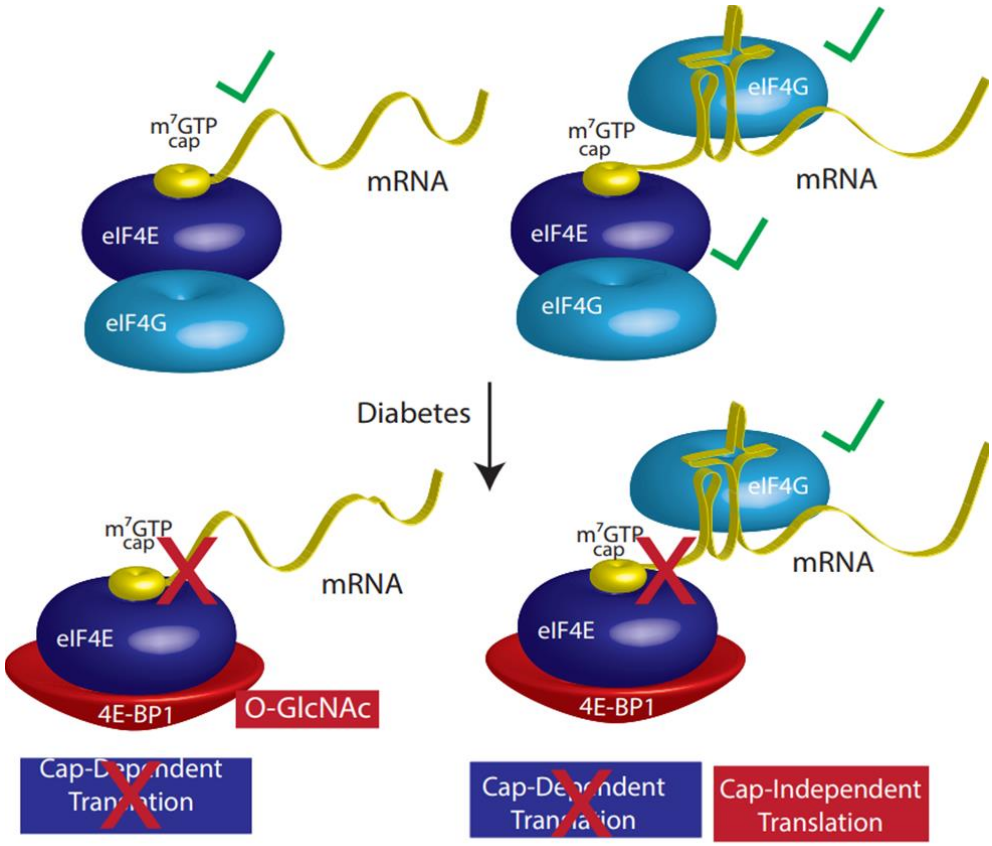

Figure 1-2. Enhanced O-GlcNAcylation promotes eIF4E binding to 4E-BP to promote cap-independent translation. eIF4E is only utilized in cap-dependent mechanisms of mRNA translation. When 4E-BP is O-GlcNAcylated, such as in diabetes, it sequesters the cap-binding protein eIF4E away from eIF4G. eIF4E binding with eIF4G is necessary for formation of the eIF4F cap-binding complex, and cap-dependent mRNA translation. However, mRNAs that contain highly structured RNA elements can also recruit ribosomes independently of eIF4E to mediate cap-independent mRNA translation.

cap-independent mRNA translation (Fig. 1-2) [94]. Therefore, O-GlcNAcylation can regulate the pattern of mRNAs selected for translation via 4E-BP (Fig. 1-2).

Interaction of 4E-BP1 with eIF4E is also enhanced in the retina of diabetic rodents and retinal cells in culture upon exposure to hyperglycemic conditions [95-97]. A key consequence of this interaction is enhanced cap-independent translation of the IRES-containing mRNA encoding VEGF in both retina of diabetic rodents and retinal cells exposed to hyperglycemic cell culture conditions [96, 97]. In rodents, expression of 4E-BP1 protein is elevated after administration of thiamet G (TMG), an inhibitor of OGA, and 4-6 weeks after induction of diabetes [95, 97].

Administering phlorizin to reduce serum glucose concentrations concomitantly reduced 4E-BP1 protein expression in the retina of diabetic mice to a value not significantly different from that in nondiabetic rodents [95]. This hyperglycemia- or O-GlcNAc-mediated induction of 4E-BP1 was determined to be due to a reduction in its rate of degradation [95]. Miller and colleagues identified a unique PEST motif in 4E-BP1 that is absent in the 4E-BP2 isoform and is associated with targeting proteins for degradation through the ubiquitin-proteasome pathway [98]. Disrupting a key phosphorylation site at threonine 82 of 4E-BP1 was sufficient to prevent polyubiquitination and degradation of the protein [95]. Therefore, one potential mechanism whereby O-GlcNAcylation of 4E-BP1 blocks ubiquitination is by promoting protein stability via interference with PEST motif phosphorylation. Notably, 4E-BP deficient mice were protected from early diabetes-induced visual dysfunction [95].

Other core translation initiation factors have also been reported as O-GlcNAc modified. eIF2α is a major mediator of the unfolded protein response (UPR), a mechanism induced by ER stress that inhibits global translation initiation, with the exception for that of a few specific, stress-related mRNAs. O-GlcNAcylation of eIF2α inhibits its phosphorylation at a critical serine residue necessary to carry out the UPR, and thereby prevents ER stress-induced apoptosis [99]. O-GlcNAcylation of eIF4G enhances its stability [100]. In human HEK293T cells, O-GlcNAcylation of eIF4G promotes its interaction with poly(A)-binding protein (PABP) and poly(A) mRNA, which facilitates the interaction of the 5'-cap and 3'-end of mRNA to form a closed loop and stimulate cap-dependent translation [101, 102]. Alternatively, a closed-loop formation could also promote cap-independent translation by enabling terminating ribosomes to come into close proximity with the start codon. eIF4G O-GlcNAcylation did not affect its ability to bind eIF4A or eIF4E [101]. However, in MEF cells, the O-GlcNAc modification on eIF4G facilitates the preferential translation of stress mRNAs during the heat shock response, a signaling

pathway that results in rapid induction of genes encoding molecular chaperones necessary for recovery from cellular damages [103]. Heat stress-induced eIF4G O-GlcNAcylation prevents binding of PABP [104]. Therefore, by opening the mRNA loop, heat stress-induced eIF4G O-GlcNAcylation not only suppresses cap-dependent translation, but simultaneously enables eIF4G to preferentially bind stress mRNAs and initiate translation via a cap-independent mechanism [104]. Li and colleagues also demonstrated the core translation factor eIF4A, an ATP-dependent RNA helicase, is O-GlcNAc modified [101]. O-GlcNAcylation of eIF4A disrupts assembly of the heterotrimeric eIF4F complex and inhibits the duplex unwinding activity of eIF4A, thereby resulting in an overall inhibition in protein synthesis and cellular proliferation [101].

Given the differential effects of O-GlcNAcylation on core translation initiation proteins, it is likely the modification exists to fine-tune protein synthesis in response to various biological cues and fluctuations in nutrient status. Protein synthesis is a tightly regulated process that is fundamental to cell growth and proliferation. While many studies have begun to uncover the role the nutrient- and stress-responsive post-translational O-GlcNAc modification may play in mRNA translation, more studies are necessary to fully appreciate this mechanism whereby the cell integrates nutritional status with the fundamental cellular process of synthesizing proteins.

Protein O-GlcNAcylation, Cellular Signaling, and the Ocular Renin Angiotensin System: Cross-Roads for Novel DR Therapies?

O-GlcNAc-Mediated Modulation of Signaling

The ability of O-GlcNAcylation to trigger changes in protein stability, activity, and localization makes it well-suited to facilitate signal transduction and propagation. Given the

interplay of O-GlcNAcylation with phosphorylation, it is becoming clear O-GlcNAcylation plays a critical role in regulating signaling pathways in response to nutrients and stress [43, 105]. For example, inhibition of GSK3β had a bidirectional effect on protein O-GlcNAcylation: the modification increased primarily on cytoskeletal and heat shock proteins while it was attenuated on primarily transcription factors and RNA-binding proteins [106]. Similarly, upon exposure to TMG, nearly every actively cycling 700 mapped phosphorylation sites were either increased or decreased in response to enhanced O-GlcNAcylation [107]. OGT itself can be phosphorylated by signaling partners such as AMP-activated protein kinase (AMPK), GSK3β, and the insulin receptor, and thereby integrate various inputs to generate a cellular output appropriate to the environmental cue [108]. Aside from phosphorylation, O-GlcNAcylation can regulate many calcium handling proteins [47, 109]. Calcium is a universal second messenger that activates and coordinates a vast spectrum of cellular functions. Enhanced O-GlcNAcylation also increases the activity of Protein Kinase A (PKA), a kinase activated by the second messenger cyclic adenosine monophosphate (cAMP) [110]. Intriguingly, global patterns of O-GlcNAcylation and cAMP-mediated signaling pathways seem to be inversely dysregulated in various behavioral models of sleep deprivation, fear conditioning, and stress [111, 112]. The collective whole of these findings thus suggest protein O-GlcNAcylation dynamically integrates cellular nutrient status by regulating intracellular signaling pathways. Dysregulation of such integration induced by aberrant O-GlcNAc cycling can subsequently produce pathogenic effects, particularly in metabolically sensitive tissues such as the retina.

A Role for the Ocular RAS in DR

The pathogenesis of DR encompasses dysregulation of a multitude of signaling pathways. However, recent evidence indicates dysregulation of the retinal renin angiotensin system (RAS)

may play a prominent role in the disruption of the retinal neurovascular unit that is associated with DR pathology [113]. The classic RAS is typically defined by its systemic physiological functions, but it is becoming increasingly evident that local, tissue-specific RAS systems play an important role in disease pathologies, including DR. The RAS is one of the oldest studied hormone systems and is well known for its role in systemic vascular control and fluid homeostasis. The retina is one of several tissues that possess a local RAS, and it is well-established that all components of the RAS are expressed in the retina, including angiotensinogen, prorenin, renin, angiotensin I (Ang I), angiotensin II (Ang II), angiotensin converting enzyme (ACE), Ang II type 1 receptor (AT1R), and Ang II type 2 receptor (AT2R) [Reviewed in [114]]. Secreted renin serves to cleave the pro-peptide angiotensinogen into Ang I. ACE cleaves Ang I into the primary effector peptide of the RAS, Ang II. Ang II stimulates vasoconstriction, aldosterone synthesis and subsequent sodium resorption, fibrosis, and inflammation, mediated through binding to the AT1R G protein-coupled receptor [115]. The mechanisms induced by AT2R binding are less well understood; although, it is thought activation of AT2R may mediate opposing actions of AT1R, such as stimulating vasodilation [116].

The role of Ang II in a healthy, functioning retina is likely related to regulation of retinal blood vessel tonicity, glial function, and neuronal function [117]. In DR, Ang II formation is elevated, potentiates VEGF-mediated angiogenesis, and increases retinal blood vessel permeability [Reviewed in [114]]. Interest in further understanding the role of Ang II and other components of the RAS increased after clinical studies revealed that blocking either Ang II signaling with ARBs (Angiotensin Receptor Blockers) or preventing Ang II formation with ACE inhibitors (ACEi) reduced the risk for both incidence and progression of DR [118]. These intriguing clinical results prompted a question that could only be answered on a molecular level: how do ARBs and ACEi mediate beneficial effects in the retina?

The hypothesis that was subsequently developed to answer that question involved the action of the more recently discovered arm of the RAS that is mediated by the effector peptide angiotensin-(1-7) (Ang 1-7). Ang1-7 is generated by cleavage of Ang II by the enzyme ACE2 or by cleavage of Ang I by various endopeptidases (Fig. 1-3). Ang I may be alternatively degraded by ACE2 to generate angiotensin-(1-9), which in turn may be cleaved by neutral endopeptidase or ACE to generate Ang 1-7 (Fig. 1-3). Ang1-7 binds to the G protein-coupled receptor Mas to elicit systemic vasodilatory and antihypertensive effects. A handful of recent studies have provided evidence that some of the positive cardiometabolic effects observed in rodents administered RAS blockers are due to increased circulating levels of Ang 1-7 [119-121]. In the case of ACEi, the basis for this rise in Ang1-7 is due to decreased degradation of Ang 1-7 to angiotensin-(1-5) by ACE and increased Ang I resulting from a reduction in Ang II formation [122, 123]. Importantly, the positive effects of Ang1-7 thus far reported are independent of changes in blood pressure [124, 125].

Pharmacological blockade of the RAS also produces visually beneficial effects. Administration of the ACEi perindopril in diabetic rodents improved both photoreceptoral and inner retinal function comparable to that of nondiabetic rodents [126]. ACEi also reduces VEGF expression and vascular permeability in retinas of diabetic rodents [127, 128]. Systemic administration of the ACEi captopril enhances expression of Ang1-7 in the retina with a concomitant decrease in diabetes-induced Ang II expression [129]. Intra-vitreal delivery of adeno viral encoded Ang1-7 also ameliorates hallmark characteristics of DR, including diabetes-induced retinal vascular permeability, formation of acellular capillaries, infiltration of inflammatory cells,

and oxidative damage in diabetic rodents [130]. These pioneering descriptive studies have done much to demonstrate the existence of an ocular RAS and have established a convincing line of evidence that targeting the ACE2/Ang 1-7/Mas axis of the RAS in retina could have promising therapeutic effects in ameliorating the deleterious consequences of DR.

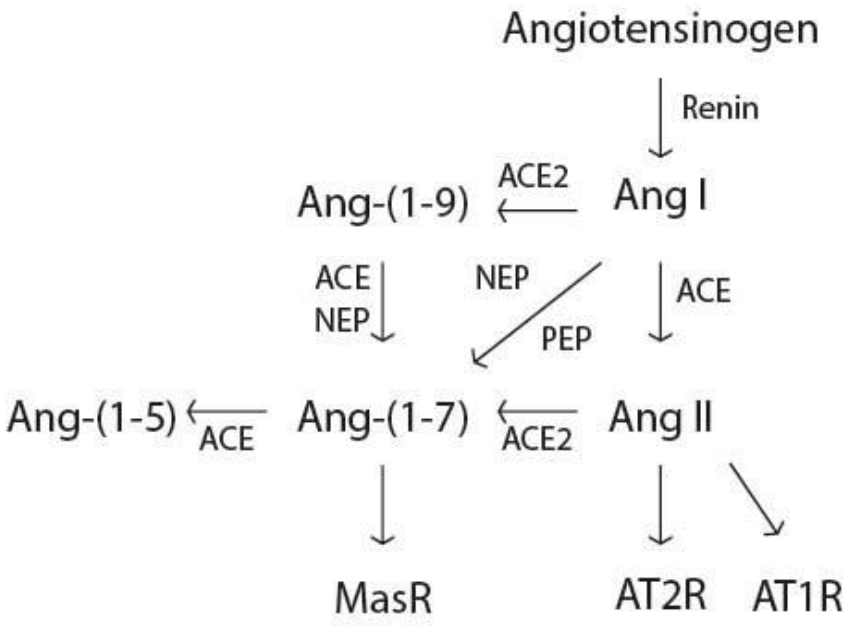

Figure 1-3. Generation of Angiotensin-(1-7). AngI may be cleaved by ACE to generate AngII which in turn is cleaved by ACE2 to generate Ang1-7. Alternatively, ACE2 cleaves AngI to generate Ang1-9 which may be degraded by ACE or NEP (neutral endopeptidase) to produce Ang1-7. Finally, AngI may be degraded by endopeptidases such as NEP or PEP (prolyl endopeptidase) to directly form Ang1-7.

Evidence for Interplay between Protein O-GlcNAcylation and the RAS

Studies examining how O-GlcNAc modified proteins affect signaling events of the RAS are limited; studies examining how the RAS modulates protein O-GlcNAcylation are largely nonexistent. However, in diabetic rats, pharmacological blockade of the RAS prevented the diabetes-induced increase in global O-GlcNAcylation in kidney [131]. Furthermore, both high glucose and glucosamine stimulated angiotensinogen gene expression in mesangial and proximal

tubular cells [132-134]. Other studies suggest activation of the HBP and enhanced protein O-GlcNAcylation modulate hypertrophic pathways associated with cardiovascular dysfunction in diabetes. Activation of the HBP in cardiomyocytes isolated from diabetic *db/db* mice resulted in an attenuated hypertrophic response upon exposure to Ang II as compared to cardiomyocytes isolated from nondiabetic control mice [135]. Inhibiting the HBP partially restored the hypertrophic signaling response in diabetic cardiomyocytes [135]. In adipose tissue, attenuation of protein O-GlcNAcylation resulted in a concomitant decrease in angiotensinogen, AT1R, OGT, and GFAT transcripts [136]. Similarly, infusion of glucosamine increased expression of angiotensinogen in adipose tissue [137].

Taken together, the results of the studies mentioned herein provide evidence to support a role for O-GlcNAc-mediated regulation of local and systemic RAS. However, studies examining specific signaling cascades that generate these results are lacking. Therefore, understanding how protein O-GlcNAcylation modulates the RAS (and vice versa) would undoubtedly prove to be additive to the current body of knowledge that has yet only scratched the surface of the complex interplay between these two pathways. Given the integral role of both protein O-GlcNAcylation and the RAS in DR, defining specific molecular events associated with the intersection of these pathways may result in identification of novel therapeutic targets for diabetic eye disease.

Conclusion

The retina has the unique function of transmitting visual information to the brain to elicit a behaviorally useful response. Retinal glial, endothelial, and neuronal cells cooperate to form a retinal neurovascular unit. The retina has one of the highest metabolic demands of the body, and therefore is particularly susceptible to hyperglycemia-mediated tissue damage. Disintegration of

the neurovascular unit results in a progressive deterioration of retinal vascular integrity and function, culminating in a diagnosis of DR. One hypothesized mechanism for hyperglycemia-mediated retinal damage is increased flux through the HBP and a subsequent increase in protein O-GlcNAcylation. O-GlcNAcylation is a post-translational modification that is associated with the pathogenesis of DR. Aberrant cycling of the O-GlcNAc modification can have deleterious consequences for many fundamental cellular processes. Many early efforts were focused on understanding the role of protein O-GlcNAcylation in modulating the transcriptional activity of transcription factors, and thus established a role for the nutrient-sensing HBP in modulating gene expression. This work has been extended upon by more recent studies demonstrating many core translation initiation factors are O-GlcNAc modified. Therefore, protein O-GlcNAcylation may also play a role in regulating gene expression at the level of mRNA translation. Protein O-GlcNAcylation also contributes to diabetes-associated defects in cellular signaling. Indeed, there is emerging evidence linking disruptions in the RAS with aberrant alterations in levels of protein O-GlcNAcylation. Pharmacological blockade of the classic RAS, mediated by the effector peptide Ang II, reduces risk for both the incidence and progression of DR. It is hypothesized these beneficial effects are due to increased levels of Ang1-7; however, specific signaling events mediated by Ang1-7 are not well defined in retina. These lines of evidence, although limited, indicate nutrient status may be integrated via the HBP to influence one of the most well-characterized systemic hormonal axes in that of the RAS.

The overarching aim of the studies included in this dissertation is to better understand the deleterious effects of enhanced retinal protein O-GlcNAcylation and identify a mechanism to attenuate it. Specifically, our work addresses three hypotheses: *1*) enhanced retinal protein O-GlcNAcylation alters the pattern of mRNAs selected for translation, *2*) diabetes-induced O-GlcNAcylation enhances translation of the immunostimulatory molecule Cluster of

Differentiation 40 (CD40), and *3*) the Ang1-7 signaling axis attenuates retinal protein O-GlcNAcylation via regulation of the HBP.

Chapter 2

Materials & Methods

Animals

At 4-weeks of age, male and female wild-type and 4E-BP1/2 double knockout C57BL/6J mice received 50 mg/kg TMG or phosphate buffer saline as a control via intraperitoneal injection. Retinas were extracted 24 h after TMG injections. Alternatively, male mice were administered 50 mg/kg STZ for 5 consecutive days to induce diabetes. Control mice were injected with equivalent volumes of sodium citrate buffer. Diabetic phenotype was confirmed by blood glucose concentration >250 mg/dL in fasted animals. Retinas were extracted after 4 weeks or 3 months of diabetes.

For studies involving the ACEi captopril, three groups of male C57Bl/6J mice (Jackson Laboratory) were placed on a diet containing 60% kcal from fat (HFD) beginning at 5 weeks of age: 1) saline (n=6 saline infusion plus normal water); 2) captopril (n=6 saline infusion plus captopril water); 3) captopril + A779 (n=5 A779 infusion [400 ng/kg/min] plus captopril water). The mice described here are a subset of those presented in our previous study [138]. After 8 weeks of HFD, mice were implanted with a subcutaneous osmotic mini-pump (Alzet Model 2004) for chronic 3-week infusion of saline or the Ang1–7 Mas receptor antagonist A779 (Bachem). Immediately following mini-pump implantation, mice received either tap water or water containing the ACE inhibitor captopril (50 mg/L; Tocris Bioscience). There were no differences in daily water intake between mice receiving tap water and water containing captopril [138]. The dose of captopril was previously demonstrated to be equivalent to captopril doses used

for treatment of patients with hypertension [139]. Body weight, arterial glucose levels, and plasma AngII and Ang1-7 concentrations were analyzed as previously described [138].

All procedures were approved by the Pennsylvania State College of Medicine Institutional Animal Care and Use Committee.

RiboTag Mouse Model

B6J.129(Cg)-Rpl22$^{tm1.1Psam}$/SjJ (RiboTag) mice carrying a targeted homozygous mutation of the ribosomal protein L22 locus to enable Cre-mediated hemagglutinin (HA) epitope tagging of ribosomes from specific cell types were purchased from Jackson Laboratories. To enable expression of HA-tagged ribosomes in Müller glia, RiboTag mice were crossed with heterozygous C57Bl/6-Tg(Pdgfra-cre)1Clc/J (PDGFRa-CRE; Jackson Laboratories) to generate heterozygous RiboTag mice. The resulting heterozygous generation was crossed with homozygous RiboTag mice to produce offspring with a PDGFRa-cre recombinase-expressing mouse with deletion of wild-type exon 4 of the Rpl22 locus and replacement with the Rpl22^{HA} exon specifically in Müller cells of the retina.

Protein Analysis

Retinas were extracted, flash-frozen in liquid nitrogen, and later homogenized in 250 μL of extraction buffer as previously described [97]. The homogenate was centrifuged at 1000 x *g* for 5 min at 4^{o}C and the supernatant was collected for analysis. A fraction of the supernatant was added to 1x SDS sample buffer, boiled for 5 min, and analyzed by Western blot analysis as previously described [97]. Briefly, lysates were fractionated using Criterion pre-cast 4-15% or 4-20% gels (Bio-Rad). Proteins were transferred to PVDF, blocked in 5% bovine serum albumin

(BSA) or 5% nonfat dried milk in Tris buffered saline Tween 20 (TBS-T) for 1 h, washed, and incubated overnight at 4˚C with the appropriate antibody. Incubations with the *O*-GlcNAc antibody were permitted to incubate for 48 h. The antigen-antibody interaction was visualized with enhanced chemiluminescence (Clarity Reagent; Bio-Rad Laboratories, Inc.; Hercules, CA) using a ProteinSimple Fluorochem E imaging system (Santa Clara, CA, USA). Blots were quantified using Image J software (NIH, Bethesda, MD, USA).

Antibodies used included *O*-GlcNAc (Cell Signaling Technology; Cat # 9875), α-actin (Cell Signaling Technology; Cat # 4970), GAPDH (Santa Cruz; Cat # sc-32233), OGA (Novus, Cat # NBP-81244), OGT (Cell Signaling Technology; Cat # 24083), DDK (Origene; Cat # TA5011-100), and HA (Santa Cruz, Cat # sc-805). Preparation of the eIF4E, 4E-BP1, and eIF4G antibodies has been previously described [140, 141]. Immunoprecipitations were performed by incubating supernatants of retina homogenates with monoclonal anti-eIF4E antibody as previously described [142].

RNA Analysis

Retinal RNA was extracted using TRIzol reagent (Invitrogen) according to the standard manufacturer's protocol. An equal amount of RNA was converted into cDNA using a High Capacity cDNA Reverse Transcription Kit (Applied Biosystems) and subjected to quantitative real-time PCR using QuantiTect SYBR Green master mix (Qiagen). Primer sequences can be found in Table 2-1. Changes in mRNA expression were normalized to GAPDH mRNA expression using the $2^{-\Delta\Delta CT}$ calculations as previously described [143].

Cell Culture

Cultures of wild-type and *Eif4ebp1;Eif4ebp2* double knockout (4E-BP1/2 DKO) mouse embryonic fibroblasts (MEF) were obtained from Dr. N. Sonenberg (McGill University) and were maintained in DMEM supplemented with 10% FBS and 1% penicillin/streptomycin. TMG was prepared in PBS and added to culture medium at a final concentration of 50 nM

MIO-M1 human Müller cells (obtained from the UCL Institute of Ophthalmology, London, UK) were maintained in DMEM (Gibco) containing 5.6 mM glucose, and supplemented with 10% heat inactivated (55˚C, 30 min) fetal bovine serum (FBS) and 1% penicillin-streptomycin (Invitrogen). For cell culture experiments, Ang1-7 acetate salt hydrate (Sigma Aldrich) was prepared in sterile water and added to culture medium at a final concentration of 10 μM, except where indicated. TMG was prepared in PBS and added to culture medium at a final concentration of 50 nM. TMG and Ang1-7 were added to cell culture wells simultaneously and treatment proceeded for 24 h. Forskolin (Fsk) was prepared in DMSO and added to cell culture medium at a concentration of 100 μM. The Mas receptor agonist AVE 0991 (Apex Bio) was prepared in DMSO and added to culture medium at a final concentration of 10 μM. Cells were pre-treated with Fsk and AVE 0991 for 1 h or 30 min, respectively prior to TMG. TMG exposure proceeded for 24 h. To quantify levels of cAMP, cells were stimulated with Ang1-7 for 30 min and then lysed with 0.1 M HCl. cAMP from cell lysates was then quantified via a cAMP competitive ELISA kit (Invitrogen) according to manufacturer's instructions. The PKA inhibitor H89 (N-[2-p-bromocinnamylamino-ethyl]-5-isoquinolinesulfonamide) and the EPAC inhibitor ESI-09 (α-[2-(3-Chlorophenyl)hydrazinylidene]-5-(1,1-dimethylethyl)-b-oxo-3-isoxazolepropanenitrile) were prepared in DMSO and added to cell culture medium at final concentrations as indicated in the figures. H89 and ESI-09 were added to cell culture medium for 1 h prior to the addition of Fsk for 1 h, followed by the addition of TMG for 24 h. D-(+)-

Glucosamine hydrochloride (GlcN) was prepared in sterile water and added to culture medium at a final concentration of 30 mM. Where indicated, mannitol (Man) prepared in sterile water was added at a final concentration of 30 mM. The membrane-permeable EPAC agonist 8-pCPT-2'-O-Me-cAMP-AM (8-CPT; Axxora) was prepared in DMSO and added to culture medium at a final concentration of 10 μM. Cells were stimulated with Fsk for 1 h prior to addition of GlcN or Man to culture medium for 24 h. Alternatively, cells were serum starved for 15 min prior to addition of 8-CPT to culture medium. Following 30 min of pre-treatment, GlcN was added to culture medium for 24 h.

Transfections

Transfections were performed using Lipofectamine 2000 (Life Technologies) according to the manufacturer's instructions. Plasmids for expression of HA-tagged 4E-BP1, HA-tagged 4E-BP1-Y54A, and HA-tagged 4E-BP1-F113A were obtained from Dr. J. Blenis (Weill Cornell Medical College). Plasmid for expression of pcDNA2.1HA-OGT was a gift from Gerald W. Hart (University of Georgia). Plasmids for expression of pAXEF-Rap1-WT (WT) and pAXEF-Rap1-E63(GTP) (Rap1E63) were a gift from Vicki Boussiotis (Addgene plasmids #32697 and #32698; http://n2t.net/addgene:32697; RRID:Addgene_32697; http://n2t.net/addgene:32698; RRID:Addgene_32698). pYIC was a gift from Han Htun (Addgene plasmid # 18673 ; http://n2t.net/addgene:18673 ; RRID:Addgene_18673).

Sequencing Library Preparation

Total RNA and Ribosome Protected Fragment (RPF) libraries for deep sequencing were prepared from mouse retina using a TruSeq Ribo Profile Kit (Ilumina). Briefly, 10 retinas per

group were dounce homogenized in 500 μL of polysome buffer containing 10% Triton X-100, 100 mM DTT, 100 mM EGTA, 0.5 U DNaseI, and 50 μg cycloheximide. For the RPF, 300 μL of retinal homogenate was treated with 0.6 U Nuclease/OD unit measured at A_{260} and purified using an illustra MicroSpin S-400 HR column (GE Healthcare Life Sciences). Ribosomal RNA depletion was performed with a Ribo-Zero Gold rRNA Removal Kit (Illumina). Total RNA was prepared from the remaining retinal homogenate and heat fragmented according to the manufacturer's instructions. RPF RNA and fragmented total RNA were end repaired with TruSeq Ribo Profile PNK for 3´adapter ligation and cDNA was reverse transcribed with EpiScript RT. cDNA libraries were PAGE purified, circularized with CircLigase, and amplified by PCR. Libraries were purified with Agencourt AMPure XP beads (Beckman Coulter) and sequenced on an Ilumina HiSeq 2500 to a depth of 15 million total reads per sample.

Sequence Analysis

Sequencing reads were mapped to 19,411 principal transcripts for each gene in the APPRIS database [144] referenced by GENCODE release M14 (GRCm38.p5) mouse genome. Principal transcripts for each gene were selected using script_for_transcript_annotation from RiboViz tool-kit package [144]. Transcript and ribosome footprint abundances for each transcript/gene were estimated using Kallisto v0.45.0 [145]. Given the small size of RPF and RNAseq inserts in our libraries (~30 bp), Kallisto indices were generated using a lower k-mer value (-k 19). Gene-specific fold-changes in RNA and footprint abundances were estimated using DESeq2 packages in R [146] using default log-fold-change shrinkage options. Changes in ribosome-densities (translation efficiencies) were estimated using the Riborex package in R [147]. Unless otherwise specified, significant changes in RNA, RPF, and ribosome densities were estimated at an adjusted p-value < 0.01 (Benjamini & Hochberg adjusted p-value). Functional

analysis of GO categories and KEGG pathways were conducted using clusterProfiler packages in R [147]. The data obtained from sequencing analysis was also analyzed using the software Ingenuity Pathways Analysis (IPA) (www.ingenuity.com) and Gene Ontology (GO) Enrichment Analysis (www.geneontology.org).

Polysome Fractionation by Sucrose Density Gradient Centrifugation and RNA Isolation

Sucrose density gradient centrifugation was employed to separate the sub-polysomal from the polysomal ribosome fractions. Retinas were harvested, and 10 retinas from the respective treatment groups were pooled. Retinas were homogenized in 600 μL of homogenization buffer [50 mM HEPES, 75 mM KCl, 5 mM $MgCl_2$, 250 mM sucrose, 2 mM DTT, 100 μg/mL cycloheximide, and 20 units/μL SUPERase-In™ RNase inhibitor (Invitrogen)]. Homogenates were incubated on ice for 5 min and 75 μL of Tween-deoxycholate solution (1.34 mL Tween 20, 0.66 g deoxycholate, 18 mL sterile water) was added for 15 min. Lysates were centrifuged at 1000 x *g* for 3 min at 4˚C

Alternatively, two 10 cm dishes of wild type or 4E-BP1/2 DKO MEFs were pooled together in 600 μL of homogenization buffer. Five minutes prior to the end of TMG exposure, cycloheximide (100 μg/mL) was added to cell culture media. Dishes were then washed twice with cold PBS supplemented with cycloheximide. Lysates were rocked for 20 min at 4˚C and then centrifuged at 3000 x g for 15 min at 4˚C.

The resulting supernatant was layered on a 20-47% linear sucrose gradient (10 mM HEPES, 75 mM KCl, 5 mM $MgCl_2$, 0.5 mM EDTA) and centrifuged in a SW41 rotor at 34,000 rpm for 225 minutes at 4˚C. Following centrifugation, the gradient was displaced upward (3 mL/min) in the fractionation system (Brandel) using Fluorinert (Sigma) through a spectrophotometer, and OD at 254 nm was continuously recorded (chart speed, 150 cm/h). Two

sucrose fractions representing the sub-polysomal and polysomal portions of the gradient were collected directly into an equal volume of TRIzol Reagent (Invitrogen). To improve the recovery of RNA from dense sucrose portions of the gradient, the polysomal fraction was diluted 2x with RNase-free water (HyClone), and the appropriate amount of TRIzol was added. RNA was extracted using the standard manufacturer's protocol and resuspended in 14 µL RNA Storage Solution. Sequences of primers used may be found in Table 2-1.

Bioenergetics Analysis of Oxygen Consumption Rate (OCR)

The Seahorse XF^{e}96 Extracellular Flux Analyzer (Seahorse Bioscience, North Billerica, MA) was used to assess mitochondrial respiration. Prior to use of the Extracellular Flux Analyzer, cells were seeded (30,000 cells/well; following optimization of cell seeding number) into the XF96 cell culture microplate, allowed to adhere, and then exposed to medium containing 50 nM TMG for 24 h. Cell culture media was then replaced with XF media (Seahorse Bioscience) and cells were placed in a non-CO_2 37˚C incubator for 1 h, prior to the start of the extracellular flux analysis. The Cell Mito Stress kit was applied according to manufacturer's instructions (Seahorse Bioscience). Prior to commencement of these experiments, dose response curves were carried out to establish the concentration of FCCP needed to achieve maximal OCR. Additionally, dose response curves were carried out to establish the optimal concentration of oligomycin required to inhibit oxygen consumption, as cells did not respond to the manufacturer's recommended 1 µM. Both cell lines achieved a plateau of maximal OCR at 0.5 µM FCCP, and inhibition of OCR at 2 µM oligomycin.

ROS Detection

MitoSOX Red mitochondrial superoxide indicator (Invitrogen) was used in wild type MEF, 4E-BP1/2 DKO MEF, and MIO-MI cells to detect mitochondrial superoxide according to the manufacturer's instructions. Briefly, cells were seeded at 300,000 cells (MEFs) or 200,000 cells (MIO) per dish in 35 mm, No. 1.5 coverglass, Poly-d-lysine coated dishes (MatTek Corporation). Cells were then exposed to 50 nM TMG for 24 h. One mL of 5 μM MitoSOX diluted in HBSS/Ca/Mg (Life Technologies) was applied to cells. The dye-loaded cells were incubated for 10 min at 37˚C in the dark and then washed with HBSS buffer. Live cells were imaged using an inverted Leica TCS SP8 confocal microscope.

To evaluate retinal ROS levels, whole eyes were harvested from mice, embedded in optimal cutting temperature compound (OCT, Sakura Finetek) and flash frozen. Cryosections (10 μm) were fixed with 2% paraformaldehyde in PBS (pH 7.4). Cryosections were stained with 1.6 μM Hoechst and 10 μM 2,7-dichlorofluoroscein (DCF). Live cells and cryosections were imaged using an inverted Leica TCS SP8 confocal microscope.

Glycosyltransferase Activity Assay

EZview red anti-HA affinity gel beads (Sigma, cat# E6779) were twice washed with lysis buffer (20 mM HEPES, 2 mM EGTA, 50 mM NaF, 100 mM KCl, 0.2 mM EDTA, 50 mM β-glycerophosphate, pH 7.4). After exposure to 10 μM Ang1-7 for 30 min, MIO-MI cells transfected with OGT were harvested in 1 mL PBS, spun at 1000 x g for 5 min at 4˚C, and cell pellet was re-suspended in 500 μL lysis buffer plus inhibitors (1M DTT, 200 mM benzamidine, 200 mM sodium vanadate, Sigma protease inhibitor cocktail [#P8340]). Clarified cell lysate was added to the prepared anti-HA beads and incubated for 2 h at 4˚C with gentle rocking.

Lysate/bead mix was spun for 30 s at 8200 x g, unbound fraction aspirated, and bead pellet washed three times in 750 µL lysis buffer. OGT activity was assessed using a UDP-Glo™ glycosyltransferase assay (Promega, cat# V6961). Bound OGT-HA fusion proteins were re-suspended in 50 µL OGT transferase buffer (25 mM HEPES, pH 7.2, 10 mM $MnCl_2$, 1 mM EDTA, and 1 mM PMSF) with 100 µM OGT peptide substrate (AnaSpec, Inc.) and 100 µM UDP-GlcNAc (Promega, cat# V7071). After 1 h at room temperature, reactions were quenched with UDP-Glo detection reagent and luminescence was measured using a SpectraMax M5 plate reader (Molecular Devices).

Bicistronic CD40 Reporter

A dsDNA gBlock fragment (IDT) encoding the 5'UTR of CD40 (TTTCCTGGGCGGGGCCAAGGCTGGGGCAGGGGAGTCAGCAGAGGCCTCGCTCGGGCGCCCAGTGGTCCTGCCGCCTGGTCTCACCTCGCTATG) was cloned into pCR2.1TOPO using the TOPO TA cloning kit (Invitrogen) according to manufacturer's instructions. pYIC and TOPO plasmids were digested with EcoRI-HF (New England BioLabs) and BamHI-HF (New England BioLabs). A 4700 base pair fragment and 100 base pair fragment were gel-purified from pYIC and TOPO digested plasmids, respectively. The fragments were ligated and cloned into XL-1 blue supercompetent cells (Agilent). The resulting construct was digested with Bstx1 (New England BioLabs) to remove the ECMV IRES. The digested construct was gel-purified, ligated, and cloned into XL-1 blue supercompetent cells. Clones were sequence verified using the YFP C terminus forward primer (ATCACATGGTCCTGCTGG).

Statistical Analysis

Data are presented either as means ± standard error of the means or means + standard error of the means. The distinction is noted in each figure legend. Analyses were performed using GraphPad Prism (Version 7.0) with p value <0.05 defined as statistically significant. Statistical tests used for each figure are noted in figure legends.

Table 2-1. Oligonucleotides used in qPCR analysis.

Gene Name	Species		Sequence
GFAT1	Mouse	*Forward*	TAAGGAGATCCAGCGGTGTC
		Reverse	CAGCTGTCTCGCCTGATTGA
GFAT2	Mouse	*Forward*	GTCATTCAGCAGTTGGAAGGC
		Reverse	CTTCGTACCCCGATGAGCAA
OGA	Mouse	*Forward*	AGCGAAGATGGCAGAGGAGT
		Reverse	CCGTGCTCGTAAGGAAGGTA
OGT	Mouse	*Forward*	GTGCACTGTTCATGGATTACATCATC
		Reverse	TCCATTGTGTATTGTTTGGTGTTG
Fam122a	Mouse	*Forward*	AGCAGTGTTTCTCACCGTCC
		Reverse	GGGTGGTAAATCGGGTGGTT
Nr6a1	Mouse	*Forward*	CTTCGGCAGAACTTCTCAGC
		Reverse	TCCCATAGTGCAAGCCCGTA
Mrpl47	Mouse	*Forward*	CGGTCAAGAAAAGCCCAGAC
		Reverse	CGATCCACATAAGGCATTGCG
Tufm	Mouse	*Forward*	GCCCAGGTTTATATCCTCAGCA
		Reverse	GTCAGGGAGAACATGACGGG
Sod2	Mouse	*Forward*	GTCGCTTACAGATTGCTGCC
		Reverse	AATCCCCAGCAGCGGAATAA
Elmsan1	Mouse	*Forward*	CGTCCCGAGAGCAACAAAGT
		Reverse	CTCTTGCGCTCAGCTACACT
Il1rap	Mouse	*Forward*	TGACGCTGCGTGGAGTTTTG
		Reverse	TTGGGACTTAGGACAACCAGG
Mettl14	Mouse	*Forward*	CGAAGCTGGGGCATGGATA
		Reverse	CACCAATGCTATCCGCACTC
Nat8l	Mouse	*Forward*	CGCAAGGTGATTCTGGCCTA
		Reverse	AGCCACCCAGAAACAGGAAC

Chapter 3

O-GlcNAcylation alters the selection of mRNAs for translation and promotes 4E-BP1-dependent mitochondrial dysfunction in retina

Introduction

As previously discussed, the principal underlying cause of diabetic retinopathy is hyperglycemia, as intensive glycemic control is associated with a reduction in both the onset and progression of neurovascular complications in retina [148]. However, the molecular mechanisms whereby hyperglycemia mediates neurovascular dysfunction remain undefined. One potential mechanism that is largely unexplored in retina is altered gene expression in response to enhanced flux through the nutrient- and stress-sensing HBP.

Hyperglycemia and diabetes promote flux through the HBP and resultant protein O-GlcNAcylation. O-GlcNAcylation of proteins has been observed to alter function through a number of mechanisms, including changes in subcellular localization, protein-protein interactions, enzymatic activity, and degradation rates [149-153]. One unexplored mechanism by which O-GlcNAcylation may alter functional outcomes in the cell is protein synthesis. Mounting evidence suggests the O-GlcNAc modification may play a prominent role in regulating mRNA translation. For example, the O-GlcNAc cycling enzymes OGT and OGA strongly associate with cytosolic ribosomes, suggesting they play an important role in regulating mRNA translation [154]. In retinal pericytes exposed to hyperglycemic conditions, O-GlcNAcylated proteins are most heavily represented in the functional category *Protein Synthesis and Processing* [62]. Indeed, O-GlcNAcylation has been detected on 34 of the ~80 proteins that compose the mammalian ribosome [154]. Among translation initiation factors, subunits of eIF2 [155], eIF3

[155, 156], eIF4 [157, 158], eIF5 [155], poly(A)-binding protein [106] and 4E-BP1 [159] are all O-GlcNAcylated; however the functional consequence of these modifications on gene expression remains to be established.

Recruitment of ribosomes to mRNA is altered in response to hyperglycemic conditions [94] or overexpression of OGT [154]. In the retina of diabetic rodents, global rates of protein synthesis are reduced; however, all mRNAs are not affected equally [160]. Diabetes promotes ribosome-association for a number of retinal mRNAs, including the synaptic proteins Snap25 and snaptophysin 1 [160]. Importantly, hyperglycemia also promotes translation of the mRNA encoding the proangiogenic cytokine VEGF [96]. VEGF concentrations are elevated in the eyes of patients with diabetic macular edema and the cytokine is considered to play a causal role in the proliferative stages of DR. In the retina of mice lacking the translational repressor 4E-BP1, VEGF expression remains unchanged in response to diabetes [97] and diabetes-induced visual dysfunction is delayed [95].

4E-BP1 regulates the selection of mRNAs for translation through binding and sequestration of the cap-binding protein eIF4E that recognizes the m^7GTP cap structure found at the 5´-terminus of all eukaryotic mRNAs [161]. It has been shown previously that in the retina of diabetic mice, hyperglycemia promotes 4E-BP1 O-GlcNAcylation and binding to eIF4E [95]. Given the dependence of mRNAs on eIF4E for translation, availability of eIF4E can serve to determine global patterns in gene expression. Some messages, such as the one that encodes VEGF, contain internal RNA elements that facilitate ribosome recruitment and translation independent of eIF4E in a cap-independent mechanism [162]. While 4E-BP1 reduces eIF4E availability and cap-dependent translation, mRNAs that are capable of recruiting ribosomal subunits independent of the 5´-cap often exhibit an increase in their relative rates of translation due to reduced competition for binding [94]. Thus, altered selection of mRNAs for translation

represents an intriguing target for novel clinical therapies that attempt to address the underlying molecular cause of DR.

In the present chapter, we evaluated the hypothesis that enhanced O-GlcNAcylation alters retinal gene expression. We used next-generation sequencing to evaluate changes in retinal mRNA abundances, and performed ribosome profiling to reveal which of those mRNAs were actually being translated into proteins (although this methodology cannot account for stalled ribosomes). This technique goes beyond more commonly used methods for assessing gene expression by isolating and sequencing nuclease-resistant 28-nucleotide ribosome protected mRNA fragment (RPFs). While a few genes exhibited altered mRNA abundances, the principal effect of enhanced O-GlcNAcylation on retinal gene expression was observed at the level of mRNA translation. Overall, the findings provide new insights into the impact of O-GlcNAcylation on retinal gene expression and identify a molecular network of translationally regulated mRNAs that potentially underlie dysfunctional mitochondrial respiration and superoxide production in diabetic retinopathy.

Results

O-GlcNAcase inhibition alters mRNA translation

To evaluate the effect of enhanced protein *O*-GlcNAcylation on retinal gene expression, mice were administered the O-GlcNAcase inhibitor TMG. Twenty-four hours later, global protein O-GlcNAcylation levels were enhanced in retina (Fig 3-1A). To evaluate the impact of TMG on gene expression we used next-generation sequencing to assess changes in retinal mRNA abundances and ribosome-bound mRNAs undergoing translation via RNAseq and RiboSeq, respectively (Fig 3-1B). Overall, sequencing reads in the total mRNA and RPF that was obtained

following nuclease digestion and ribosome isolation from whole retina were mapped to principal transcripts of 19,411 genes [See Reference [163]for electronic access to dataset]. For both TMG and PBS administration, replicates from two independent runs were highly similar in total mRNA abundance ($R^2 \geq 0.95$, Fig 3-S1A) and RPF ($R^2 \geq 0.95$, Fig 3-S1B).

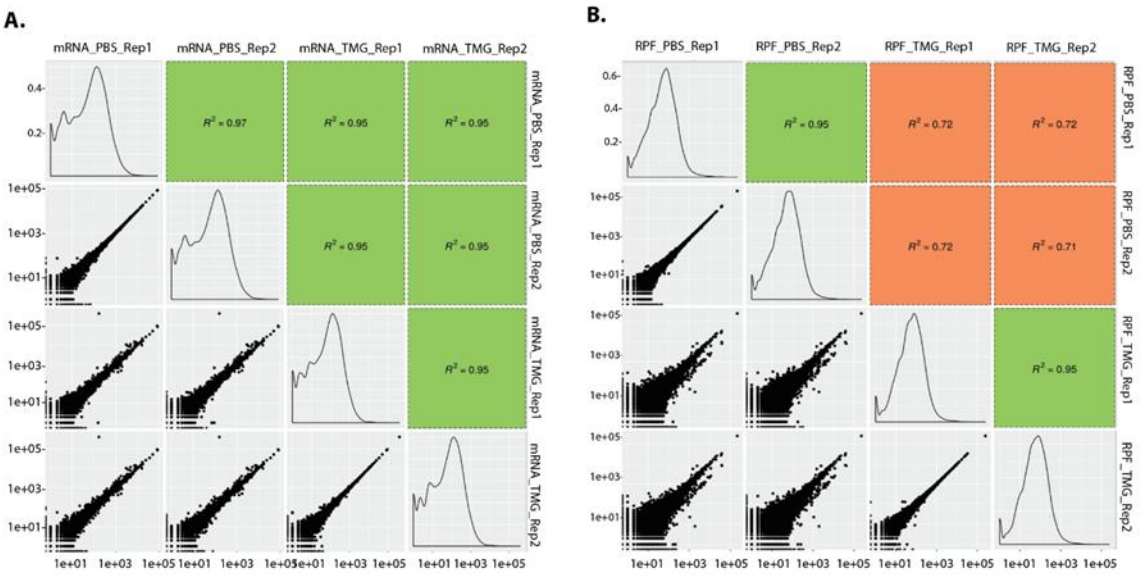

Figure 3-S1. *O*-GlcNAcase inhibition principally alters retinal mRNA translation. Mice were administered the *O*-GlcNAcase inhibitor Thiamet G (TMG) or PBS vehicle. Retinal gene expression changes were assessed in two independent runs by RNASeq in combination with RiboSeq to compare changes in retinal mRNA abundance (*A.*) and mRNA translation as assessed by mRNA in the nuclease resistant Ribosome Protected Fragment (RPF) (*B.*).

In response to TMG, the majority of transcripts observed in retina did not exhibit a change in total mRNA abundance or RPF. We observed minimal differences in mean mRNA abundances from the retina of PBS control versus TMG exposed mice (Fig 3-1C, R^2=0.96). In total, 148 retinal mRNAs exhibited a change in abundance 24 h after administration of TMG as compared to vehicle. Alternatively, the principal effect of TMG on retinal gene expression was observed at the level of mRNA translation (R^2=0.74, Fig 1D). Specifically, ~19% of the transcriptome showed significant changes in ribosome density, as 1683 mRNAs exhibited increased and 1912 mRNAs exhibited reduced ribosome association with TMG administration

(Fig 3-1E). To assess effects on mRNA translational efficiency (TE), we compared the relative RPF and total mRNA abundance observations between retinas of mice receiving TMG and vehicle (Fig 3-1F) using riborex package [147]. While the TE of most mRNAs was not different, 3185 mRNAs exhibited altered TE in the retina of mice receiving TMG as compared to vehicle (adjusted p-value ≤ 0.01). While 1360 mRNAs had enhanced TE, 1825 mRNAs had attenuated TE in the retinas of mice receiving TMG as compared to vehicle. For orthogonal validation, we performed polysome fractionation by sucrose density gradient centrifugation and analyzed mRNA distribution profiles. Actively translating mRNAs associate with multiple ribosomes to form heavy polysomes, whereas poorly translated mRNAs are associated with few or no ribosomes and localize to the sub-polysomal fraction. Consistent with the results of next-generation sequencing (Fig 3-2A), mRNAs encoding Nr6a1 (nuclear receptor subfamily 6 group A member 1) and Fam122a (family with sequence similarity 122A) dramatically shifted from the polysome fraction, such that they were almost exclusively observed in the sub-polysome fraction in the retinas of mice administered TMG (Fig 3-2B-D). In addition, mRNAs encoding Elmsan1 (ELM2 and Myb/SANT Domain Containing 1), Mettl14 (Methyltransferase Like 14), Nat8l (N-acetyltransferase 8 like), and IL1Rap (Interleukin 1 receptor accessory protein) exhibited shifts with polysome profiling that supported the results obtained from ribosome profiling (Fig 3-2D).

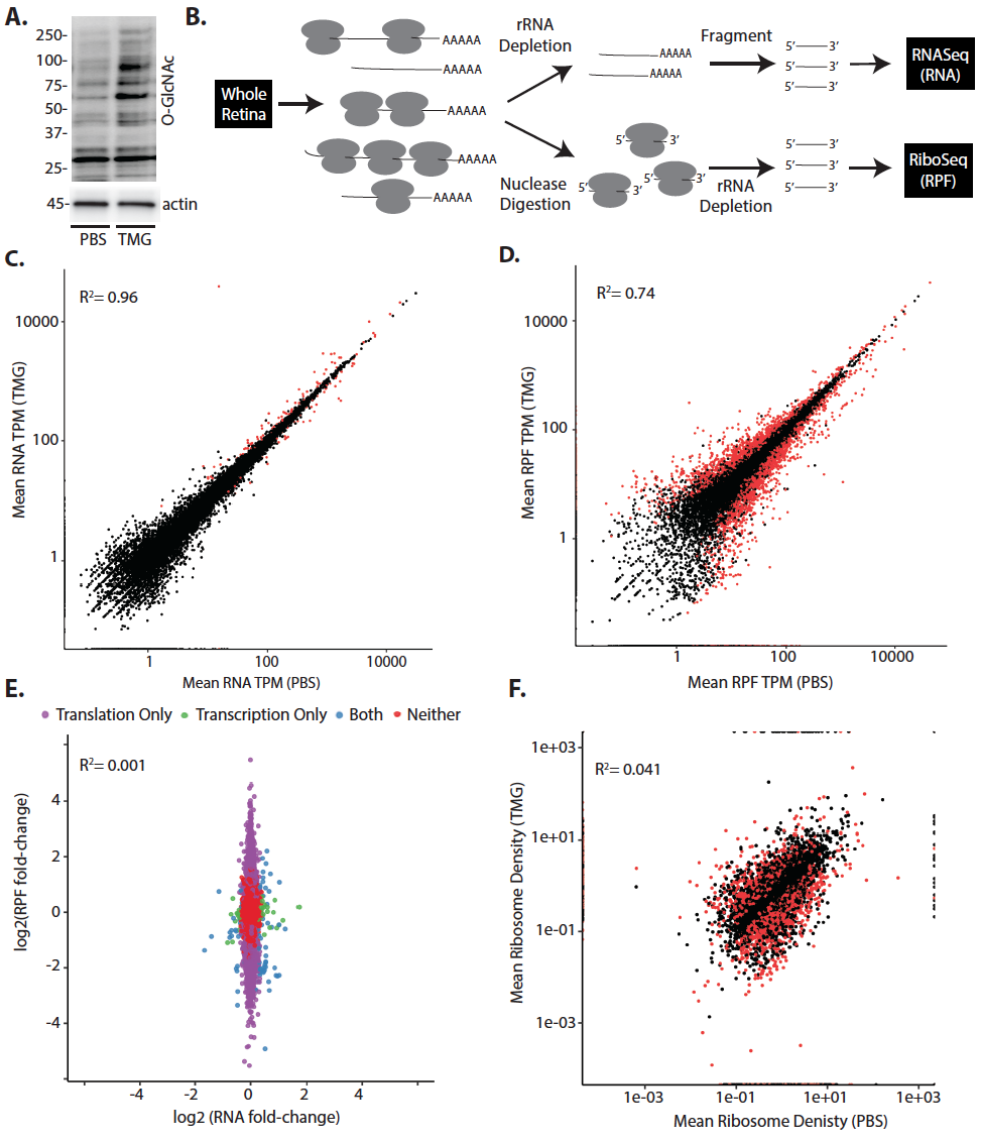

Figure 3-1. *O*-GlcNAcase inhibition alters the selection of mRNAs for translation in retina. Mice were administered the *O*-GlcNAcase inhibitor thiamet G (TMG) or PBS vehicle as a control. *A.* Total protein *O*-GlcNAcylation was assessed in retinal lysates by Western blot analysis 24 h after TMG administration. Protein molecular mass (kDa) is indicated at the *left* of blots. *B.* Workflow for analysis of retinal gene expression to assess changes in total mRNA abundance by RNAseq and nuclease resistant ribosome protected fragments (RPF) by RiboSeq. Retinal gene expression changes were assessed in two independent runs by RNASeq in combination with RiboSeq to compare mean variation in retinal mRNA abundance (*C.*) and mRNA translation (*D.*), respectively. *E.* Changes in mRNA abundance and mRNA translation following TMG administration were compared. Translational efficiency as assessed by mean ribosome density was compared in mice administered either TMG or PBS vehicle. In *C*, *D*, and *F*, significant differences (adjusted p-value ≤ 0.01) are indicated in red. In *E*, significant differences are indicated in purple (translation), green (transcription), or blue (both translation and transcription). TPM, transcripts per million mapped reads. Gene-specific fold-changes in RNA and footprint abundances were estimated using DESeq2 packages in R using default log-fold-change shrinkage options. Changes

in ribosome-densities (translation efficiencies) were estimated using the Riborex package in R. Unless otherwise specified, significant changes in RNA, RPF, and ribosome densities were estimated at an adjusted p-value < 0.01 (Benjamini & Hochberg adjusted p-value).

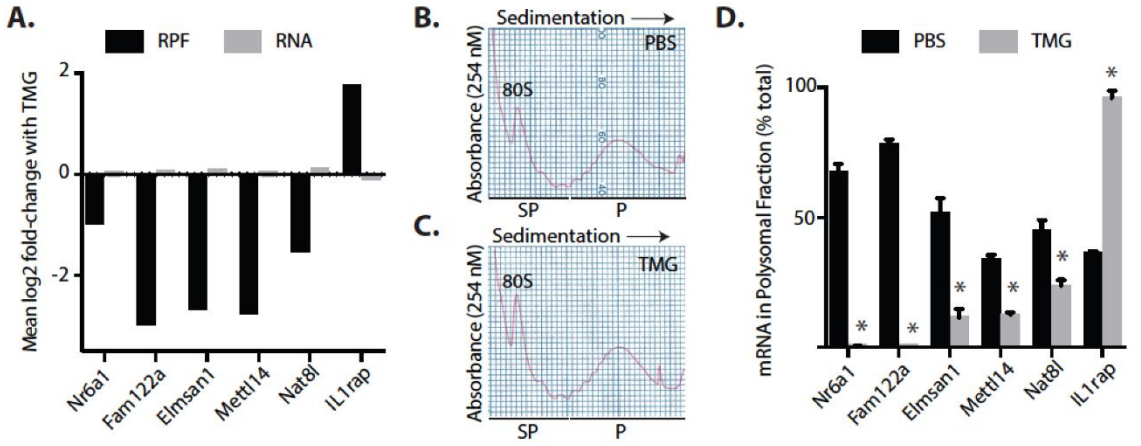

Figure 3-2. The effect of *O*-GlcNAcase inhibition on polysome association is consistent with sequencing analysis. Mice were administered TMG or PBS vehicle. *A.* Summary of results from sequencing analysis described in *Fig 1* for mRNAs encoding Nr6a1, Fam122a, Elmsan1, Mettl14, Nat8l, and Il1Rap. *B-D.* Ribosomes were separated into either sub-polysomal (SP) or polysomal (P) fractions via sucrose density gradient centrifugation. The distribution of mRNAs encoding Nr6a1, Fam122a, Elmsan1, Mettl14, Nat8l, and Il1Rap were assessed in SP or P fractions via RT-PCR. Results are expressed as a relative percentage of the mRNA in the P fraction and are representative of 2 independent experiments. Data were analyzed by unpaired t test. Values are means ± SE for three replicates assessing a pooled sample obtained from 10 retinas. *, represents $p<0.05$ versus PBS vehicle. RPF, ribosome protected fragment.

O-GlcNAcase inhibition alters the translation of mitochondrial proteins

To assess the potential impact of the observed gene expression changes, functional relationships between genes that exhibited altered TE in retina following O-GlcNAcase inhibition were investigated. The Top Canonical Pathways identified by IPA as being altered by TMG included acute phase response signaling, pattern recognition receptors, coagulation system, and LXR/RXR activation (Table 3-1). This analysis also identified toxicologic lists pathways associated with mitochondrial dysfunction and oxidative stress (Fig 3-S2). GO enrichment analysis showed our gene set to be enriched 1.66-fold for genes associated with the annotation mitochondrion organization and 1.55-fold for genes associated with the annotation mitochondrial

membrane (Table 3-2). Top-scoring mRNAs encoding mitochondrial proteins with TMG-induced changes in translation are listed in Fig 3-3A and Table 3-3.

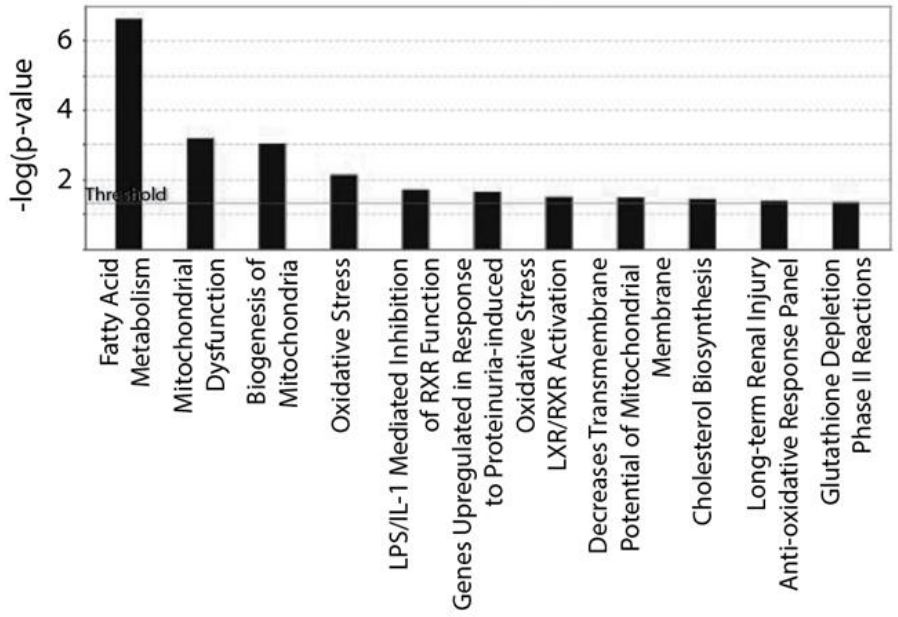

Figure 3-S2. *O*-GlcNAcase inhibition alters the translation of mRNAs encoding mitochondrial proteins. Ingenuity Pathway Analysis was used to identify functionally grouped gene sets and pathways for transcripts with altered mRNA translation in the retina following *O*-GlcNAcase inhbition.

O-GlcNAcase inhibition regulates translation of mitochondrial proteins via 4E-BP1

4E-BP-dependent translational control has been previously implicated in regulating the expression of mitochondria-related proteins [164]. Moreover, we previously demonstrated that elevated *O*-GlcNAcylation promotes sequestration of eIF4E by 4E-BP1 in cells in culture [159]. To determine if enhanced *O*-GlcNAcylation had a similar effect in retina, we performed immunoprecipitation of eIF4E from retinal lysates. Retinas from mice administered TMG exhibited enhanced interaction of 4E-BP1 and reduced interaction of eIF4G with eIF4E (Fig 3-3B-D). We previously demonstrated that hyperglycemia promotes 4E-BP1 *O*-GlcNAcylation and alters the translation of specific mRNAs in a manner that is dependent on 4E-BP1 [94]. To

evaluate the role of 4E-BP1 *O*-GlcNAcylation in regulating the translation of mRNAs encoding mitochondrial proteins, wild-type and 4E-BP1/2 knockout mice were administered TMG. In the retina of both wild-type and 4E-BP1/2-deficient mice, TMG enhanced global protein *O*-GlcNAcylation (Fig 3-3E). Consistent with Fig 3B-D, TMG promoted 4E-BP1 co-immunoprecipitation with eIF4E in the retina of wild-type mice; whereas the protein could not be detected in 4E-BP1/2-deficient mice (Fig 3-3E-F). Next-generation sequencing demonstrated down-regulated translation of mRNAs encoding the mitochondrial proteins Tufm (Tu translation elongation factor, mitochondrial), Mrpl47 (mitochondrial ribosomal protein L47), and SOD2 (superoxide dismutase 2) in the retina of wild-type mice with enhanced protein *O*-GlcNAcylation (Fig 3-3A, Table S1). In polysome profiles, Tufm and Mrpl47 were observed in the polysomal fraction obtained from the retina of wild-type mice receiving PBS (Fig 3-3G & H, respectively). TMG caused both mRNAs to shift almost exclusively into the sub-polysomal fraction. In the

retina of 4E-BP1/2 deficient mice, the ratio of Tufm and Mrpl47 observed in the polysomal fraction was similar with PBS and TMG administration. Similarly, the mRNA encoding SOD2

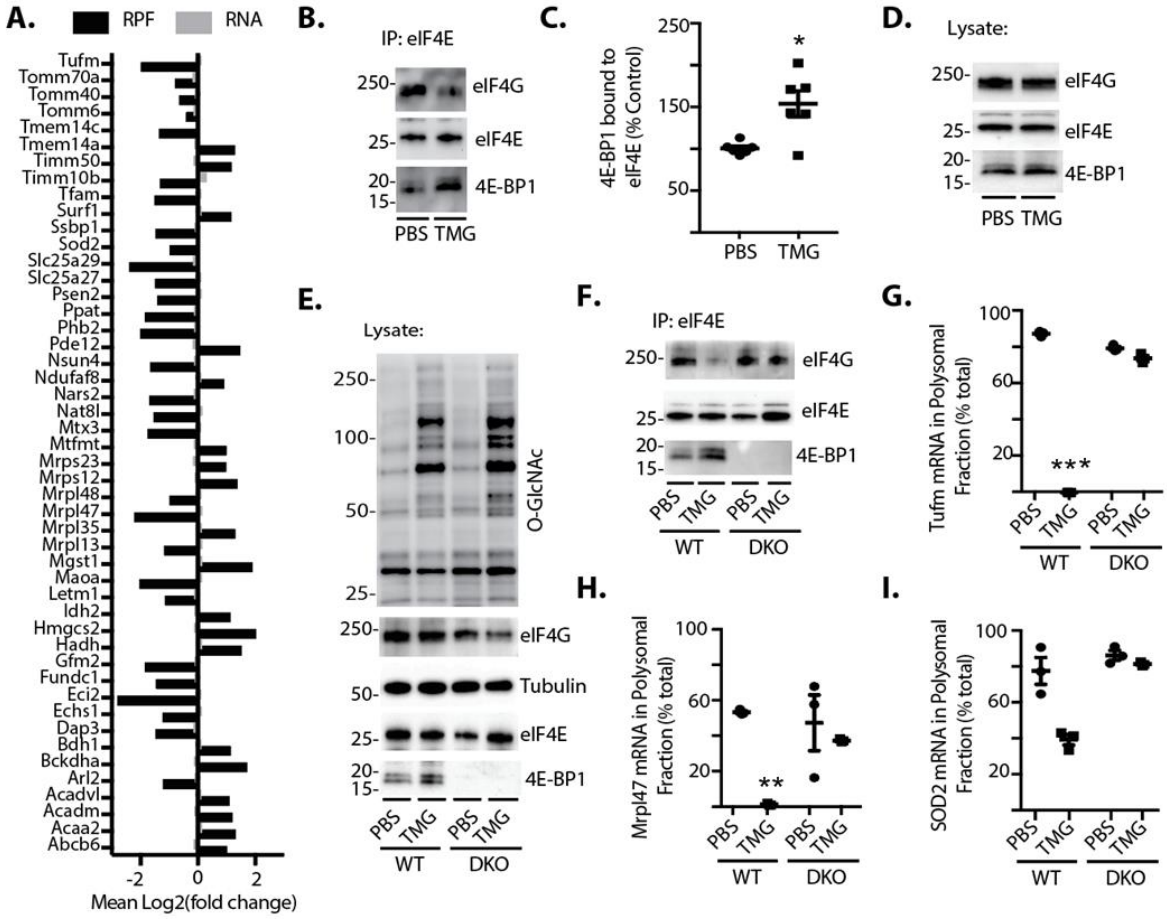

Figure 3-3. *O*-GlcNAcase inhibition alters the translation of mRNAs encoding mitochondrial proteins in a 4E-BP1/2-dependent manner. Mice were administered TMG or PBS vehicle. *A.* The sequencing analysis described in *Fig 1* identified TMG-induced changes in translation of mRNAs encoding mitochondrial proteins. *B.* The interaction of 4E-BP1 and eIF4G with eIF4E was examined by immunoprecipitating eIF4E from retinal supernatants and measuring the amount of eIF4G and 4E-BP1 in the immunoprecipitate (IP) by Western blot analysis. Protein molecular mass (kDa) is indicated at the *left* of blots. *C.* The interaction of 4E-BP1 with eIF4E in *B.* was quantified and analyzed via an unpaired t-test. *D.* Western blot analysis was used to evaluate eIF4G, eIF4E, and 4E-BP1 protein expression in retinal lysates. *E-I.* Wild-type (WT) and 4E-BP1/2 double knockout (DKO) mice were administered TMG or PBS vehicle as previsouly described. *E.* Retinal protein *O*-GlcNAcylation, as well as eIF4G, tubulin, eIF4E, and 4E-BP1 protein expression, were assessed by Western blot analysis. *F.* The interaction of 4E-BP1 and eIF4G with eIF4E was examined as described in *B. G-I.* Ribosomes from the retinas of WT and DKO mice administered either TMG or PBS vehicle were separated into either sub-polysomal or polysomal fractions as described in *Fig 2.* The distribution of mRNAs encoding the mitochondrial proteins TufM (*G.*), Mrpl47 (*H.*) and SOD2 (*I.*) were assessed in sub-polysomal and polysomal fractions via RT-PCR. Data in *G-I* were analyzed by two-way ANOVA with Dunnett's post-hoc analysis. Results are

expressed as a relative percentage of the mRNA in the polysomal fraction and are representative of 2 independent experiments. Values are means ± SE for three replicates assessing a pooled sample obtained from 10 retinas. *, p<0.05 *versus* PBS; **, p<0.01 *versus* WT PBS; ***, p<0.001 *versus* WT PBS.

trended towards shifting out of the polysomal fraction with enhanced *O*-GlcNAcylation in wild-type mice, but a similar effect was not observed in mice deficient for 4E-BP1/2 (Fig 3-3I). There was a significant interaction detected by two-way ANOVA between TMG exposure and genotype on distribution of Mrpl47 (p=0.0389) and Sod2 (p=0.0068) mRNA in polysomal fractions. Though the distribution of Sod2 mRNA was trending towards shifting out of the polysomal fraction, no significant TMG effect was detected by two-way ANOVA (p=0.0857).

O-GlcNAcase inhibition promotes mitochondrial ROS via 4E-BP1

To determine if increased *O*-GlcNAcylation could affect mitochondrial respiration in a manner that is dependent on 4E-BP1, cultures of wild-type and 4E-BP1/2-deficient mouse embryonic fibroblasts (MEF) were exposed to TMG. In both wild-type and 4E-BP1/2-deficient MEF, exposure to TMG enhanced protein *O*-GlcNAcylation (Fig 3-4A) and altered cellular respiration (Fig 3-4B). TMG did not significantly increase basal oxygen consumption rate (OCR; p=0.0704) (Fig 3-4C), but did significantly increase maximal OCR (Fig 3-4D) and ATP production (Fig 3-4E) in both wild-type and 4E-BP1/2-deficient MEF. In two-way ANOVA analysis, effect of TMG exposure and presence of 4E-BP1/2 were significant for maximal OCR (p<0.0001) and ATP production (p<0.0001 and p=0.0031, TMG exposure and presence of 4E-BP1 respectively). There were no signifcant interaction effects between genotype and TMG exposure on basal OCR, maximal OCR, or ATP production. While TMG enhanced cellular respiration in both wild-type and 4E-BP1/2-deficient cells, maximal OCR in 4E-BP1/2-deficient MEF in both the presence and absence of TMG was attenuated as compared to wild-type (Fig 3-

4D). In addition to changes in oxidative phosphorylation, mitochondrial dysfunction can also involve the generation of ROS. To determine if TMG altered cellular ROS production, we assessed mitochondrial superoxide. Superoxide levels were similar in vehicle treated wild-type and 4E-BP1/2-deficient MEF cultures (Fig 3-4F-G). In two-way ANOVA analysis, effect of TMG exposure and presence of 4E-BP1/2 were significant ($p=0.0319$ and $p=0.0001$, respectively). There was also a signifcant interaction effect between genotype and TMG exposure ($p=0.0062$) upon superoxide levels. TMG exposure increased superoxide in wild-type MEF. However, the effect of TMG was absent in 4EBP1/2-deficient MEF, as superoxide levels were similar to those observed in WT MEF exposed to vehicle alone. This supports that acute elevations in *O*-GlcNAcylation promote mitochondrial superoxide levels via a 4E-BP1/2-dependent mechanism.

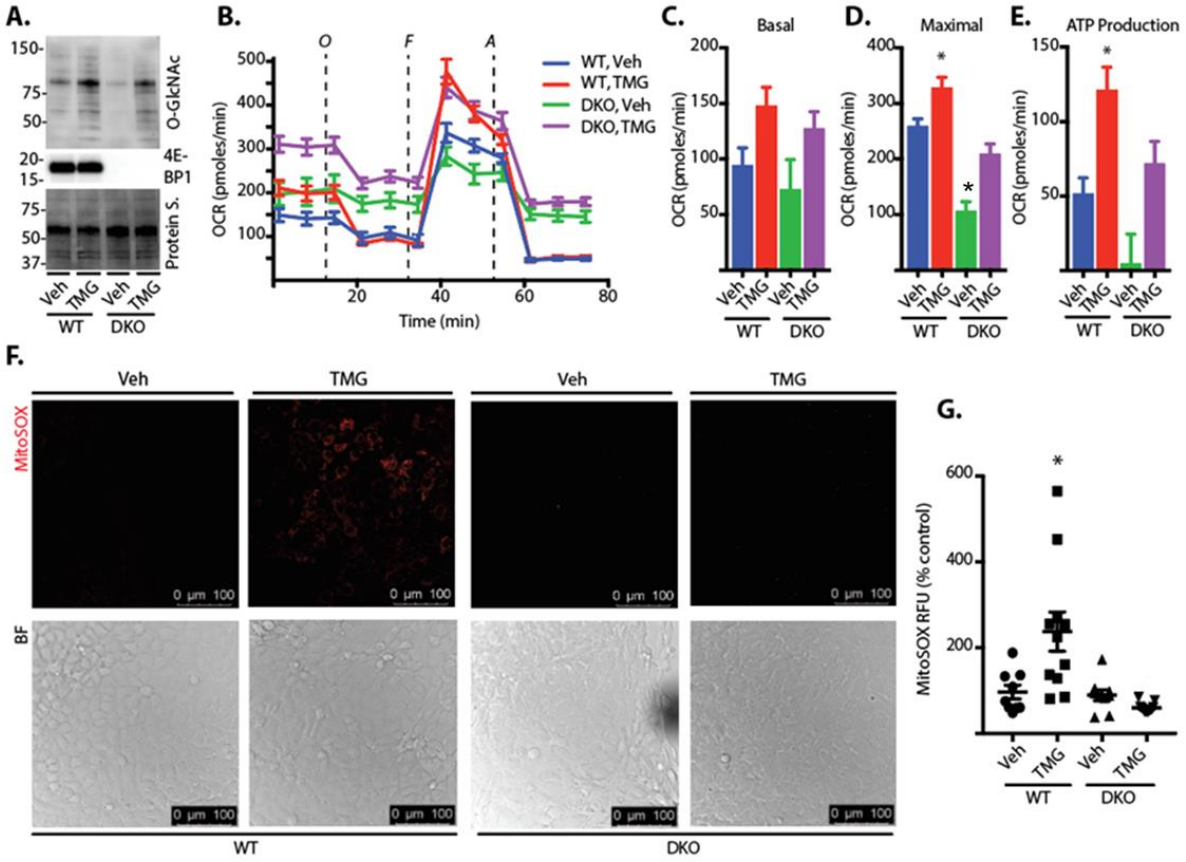

Figure 3-4. *O*-GlcNAcase inhibition promotes mitochondrial ROS via 4E-BP1. Wild-type (WT) and 4E-BP1/2 doube knockout (DKO) mouse embryonic fibroblasts were cultured in the presence of TMG or vehicle (Veh) for 24 h. *A.* Protein *O*-GlcNAcylation and 4E-BP1 expression were assessed by Western blot analysis. Protein Staining (Protein S.) is shown as a loading control. Protein molecular mass (kDa) is indicated at the *left* of blots. *B.* Mitochondrial respiration was assessed by Seahorse XF Cell Mitochondrial Stress Test. Basal respiration (*C.*), maximal respiration (*D.*), and ATP production (*E.*) were compared. *C-E.* Data were analyzed by two-way ANOVA with Dunnet's post-hoc analysis. *F-G.* Mitochondrial superoxide was assessed in live cells using MitoSOX Red superoxide indicator. MitoSOX fluorescence was visualized by confocal laser microscopy (*F.*) and quantified and analyzed via two-way ANOVA with post-hoc analysis by Dunnet's multiple comparison test (*G.*) Results are representative of three experiments. Within each experiment 2-3 independent samples were analyzed. Values are means ± SE. *, $p<0.05$ versus Veh. OCR, oxygen consumption rate; RFU, relative fluorescent units.

To further investigate the role of 4E-BP1 in *O*-GlcNAcylation-induced mitochondrial superoxide levels, we restored 4E-BP1 expression in 4E-BP1/2-deficient MEF in culture (Fig 3-5A). TMG enhanced mitochondrial superoxide in cells expressing wild-type 4E-BP1 (Fig 3-5A-

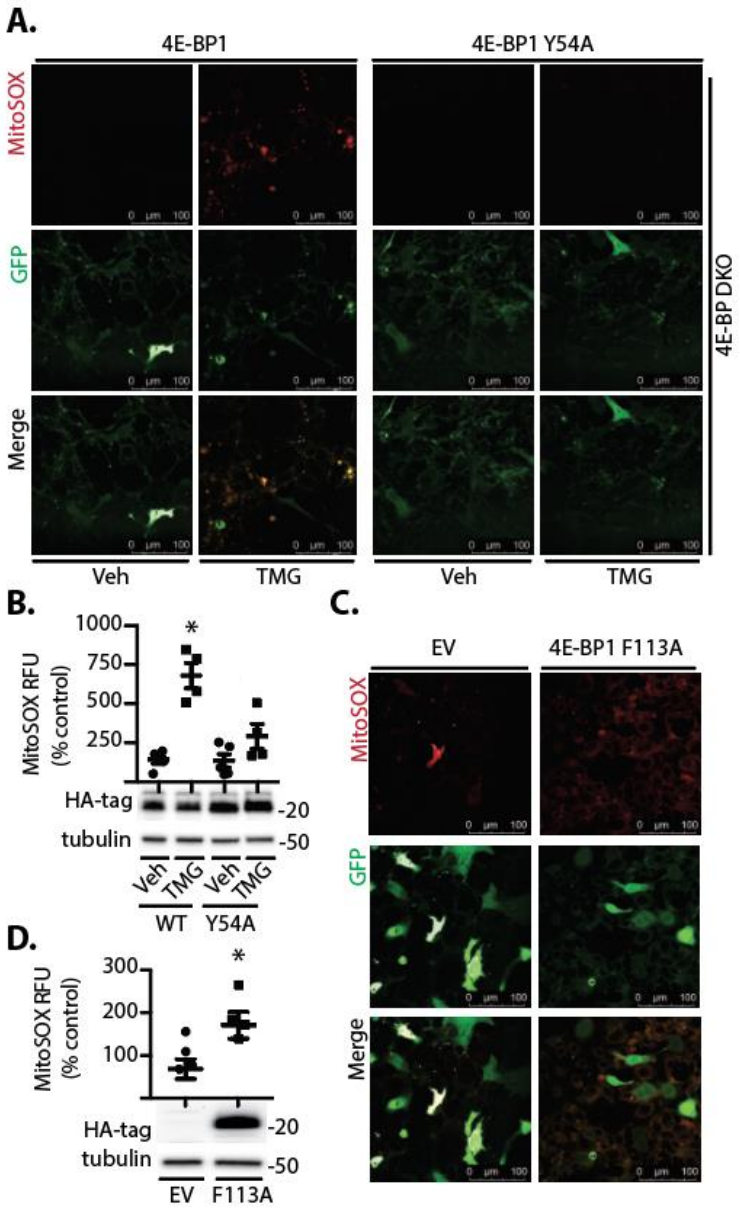

Figure 3-5. 4E-BP1 regulates mitochondrial superoxide levels. *Figure legend on next page.*

Figure. 3-5. *A-B.* Wild-type (WT) or 4E-BP1/2 double knockout (4E-BP DKO) mouse embryonic fibroblasts were cultured in the presence of TMG or vehicle (Veh) for 24 h. Cells were co-transfected with plasmids that express GFP and either a wild-type 4E-BP1 or a 4E-BP1 variant (Y54A) that is deficient in binding to eIF4E. *C-D.* Wild-type cells were co-transfected with plasmids that express GFP and either an empty vector (EV) control or a plasmid that expresses a 4E-BP1 F113A variant that is unable to be phosphorylated by mTORC1 resulting in constituitive eIF4E binding. MitoSOX fluoresence and GFP expression were visualized by confocal laser microscopy (*A. & C.*) and relative MitoSOX fluoresence was quantified (*B. & D.*). Data were analyzed via two-way ANOVA with multiple comparisons conducted by Dunnett's post-hoc analysis (*B.*) or one-way ANOVA with Tukey's post-hoc analysis(*D.*). Values are means ± SE. Results are representative of two experiments. Within each experiment 2-3 independent samples were analyzed. *, $p<0.05$ versus WT Veh or EV. RFU, relative fluorescent units.

B). However, in cells expressing a 4E-BP1 variant (Y54A) that is deficient in binding to eIF4E [165], TMG did not enhance mitochondrial superoxide levels (Fig 3-5A-B). In two-way ANOVA analysis, the effect of TMG exposure or Y54A expression on MitoSox intensity was significant ($p<0.0001$ and $p=0.0038$, respectively). There was also a significant interaction between TMG exposure and Y54A expression ($p=0.0049$). Expression of a 4E-BP1 variant with an F113A substition that prevents mTORC1-dependent phosphorylation and promotes eIF4E binding [166] was sufficient to enhance mitochondrial superoxide levels in wild-type MEF (Fig 3-5C-D).

4E-BP1/2 deletion prevents O-GlcNAc- and diabetes-induced ROS in retina

To evaluate the role of 4E-BP1 in the effect of *O*-GlcNAcyaltion on retina, wild-type and 4E-BP1/2-deficient mice were administered TMG. Retinal cryosections were exposed to the fluorescent ROS indicator 2,7-dichlorofluoroscein (DCF) to evaluate oxidative stress. In the retina of wild-type mice, TMG administration enhanced DCF fluorescence as compared to vehicle (Fig 3-6A-B). Enhanced ROS levels were most obvious in the photoreceptor layers but could also be observed throughout the entire retina. DCF fluorescence was similar in the retina of wild-type and 4E-BP1/2-deficient mice receiving vehicle. Moreover, ROS levels were similar in the retina of 4E-BP1/2-deficeint mice administered either PBS or TMG. Importantly, ROS levels

were reduced in 4E-BP1/2-deficeint mice administered TMG as compared to wild-type controls administered TMG. There were significant effects on DCF intensity from both TMG administration and expression of 4E-BP1/2 as detected by two-way ANOVA ($p=0.01$ and $p=0.0058$, respectively). There was no significant interaction between TMG administration and expression of 4E-BP1/2 ($p=0.3403$).We previously demonstrated that 4E-BP1 *O*-GlcNAcylation was enhanced in the retina of STZ-induced diabetic mice [95]. Consistent with previous reports [e.g. [167]], STZ-induced diabetes enhanced DCF fluorescence in the retina of wild-type mice as compared to non-diabetic controls (Fig 3-6C-D). In non-diabetic 4E-BP1/2-deficient mice, DCF fluorescence was similar to that observed in diabetic 4E-BP1/2-deficient mice. Moreover, ROS levels were reduced in diabetic 4E-BP1/2-deficient mice as compared to diabetic wild-type mice. Overall, the results support a model wherein diabetes-induced 4E-BP1 *O*-GlcNAcylation alters mRNA translation in a manner that causes mitochondrial oxidative stress in retina. There were significant effects on DCF intensity from both diabetes and expression of 4E-BP1/2 as detected by two-way ANOVA ($p=0.0181$ and $p=0.0069$, respectively). There was no significant interaction between diabetes and expression of 4E-BP1/2 ($p=0.1617$).

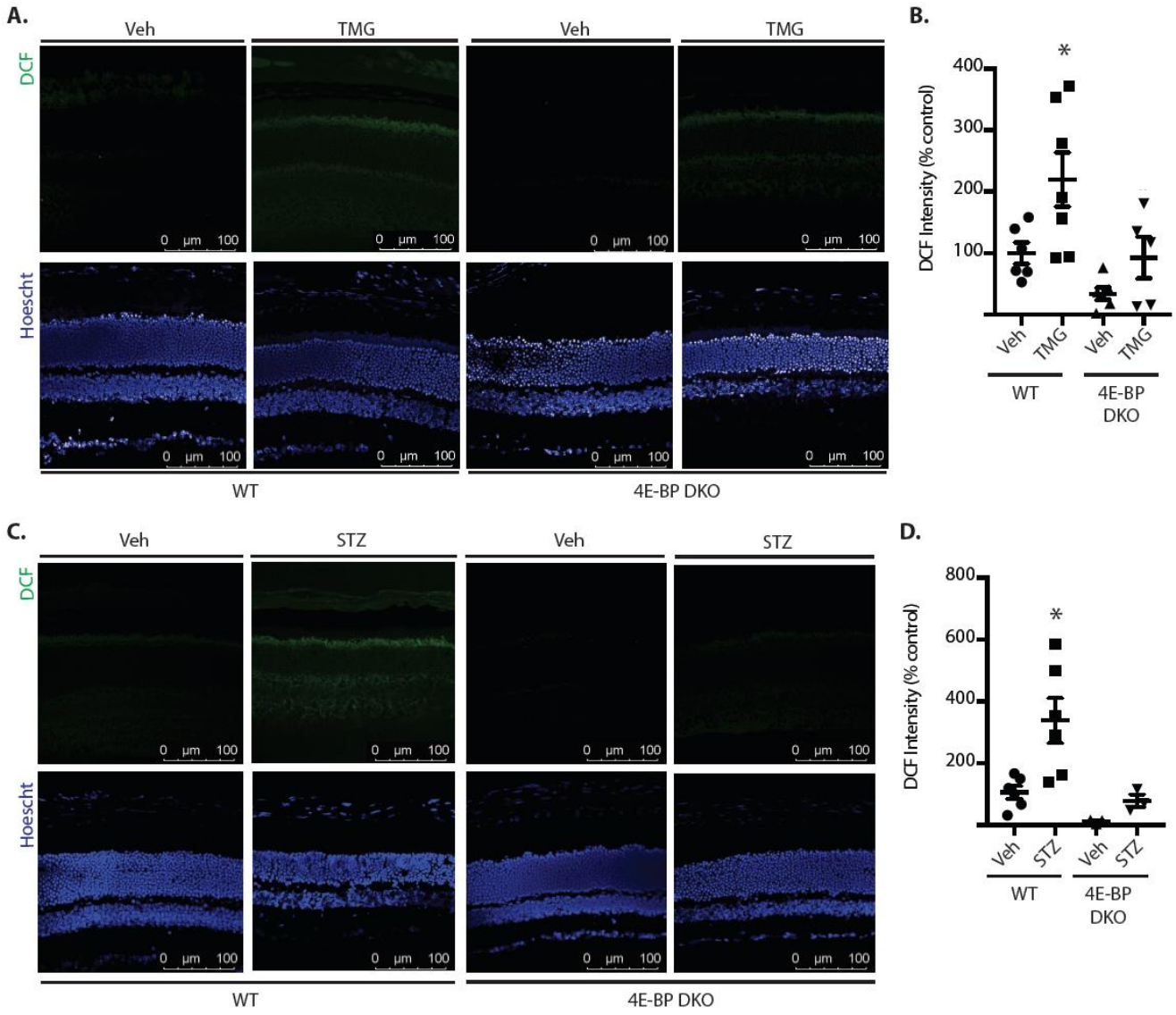

Figure 3-6. 4E-BP1/2 deletion prevents O-GlcNAcyaltion- and diabetes-induced ROS in retina. *A-B.* Wild-type (WT) and 4E-BP1/2 doube knockout (4E-BP DKO) mice were administered TMG or vehicle (Veh) as previsouly described. *C-D*. Diabetes was induced in WT and 4E-BP DKO mice by administration of streptozotocin (STZ). Non-diabetic controls were administered vehicle (Veh). Whole eyes were isolated, cryosectioned into sagittally-oriented longitudinal cross sections, stained with Hoechst, and exposed to 2,7-dichlorofluoroscein (DCF). Retinas were evaluated 24 h after TMG administration (*A-B.*) or after 4 weeks of diabetes (*C-D.*). DCF fluorescence and nuclear staining were evaluated by confocal laser microscopy (*A. & C.*) and relative DCF fluoresence was quantified (*B. & D.*). Data were analyzed via two-way ANOVA with Dunnett's post-hoc analysis. Results are representative of two experiments (n = 3-6). *, $p<0.05$ versus WT Veh.

Discussion

One potential mechanism whereby dysregulated O-GlcNAcylation contributes to diabetic retinopathy is by altering retinal gene expression, as numerous regulatory factors involved in gene transcription and mRNA translation are modified by O-GlcNAc. Thus, the present chapter investigated the impact of O-GlcNAcylation on retinal gene expression. Assessment of retinal gene expression by deep sequencing demonstrated that TMG altered translation of a molecular network of mRNAs associated with mitochondrial function and oxidative stress. Overall, the findings support a model whereby O-GlcNAcylation enhances cellular respiration and mitochondrial superoxide production.

Gene expression is the sum of events that regulate cellular protein concentrations, including transcription, translation, as well as mRNA and protein degradation. Historically, gene expression studies have utilized techniques such as microarrays, and more recently RNAseq, to assess changes in mRNA abundances. However, mRNA abundances are a relatively poor correlate for protein expression [168, 169] and some studies suggest that they only account for ~40% of the global variation in protein expression [170, 171]. Translational control facilitates the selective recruitment of ribosomes to specific mRNAs to provide a rapid and reversible response in expression of specific proteins to changes in nutrient supply, hormones, and stress [172, 173]. Thus, an assessment of ribosome protected mRNA fragments accounts for both transcriptional and translational changes that lead to variation in protein expression. Previous studies from our laboratory, demonstrate that hyperglycemic conditions alter the selection of mRNAs for translation [142]. In the present chapter, we performed genome-wide, quantitative analysis of *in vivo* translation in the retina in combination with RNAseq to assess changes in retinal gene expression. This technique utilized nuclease footprinting to produce mRNA fragments that indicate which mRNAs were associated with ribosomes. The effect of O-GlcNAcase inhibition

on retinal gene expression was largely observed at the level of mRNA translation. Remarkably, only a few genes exhibited changes in mRNA abundance (<1% of the observed transcripts) following TMG administration. However, ~19% of the transcriptome exhibited altered mRNA translation. The extremely limited transcriptional effect of O-GlcNAcase inhibition on retinal gene expression was surprising, as the activity of a number of transcription factors are regulated by O-GlcNAcylation [174]. An important caveat is that retinal gene expression was assessed 24 h after administration of the O-GlcNAcase inhibitor, and thus transcriptional effects on gene expression may be more obvious after prolonged disruption of O-GlcNAc cycling. Another important consideration of the present analysis is that the contribution of protein degradation to gene expression has not been considered. Protein concentrations in a cell are determined by the relative rates of synthesis and degradation. Enhanced rates of retinal protein degradation have been observed in diabetic rodents [160]; however, when compared to rates of synthesis, the impact of protein stability on gene expression is relatively minor [170].

In the present study, changes in ribosome density were interpreted as reflecting changes in mRNA translation. While this is a common assumption in the field, it is only accurate if there are no systemic pauses or stalls of ribosomes on transcripts. To ensure that the effects of O-GlcNAcase inhibition on ribosome density were not due to pausing/stalls, polarity scores [175] were generated to determine if TMG skewed ribosome denisty toward the 5′- or 3′-ends of mRNA. Importantly, there were no significant changes in polarity scores between the two treatments (Wilcoxon signed rank test with continuity correction, $p = 0.09$, Fig 3-S3), indicating that the large-scale effect of TMG on mRNA translation was due to changes in initiation rates.

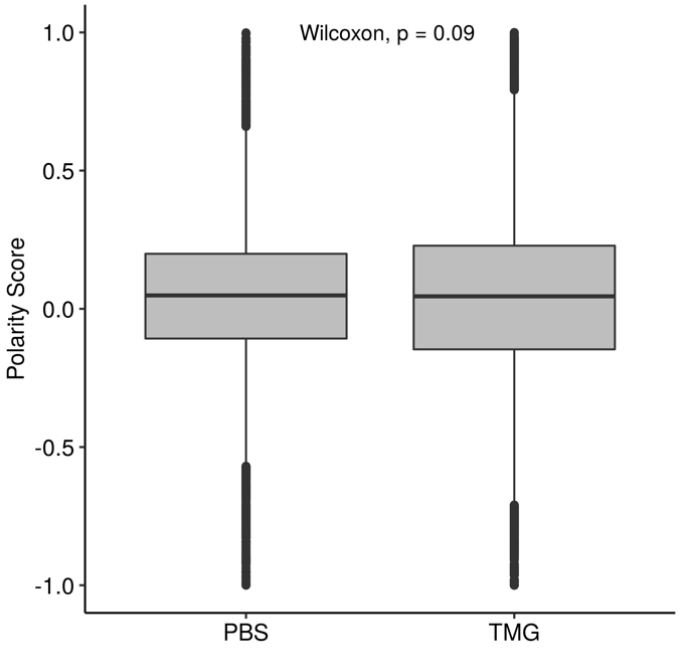

Figure 3-S3. *O*-GlcNAcase inhibition does not alter the location of ribosomes on mRNA transcripts. Mice were administered the *O*-GlcNAcase inhibitor Thiamet G (TMG) or PBS vehicle. Retinal gene expression changes were assessed by RiboSeq to compare changes in ribosome density. To determine if TMG skewed ribosome denisty toward the 5′- or 3′-ends of transcripts, ribosome positions were quantified by estimating polarity scores. This metric assigns a value between -1 and +1 to each gene based on the distribution of sequencing reads along the transcript.

One of the best-characterized mechanisms for regulating translation initiation involves 4E-BP1 binding to eIF4E to prevent eIF4F complex assembly at the 5′-end of an mRNA. We initially discovered that 4E-BP1 was directly modified by O-GlcNAcylation in the liver of diabetic rats [159]. A variety of conditions that increase O-GlcNAc levels (e.g. hyperglycemia, O-GlcNAcase inhibition, or glucosamine addition to culture medium) promote binding of 4E-BP1 with eIF4E [94, 95, 159]. Furthermore, 4E-BP1 O-GlcNAcylation inhibits its degradation via an E3 ubiquitin ligase complex containing CUL3. Specifically, we have provided evidence for a model wherein O-GlcNAcylation and GSK3-dependent phosphorylation competitively modify 4E-BP1 at T82/S86 [95]. Of importance to the work presented in this chapter, we previously

reported that 4E-BP1 O-GlcNAcylation [95] and binding to eIF4E [97] are enhanced in the retina of diabetic rodents. Herein, we found that in the retina of mice receiving TMG, O-GlcNAcylation levels were enhanced concomitant with an increase in the co-immunoprecipitation of 4E-BP1 with eIF4E.

TMG-induced O-GlcNAcylation altered the translation of mRNAs encoding numerous mitochondrial proteins, including those involved in oxidative phosphorylation (OXPhos), mitochondrial ribosomal subunits, mitochondria-specific tRNA synthetases, and subunits of the TIM/TOM translocase complex. Importantly, we demonstrated that 4E-BP1/2 were critical in mediating the effects of O-GlcNAcylation on translation of specific mRNAs encoding mitochondrial proteins and mitochondrial ROS production. This observation supports previous reports implicating 4E-BP-dependent translational control in the regulation of mitochondrial function [164, 176]. The mitochondrial electron transport chain compromises ~150 distinct proteins, including 13 hydrophobic inner membrane proteins that are encoded by the mitochondrial DNA (mtDNA) and synthesized by mitochondrial ribosomes (mitoribosomes). Alternatively, the remaining majority of OXPhos proteins are synthesized by cytosolic ribosomes and imported by the TIM/TOM complex. Proper mitochondrial function requires rapid adaptation to metabolic conditions, and involves coordinated expression from both the mtDNA and nuclear genome. Yeast ribosome profiling demonstrates that nuclear- and mitochondrial-encoded OxPhos mRNA abundances are not altered in concordance following a nutrient shift, but rather synchronized protein expression is achieved via translational control [177]. Thus it is likely that defects in mRNA translation would contribute to human pathology, as there are a variety of mitochondrial diseases that result from improper mitochondrial protein expression [reviewed in [178]].

In recent years, O-GlcNAcylation has emerged as a critical regulator of mitochondrial function [179, 180]. Overexpression of the enzymes responsible for O-GlcNAc

modification (i.e., OGT and OGA) alters mitochondrial protein levels, including specific proteins involved in OXPhos [179]. Moreover, cells with elevated O-GlcNAc levels exhibit abnormal mitochondrial morphology and hyperpolarization [180]. Numerous mitochondrial proteins are post-translationally modified by O-GlcNAcylation directly in response to diabetes and hyperglycemic conditions [181, 182]. Tan *et al* [180] have previously suggested that mitochondria undergo a two-stage adaptive process in response to O-GlcNAcase inhibition. Initially, mitochondrial proteins are O-GlcNAcylated, resulting in increased cellular respiration and enhanced ROS production [183]. However, with sustained elevation in O-GlcNAcylation, mitochondria undergo transcriptional reprogramming as ATP production and ROS levels decline [180]. Consistent with the previous studies, we observed increased cellular respiration and elevated mitochondrial superoxide levels in cells after 24 h of exposure to culture medium containing TMG. The present study extends on these previous reports by demonstrating the synthesis of mitochondrial proteins is dramatically altered by enhanced O-GlcNAcylation in response to TMG-induced O-GlcNAcase inhbition. Whereas the effect of TMG on cellular respiration was observed in 4E-BP1/2 deficient cells, TMG-induced mitochondrial superoxide was absent in cells lacking 4E-BP1/2. This observation supports a role for 4E-BP1/2-dependent translational control in increased ROS production during the first stage of the adaptive process that is initiated upon disruption of O-GlcNAc cycling.

The retina is among the most metabolically active tissues in the body, and therefore is heavily dependent on a constant supply of energy from oxidative phosphorylation in the mitochondria. However, in diabetes, retinal mitochondria contain damaged mtDNA [184] in association with increased capillary cell apoptosis, an abnormality that occurs prior to the onset of histopathological changes in the retina [185]. The dynamic nature of mitochondria necessitates tight regulation of the organelle's shape, size, formation of cristae, and transport of molecules across the mitochondrial membranes [186]. In retinas of diabetic rats, this tight control is

impaired as mitochondrial ultrastructure is disrupted [187], and the enzymes required for repairing damaged retinal mtDNA fail to access the mitochondria, despite an increase in their mRNA levels [184]. Furthermore, expression of small molecule transport proteins involved in the exchange of citric acid cycle substrates, as well as transport of antioxidant molecules into the mitochondria, are less abundant in the mitochondria of diabetic rats and diabetic donor eyes [187]. Similarly, we report in our data set a TMG-induced decrease in translation of the outer membrane translocase complex proteins Tomm6, Tomm40, Tomm70a, the mitochondrial amino acid transporter Slc25a29, and mitochondrial protein transporter Metaxin3. These findings are consistent with previous reports that suggest diabetes-induced impairment in mitochondrial transport machinery [e.g. [187]].

Hyperglycemic conditions provide an abundance of substrate for glucose oxidation, leading to increased electron transport chain flux and a higher voltage gradient across the mitochondrial membrane [188, 189]. When a critical threshold is reached, electron transfer inside complex III of the electron transport chain is obstructed, giving way to accumulation of electrons at Coenzyme Q and the formation of superoxide [37, 190]. Studies have shown this to be problematic in diabetic retinopathy, as retinal mitochondrial superoxide levels are elevated in diabetic rodents [191] while the activities of the superoxide scavenging SOD2 (aka MnSOD) and Complex III of the electron transport chain are attenuated [191, 192]. Overproduction of superoxides by mitochondria links the principle pathways, such as HBP, resopnsible for hyperglycemia-induced tissue damage [189]. Notably, long-term administration of antioxidants inhibits the development of retinopathy in diabetic rats [193] as does overexpression of SOD2 [194]. In the retina of mice administered TMG, SOD2 mRNA translation was attenuated as compared to controls. However, in the retina of 4E-BP1/2-deficient mice administered TMG, relative SOD2 mRNA translation was similar to that observed in 4E-BP1/2-deficient and wild-type controls administered vehicle alone. Thus, 4E-BP1 is necessary for the repressive effect of

O-GlcNAcylation on SOD2 mRNA translation. ROS levels were elevated in the retina of diabetic wild-type mice or non-diabetic mice administered TMG. Moreover, 4E-BP1/2 deletion was sufficeint to normalize ROS levels in the retina of both diabetic mice, as well as those administered TMG to enhance O-GlcNAcylation.

The studies herein provide new evidence that O-GlcNAcylation regulates mitochondrial function in retina. We report that enhanced O-GlcNAcylation alters retinal gene expression by principally acting at the level of mRNA translation. We provide evidence that the effect of O-GlcNAcylation on translation of specific mitochondrial mRNAs is dependent on 4E-BP1/2 and provide functional evidence that O-GlcNAcylation enhances ROS levels in retina in a 4E-BP1/2-dependent manner. Overall, the findings are consistent with a model wherein diabetes-induced *O*-GlcNAcylation acts to promote oxidative stress in retina by altering the selection of mRNAs for translation. Due to the critical role oxidative stress plays in the development of diabetic retinopathy, pharmacological targeting of O-GlcNAcylation or 4E-BP1 binding to eIF4E may represent novel targets for therapeutic intervention.

Table 3-1: IPA of Translational Efficiency (TE) changes in the retina of mice treated with the O-GlcNAcase inhibitor TMG to promote protein O-GlcNAcylation

	p-value	Overlap
Top Canonical Pathways		
Acute Phase Response Signaling	2.44E-07	23.9% 42/176
Role of Pattern Recognition Receptors in Recognition of Bacteria and Viruses	6.20E-07	25.2% 35/139
Coagulation System	8.05E-07	42.9% 15/35
LXR/RXR Activation	1.79E-06	25.6% 31/121
Role of Osteoblasts, Osteoclasts and Chondrocytes in Rheumatoid Arthritis	1.92E-06	20.9% 49/235

Table 3-2: GO analysis of Translational Efficiency (TE) changes in the retina of mice treated with the O-GlcNAcase inhibitor TMG to promote protein O-GlcNAcylation

	Number	Expected	Fold Enrichment	P value
GO Biological Process				
retina development in camera-type eye	55	21	2.61	1.87E-04
eye morphogenesis	49	22	2.22	4.88E-02
visual perception	65	31.38	2.07	1.11E-02
protein localization to membrane	121	70.97	1.7	4.28E-03
mitochondrion organization	110	66.34	1.66	4.35E-02
neuron projection development	157	98.17	1.6	2.72E-03
GO Molecular Function				
protein domain specific binding	170	105.04	1.62	1.30E-04
inorganic molecular entity transmembrane transporter activity	184	126.41	1.46	1.44E-02
ion transmembrane transporter activity	192	1.35.67	1.42	4.26E-02
protein dimerization activity	268	194.69	1.38	4.85E-03
RNA binding	339	249.52	1.36	4.85E-03
GO Cellular Component				
dendrite	163	92.19	1.66	8.29E-05
cell-substrate junction	99	61.41	1.61	4.93E-02
pre-synapse	117	74.11	1.58	2.66E-02
neuronal cell body	117	74.56	1.57	2.85E-02
Golgi-membrane	175	112.51	1.56	3.75E-04
adherens junction	125	80.53	1.55	2.53E-02
mitochondrial membrane	163	105	1.55	2.53E-02

Table 3-3: Top-scoring mRNAs encoding mitochondrial proteins with TMG-induced changes in translation

Gene	log2FC mRNA	log2FC RPF	Name	Function
Abcb6	-0.0710	0.9630	ATP Binding Cassette Subfamily B Member 6	ATP-dependent uptake of heme and porphyrins into mitochondria
Acaa2	0.0850	1.2650	Acetyl-CoA Acyltransferase 2	catalyzes last step of the mitochondrial fatty acid beta-oxidation
Acadm	-0.0276	1.0962	Acyl-CoA Dehydrogenase Medium Chain	catalyzes initial step of the mitochondrial fatty acid beta-oxidation
Acadvl	0.0262	1.0928	Acyl-CoA Dehydrogenase Very Long Chain	catalyzes initial step of the mitochondrial fatty acid beta-oxidation
Arl2	-0.0282	-1.3804	ADP Ribosylation Factor Like GTPase 2	small GTP-binding protein
Bckdha	-0.0594	1.6101	Branched Chain Keto Acid Dehydrogenase E1, Alpha Polypeptide	catalyzes second step in catabolism of BCAAs L, I, V
Bdh1	0.0383	1.0853	3-Hydroxybutyrate Dehydrogenase 1	catalyzes the interconversion of acetoacetate and (R)-3-hydroxybutyrate
Dap3	-0.0826	-1.2459	Death Associated Protein 3	mitochondrial ribosomal protein mediates interferon-gamma-induced cell death
Echs1	0.0931	-1.1399	Enoyl-CoA Hydratase, Short Chain 1	second step of the mitochondrial fatty acid beta-oxidation
Eci2	0.0151	-2.4780	Enoyl-CoA Delta Isomerase 2	involved in mitochondrial beta-oxidation of unsaturated fatty acids
Fundc1	0.0067	-1.3647	FUN14 Domain Containing 1	activator of hypoxia-induced mitophagy
Gfm2	-0.0526	-1.6467	G Elongation Factor Mitochondrial 2	mediates disassembly of mitoribosomes from mRNA
Gpx4	-0.0211	-0.0525	Glutathione Peroxidase 4	catalyze the reduction of hydrogen peroxide and hydroperoxides
Hadh	0.0438	-1.3200	Hydroxyacyl-CoA Dehydrogenase	role in the mitochondrial beta-oxidation of short chain fatty acids
Hmgcs2	-0.0280	1.8631	3-Hydroxy-3-Methylglutaryl-CoA Synthase 2	catalyzes the first reaction of ketogenesis
Idh2	-0.0218	1.0865	Isocitrate Dehydrogenase (NADP(+)) 2, Mitochondrial	catalyze the oxidative decarboxylation of isocitrate to 2-oxoglutarate
Iars2	0.0902	-0.9902	Isoeucyl-TRNA Synthetase 2, Mitochondrial	catalyze the aminoacylation of mitochondrial tRNA by isoleucine
Letm1	-0.0394	-1.1684	Leucine Zipper And EF-Hand Containing Transmembrane Protein 1	mitochondrial proton/calcium antiporter
Maoa	0.0937	-1.4106	monoamine oxidase A	catalyze the oxidative deamination of amines
Mgst1	0.0692	1.8117	Microsomal Glutathione S-Transferase 1	catalyzes conjugation of glutathione to electrophiles
Mrpl1	0.0381	-0.9622	Mitochondrial Ribosomal Protein L1	mitoribosome subunit
Mrpl13	0.0916	-1.0897	Mitochondrial Ribosomal Protein L13	mitoribosome subunit
Mrpl35	0.0241	1.1355	Mitochondrial Ribosomal Protein L35	mitoribosome subunit
Mrpl47	0.1732	-1.9064	Mitochondrial Ribosomal Protein L47	mitoribosome subunit
Mrpl48	0.1044	-1.1048	Mitochondrial Ribosomal Protein L48	mitoribosome subunit
Mrps12	-0.0261	1.3135	Mitochondrial Ribosomal Protein S12	mitoribosome subunit

Mrps23	-0.0845	0.9893	Mitochondrial Ribosomal Protein S23	mitoribosome subunit
Mrps35	0.0695	-0.9816	Mitochondrial Ribosomal Protein S35	mitoribosome subunit
Mtfmt	-0.0116	1.1853	Mitochondrial Methionyl-TRNA Formyltransferase	catalyzes the formylation of methionyl-tRNA
Mtx3	0.0245	-1.5685	Metaxin 3	transport of proteins into the mitochondrion
Nat8l	0.1171	-1.3236	N-Acetyltransferase 8 Like	neuron-specific mitochondrial N-acetylaspartate (NAA) biosynthetic enzyme
Nars2	-0.1064	-1.4961	Asparaginyl-TRNA Synthetase 2, Mitochondrial	catalyze the aminoacylation of mitochondrial tRNA by asparagine
Ndufaf8	0.0431	1.0327	NADH:Ubiquinone Oxidoreductase Complex Assembly Factor 8	mediates assembly of ETC complex I
Ndufb4	-0.1965	-1.1650	NADH:Ubiquinone Oxidoreductase Subunit B4	ETC complex I subunit
Nsun4	-0.0657	-1.2528	NOP2/Sun RNA Methyltransferase Family Member 4	involved in a final step in ribosome biogenesis
Pde12	-0.1496	1.1052	Phosphodiesterase 12	mitochondrial poly(A)-specific ribonuclease
Phb2	-0.0502	-1.9006	Prohibitin 2	regulates mitochondrial respiration
Ppat	-0.0371	-1.5198	Phosphoribosyl Pyrophosphate Amidotransferase	catalyzes first step of de novo purine nucleotide biosythesis
Prdx3	-0.0437	0.8485	Peroxiredoxin 3	antioxidant
Psen2	0.0928	-1.3085	presenilin 2	regulate gamma-secretase activity
Sco1	0.0716	-1.1969	Cytochrome C Oxidase Assembly Protein	regulates cytochrome c oxidase assembly
Slc25a20	0.0375	1.2058	Mitochondrial Carnitine/Acylcarnitine Carrier Protein	transports acylcarnitines into mitochondrial matrix for oxidation
Slc25a27	-0.0034	-1.6178	Mitochondrial Uncoupling Protein 4	reduce the mitochondrial membrane potential
Slc25a29	-0.1017	-2.1008	Mitochondrial Basic Amino Acids Transporter	transports basic amino acids into mitochondria
Sod2	-0.0906	-0.5248	Superoxide Dismutase 2, Mitochondrial	converts superoxide to hydrogen peroxide and diatomic oxygen
Ssbp1	-0.0581	-1.3922	Single-Stranded DNA Binding Protein 1, Mitochondrial	involved in mitochondrial DNA replication
Surf1	0.0498	1.1803	Cytochrome C Oxidase Assembly Factor	regulates cytochrome c oxidase assembly
Tfam	0.0138	-1.2567	Transcription Factor A, Mitochondrial	functions in mitochondrial DNA replication and repair
Timm10b	0.2988	-1.3091	Translocase Of Inner Mitochondrial Membrane 10B	imports hydrophobic membrane proteins into mitochondria
Timm50	-0.0645	1.1129	Translocase Of Inner Mitochondrial Membrane 50	recognizes mitochondrial targeting signal for import
Tmem14a	-0.0549	1.2040	Transmembrane Protein 14A	negative regulator of the mitochondrial outer membrane permeabilization
Tmem14c	0.0069	-1.2068	Transmembrane Protein 14C	Required for normal heme biosynthesis
Tomm6	-0.0946	-0.4088	Translocase Of Outer Mitochondrial Membrane 6	subunit of mitochondrial translocase complex
Tomm40	-0.0063	-0.6462	Translocase Of Outer Mitochondrial Membrane 40	channel-forming subunit of mitochondrial translocase complex
Tomm70a	-0.1726	-0.7818	Translocase Of Outer Mitochondrial Membrane 70	import of mitochondrial precursor proteins
Tufm	0.0392	-1.8307	Tu Translation Elongation Factor, Mitochondrial	promotes the GTP-dependent binding of aminoacyl-tRNA to mitoribosome

Chapter 4

Diabetes enhances translation of the mRNA encoding CD40 in Müller glia via a 4E-BP1/2-dependent mechanism

Introduction

Retinal inflammation plays a critical role in the pathogenesis of diabetic retinopathy (DR) [195, 196]. While inflammation is typically beneficial when resolved promptly, chronic low-grade inflammation can contribute to disease progression, including DR [197]. Diabetes increases the expression of pro-inflammatory molecules in retinal microglia, pericytes, endothelial cells, and Müller cells [197]. The conventional view of retinal inflammation is that microglia are the first responders that initiate Müller cell activation and gliosis [198]. Indeed, in the presence of activated microglia Müller cells increase expression of pro-inflammatory factors including IL-1β and IL-6 [199]. Counter to this conventional view, Portillo *et al* recently demonstrated that the immune co-stimulatory molecule Cluster of Differentiation 40 (CD40) in Müller glia is specifically responsible for initiating diabetes-induced retinal inflammation [200]. Activation of CD40 by its ligand CD154 results in increased protein nitration, retinal leukostasis, and capillary degeneration, which are all hallmark characteristics of DR [201, 202]. Diabetic $CD40^{-/-}$ mice fail to exhibit enhanced pro-inflammatory cytokine expression and are protected from both retinal leukostasis and degeneration of the retinal vasculature [200, 202]. Remarkably, Müller cell targeted add-back of CD40 to $CD40^{-/-}$ mice restores the retinal inflammatory response to diabetes, as well as the development of leukostasis and capillary degeneration [200].

Post-translational modification of proteins by O-GlcNAcylation regulates the inflammatory response under both physiological and pathological conditions [203]. Deficiency in

protein O-GlcNAcylation inhibits T cell proliferation and differentiation [204, 205]. Similarly, O-GlcNAcylation is necessary for B cell expansion and activation of neutrophils [206, 207]. Several immune stimulating transcription factors are O-GlcNAc modified, including NF-KB, NFAT, and SP1, resulting in enhanced transcriptional activity of these proteins and subsequent production of immunomodulatory molecules [64, 81, 208-210].

In the retina of diabetic mice, CD40 protein expression is elevated in Müller glia [200]; however, the mechanisms responsible for this increase has not been established. Expression of pro-inflammatory proteins is typically induced by transcription factors, which can promote inflammation by increasing the expression of cytokines and other pro-inflammatory molecules. Importantly, translational control also plays a critical role in the inflammatory response that is less well explored [211]. Studies evaluating the effects of the O-GlcNAcylation on mRNA translation are also lacking, in spite of evidence demonstrating widespread modification of ribosomal and other regulatory proteins, including the translational repressor 4E-BP1 [93, 157, 158, 212, 213]. In chapter 3, we demonstrated that augmented O-GlcNAcylation causes widespread variation in retinal gene expression at the level of mRNA translation. In that chapter, the top canonical pathway identified by Ingenuity Pathway Analysis as being translationally altered by O-GlcNAcylation was the “acute-phase response” (Table 3-1), which is a complex early-defense system involving a range of pro-inflammatory cytokines. Here, we explored CD40 as one gene candidate subject to translation regulation in retina.

Initiation of mRNA translation is generally limited by the recruitment of ribosomes to an mRNA to facilitate either cap-dependent or cap-independent translation. Cap-dependent recruitment of the ribosome onto mRNA occurs via assembly of the eIF4F complex (that includes eIF4E) at the 5′-cap, followed by binding of eIF4F•mRNA to the 40S ribosomal subunit [88]. Sequestration of eIF4E by the translational repressor 4E-BP1 prevents eIF4F complex assembly and represents the best-characterized mechanism for repressing cap-dependent translation

initiation. As an alternative to cap-dependent translation initiation, ~10% of mRNAs contain sequence elements that enable translation to be initiated independent of the 5′-cap [89]. These sequence elements are not conserved between genes; however, a common feature is the formation of hairpin, or stem-loop, secondary structures. Highly-structured elements in the 5′-untranslated region (UTR) of messages are thought to enable translation under physiological duress when cap-dependent translation is inhibited, such as upon exposure to diabetes-induced hyperglycemia [94, 214]. In this study, we evaluated the hypothesis that diabetes enhances translation of the mRNA encoding CD40. Overall, the findings demonstrate that protein O-GlcNAcylation promotes cap-independent CD40 mRNA translation via a 4E-BP1/2-dependent mechanism that involves sequences within its 5′-UTR.

Results

O-GlcNAcase inhibition enhances CD40 mRNA translation in retina

In chapter 3, we evaluated the impact of O-GlcNAcase inhibition on retinal gene expression using next-generation sequencing to assess changes in mRNA abundance and ribosome-bound mRNAs undergoing translation via RNA-Seq and ribosome profiling (Ribo-Seq), respectively. CD40 was identified as a candidate gene that exhibited enhanced mRNA translation in the retina of mice administered TMG as compared to PBS (Fig. 4-1A). In the retina of mice administered TMG, protein O-GlcNAcylation was enhanced as compared to mice administered PBS (Fig. 4-1B). Consistent with the results of sequencing analysis, CD40 mRNA abundance was not altered in whole retinal lysates from mice administered TMG as compared to PBS (Fig. 4-1C). Sucrose density gradient centrifugation was used to separate retinal ribosomes into either subpolysomal or polysomal fractions (Fig. 4-1D). Poorly translated mRNAs are found

in the light subpolysomal fractions, whereas actively translating mRNAs associate with multiple ribosomes and form heavy polysomes. Consistent with sequencing results in Fig. 4-1A, the mRNA encoding CD40 was shifted into the polysomal fraction obtained from the retina of mice administered TMG, as compared to PBS (Fig. 4-1E). In addition to upregulation of CD40 mRNA translation, mRNAs predicted by the sequencing analysis to exhibit downregulation (Nfe2l2 and

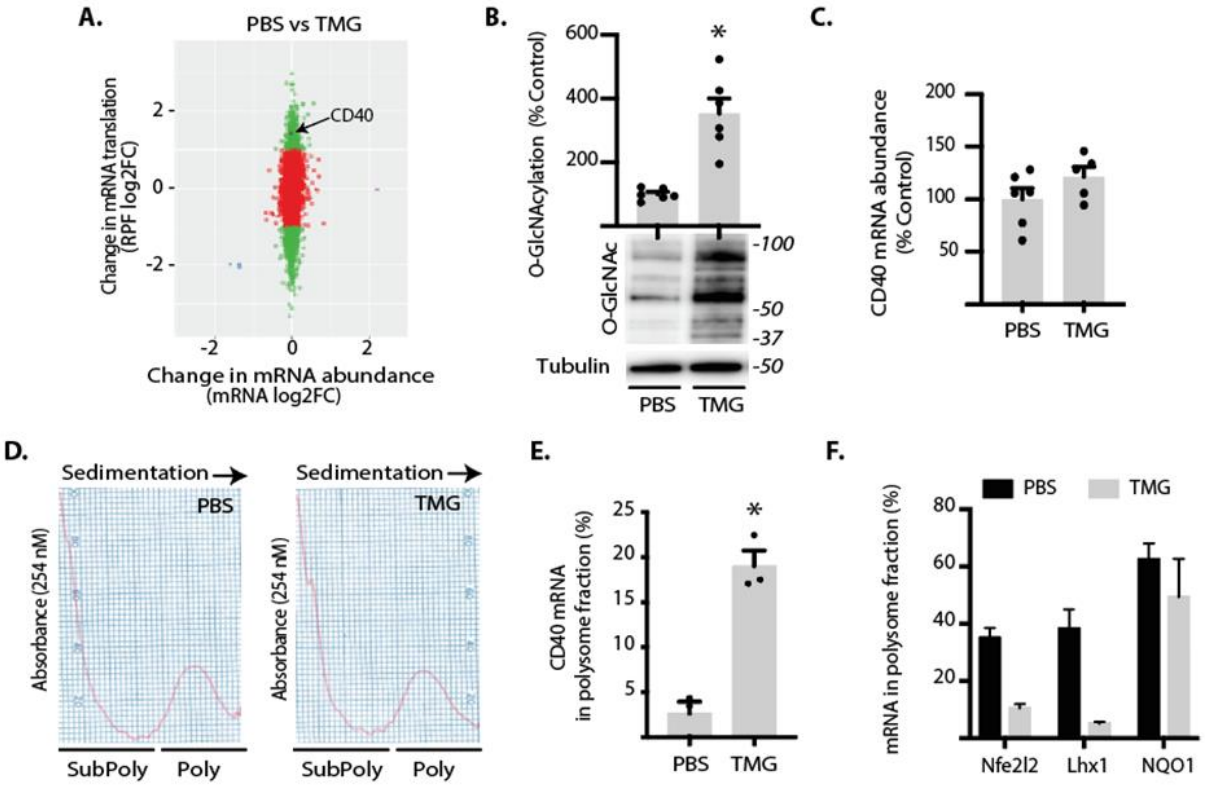

Figure 4-1. O-GlcNAcase inhibition enhances translation of the mRNA encoding CD40 in mouse retina. Mice were administered TMG or PBS vehicle. *A*, sequencing analysis (Chapter 3) revealed a TMG-induced increase in CD40 mRNA in the ribosome protected fragment (RPF) obtained from retina independent of a change in mRNA abundance. *B*, total protein O-GlcNAcylation and tubulin expression were assessed in retinal lysates by Western blot analysis 24 h after TMG administration. Protein molecular mass (in kilodaltons) is indicated on the *right*. *C*, CD40 mRNA expression in whole retina was assessed by PCR. *D*, retinal ribosomes were separated into either subpolysomal (SubPoly) or polysomal (Poly) fractions via sucrose density gradient centrifugation. The distribution of mRNAs encoding CD40 (*E*) or Nfe2l2, Lhx1, and NQO1 (*F*) was assessed in each fraction via PCR. Results are expressed as a relative percentage of the mRNA in the polysomal fraction obtained from 10 retinas. Values are means + SEM. *, $p < 0.05$ *versus* PBS vehicle. Data were analyzed by unpaired t-test.

Lhx1) or no change (NQO1) were also distributed in polysome profiles such that those sequencing results were validated (Fig. 4-1F).

Diabetes enhances CD40 mRNA translation in retina

To assess whether CD40 mRNA translation was enhanced in a model of diabetes, we generated polysome profiles from the retina of STZ-induced diabetic mice. Consistent with previous studies [50], blood glucose concentrations were significantly elevated (Fig. 4-2A) and retinal protein O-GlcNAcylation was enhanced in diabetic mice as compared to nondiabetic control mice (Fig. 4-2B). To determine if diabetes altered CD40 expression at the level of transcription, we evaluated total CD40 mRNA abundance. There was no significant change in total CD40 mRNA abundance in retina of diabetic mice as compared to nondiabetic mice (Fig. 4-2C). However, the relative distribution of the CD40 mRNA was shifted into the polysomal fraction obtained from the retina of diabetic mice, indicating enhanced translation of the CD40 mRNA (Fig. 4-2D).

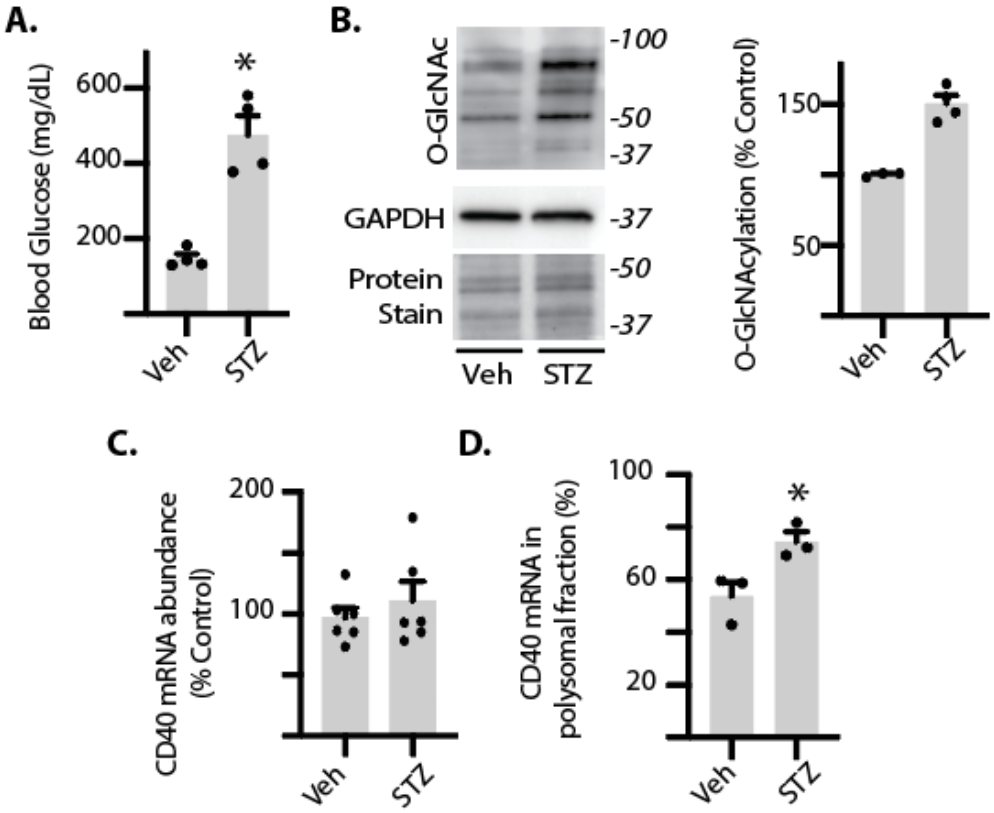

Figure 4-2. CD40 mRNA translation is enhanced in the retina of diabetic mice. Diabetes was induced in mice by administration of streptozotocin (STZ). Nondiabetic controls were administered vehicle (Veh). Retinas were collected after 3 months of diabetes. *A*, blood glucose concentrations were evaluated. *B*, protein O-GlcNAcylation and GAPDH expression were assessed in retinal lysates by Western blotting. Protein staining was used to evaluate loading. Protein molecular mass (in kilodaltons) is indicated on the *right*. *C*, CD40 mRNA expression was evaluated in retinal lysates by PCR. *D*, ribosomes from retinas were separated into either subpolysomal or polysomal fractions. The distribution of the mRNA encoding CD40 was assessed in each fraction by PCR. Means were compared by unpaired t test. Results are expressed as the relative percentage of the mRNA in the polysomal fraction. Values are means + SEM. *, $p < 0.05$ *versus* Veh.

Diabetes and O-GlcNAcase inhibition enhance CD40 mRNA translation in retinal Müller glia

To specifically assess CD40 mRNA translation in retinal Müller cells, we developed a RiboTag mouse [215] which expressed an epitope-tagged ribosomal protein under the control of the Müller cell-specific promoter PDGFRa [216]. RiboTag mice express a fully functional hemagglutinin (HA)-tagged variant of ribosomal protein L22 (Rpl22), which forms the core of the ribosomal 60S subunit and facilitates cell-type specific isolation of translationally active mRNAs [215]. PDGRa-cre recombinase expressing mice were crossed with WT RiboTag mice, resulting in deletion of the WT Exon 4 in Müller cells and replacement with an Exon 4 that included an HA-tag (Fig. 4-3A). Replacement of WT Exon 4 with the HA-tagged Exon 4 was validated by PCR (Fig. 4-3B). HA-tagged Rpl22 expression was only observed in the retina of cre-positive mice (Fig. 4-3C). HA-Rpl22 heavily co-localized with the Müller cell specific marker glutamine synthetase (GS) in retinal cryosections (Fig. 4-3D). Müller-specific HA-tagged ribosomes were immunoprecipitated from whole retinal lysates (Fig. 4-3E). HA-Rpl22 was detected in immunoprecipitations targeting the HA-tag, but not in a FLAG-tag negative control (Fig. 4-3E). RNA isolated by immunoprecipitation was high quality (Fig. 4-3F), and enriched for Müller cell markers (CRALBP, GS, and AQP4), but not the retinal pigmented epithelium marker RPE65 (Fig. 4-3G). To evaluate the effects of enhanced O-GlcNAcylation on CD40 mRNA associated with HA-tagged ribosomes, mice were administered TMG. CD40 mRNA association with HA-tagged ribosomes was enhanced in the retina of mice administered TMG as compared to those administered PBS, indicating upregulated CD40 mRNA translation (Fig. 4-3H). Similarly, diabetes also promoted Müller-specific CD40 mRNA translation (Fig. 4-3I).

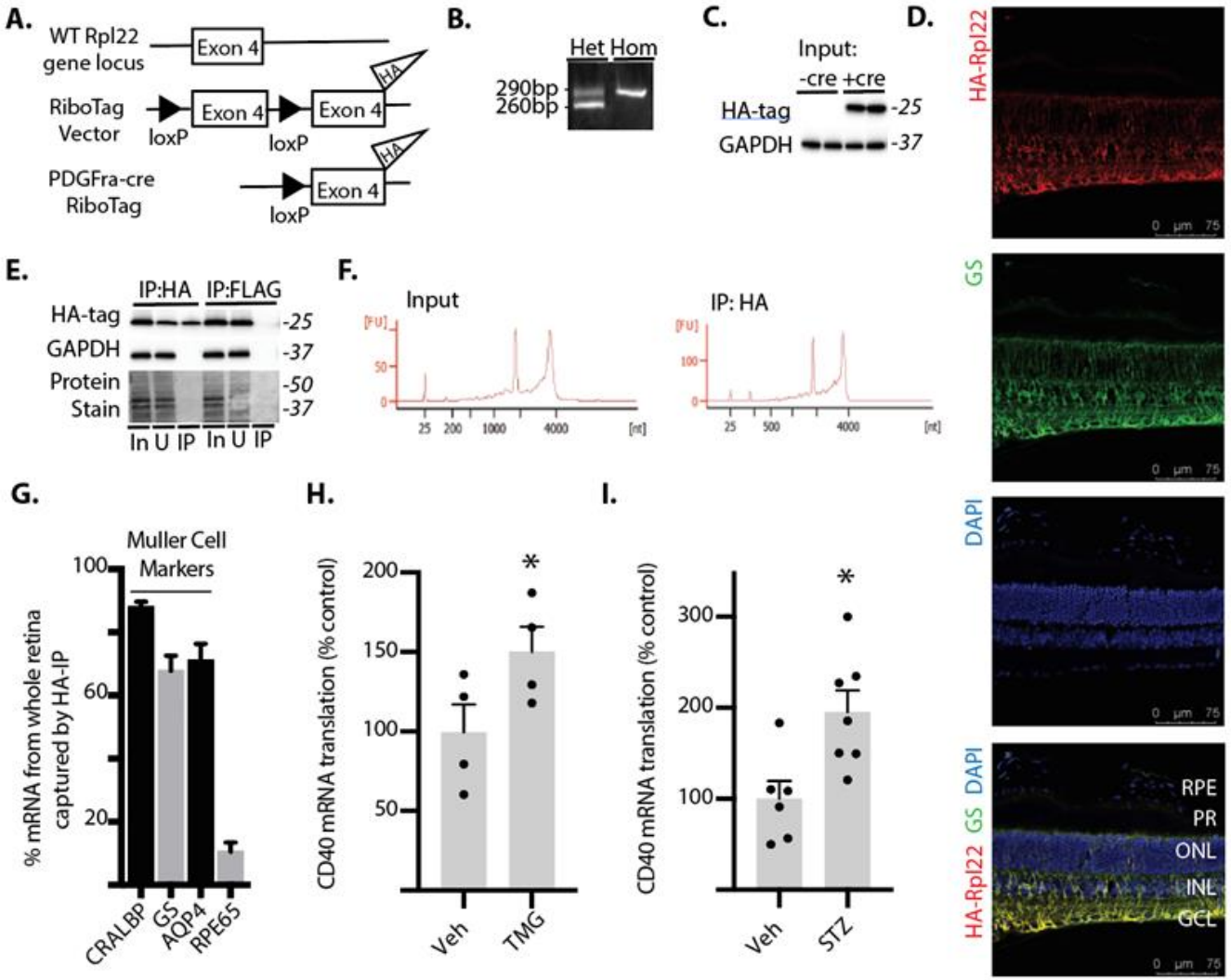

Figure 4-3. CD40 mRNA translation is enhanced in retinal Müller glia by O-GlcNAcase inhibition or diabetes. *Figure Legend on next page.*

Figure 4-3. *A,* Müller glia specific expression of HA-tagged Rpl22 protein in retina was achieved by crossing wild-type (WT) RiboTag mice to a PDGFRa-cre recombinase-expressing mouse, resulting in deletion of the wild-type exon 4 in the target cell population and replacement with the *Rpl22*^{HA} exon. *B,* PCR products were generated using oligonucleotides that amplify the loxP-containing intron sequence 5´ to the wild-type Exon 4 of the *Rpl22* gene. The wild-type PCR product is 260 bp, while the mutant PCR product is 290 bp. *C,* Western blot analysis of HA-tagged Rpl22 and GAPDH in retinal lysates from WT Rpl22 (-cre) or Rpl22^{HA} (cre+) mice. *D,* whole eyes were isolated, fixed, and cryosectioned into sagittally oriented longitudinal cross-sections. HA-Rpl22 (red) and the Müller glia specific marker glutamine synthetase (GS, green) was evaluated in retinal sections by immunofluorescence. Nuclei were visualized by DAPI (blue). Co-localization of HA-Rpl22 and GS is shown in yellow. *E,* ribosomes from Rpl22^{HA}-expressing homozygous mouse retina were isolated by immunoprecipitation. *F,* bioanalyzer analysis demonstrating recovery of high-quality RNA from both whole retina and following ribosome isolation (RIN >8.0). *G,* RNA from HA-tag immunoprecipitates was analyzed for recovery of Müller glia specific markers (CRALBP, GS, AQP4) and RPE65. *H-I,* CD40 mRNA association with ribosomes isolated from the retina of Rpl22^{HA}-expressing homozygous mice was determined by PCR. Retinas were isolated after 24 h after administration of TMG. (*H*) or 4 weeks after STZ (*I*). (*H.-I.*)Means were compared by unpaired t test. Protein molecular mass (in kilodaltons) is indicated at *right* of blots in *C* & *E.* Values are means + SEM. *, $p < 0.05$ *versus* Veh. RPE, retinal pigmented epithelium; PR, photoreceptor outer segments; ONL, outer nuclear layer; INL, inner nuclear layer; GCL, ganglion cell layer; In, immunoprecipitation input; U, unbound immunoprecipitation fraction.

Role of 4E-BP1/2 in cap-independent CD40 mRNA translation

Transcript-specific translational control is generally mediated by cis-regulatory elements encoded by the untranslated region of the target mRNA. A recent genome-wide systematic screen indicated that sequences within the 5′-UTR of the mRNA encoding CD40 were capable of promoting translation independent of a 5′ mRNA cap [217]. Evidence previously suggested that enhanced O-GlcNAcylation causes a shift from cap-dependent to cap-independent mRNA translation that is mediated by 4E-BP1 [94]. In order to investigate the role of 4E-BP1 in translation of the CD40 mRNA, we established a cell culture model of enhanced O-GlcNAcylation in WT and 4E-BP1/2-deficient MEFs. In both WT and 4E-BP1/2-deficient MEFs,

exposure to TMG enhanced protein O-GlcNAcylation (Fig. 4-4A). TMG promoted 4E-BP1 co-immunoprecipitation with eIF4E, whereas the protein could not be detected in 4E-BP1/2-deficient cells (Fig. 4-4B-C). In polysome profiles, CD40 shifted into the polysomal fraction in WT MEFs exposed to TMG (Fig. 4-4D). In 4E-BP1/2 deficient MEFs, there was not a significant shift upon TMG exposure (Fig. 4-4D). There were significant effects of both TMG exposure and expression of 4E-BP1/2 on the distribution of the CD40 mRNA in polysomal fractions ($p=0.0065$ and $p=0.0058$, respectively). There was also a significant interaction between TMG exposure and genotype on the distribution of CD40 mRNA in polysomal fractions ($p=0.0376$). To specifically evaluate the role of the 5′-UTR of CD40, it was cloned into a bicistronic reporter (pYIC) wherein a single mRNA encodes both yellow and cyan fluorescent protein (YFP and CFP, respectively). YFP expression was used as a reporter for cap-dependent translation, whereas CFP expression was used as a reporter for cap-independent translation driven by the CD40 5′-UTR (Fig. 4-4E). Mfold web server predicted that the 5′-UTR sequence of CD40 forms a hairpin structure (Fig. 4-4F). In WT MEFs, exposure to TMG resulted in an increase in the CFP/YFP expression ratio, whereas there was no change in the ratio of CFP/YFP expression in 4E-BP1/2-deficient MEFs exposed to TMG (Fig. 4-4G). There were significant effects of both TMG exposure and expression of 4E-BP1/2 on the ratio of CFP/YFP expression ($p=0.0003$ and $p=0.0185$, respectively). There was also a significant interaction between TMG exposure and genotype on the ratio of CFP/YFP expression as determined by two-way ANOVA ($p=0.0007$). We also co-expressed pYIC with a 4E-BP1 F113A variant that resists mTORC1-dependent phosphorylation and therefore constitutively binds eIF4E [166] in the human MIO-M1 Müller cell line. As compared to an empty vector, 4E-BP1 F113A increased the CFP/YFP expression ratio (Fig. 4-4H).

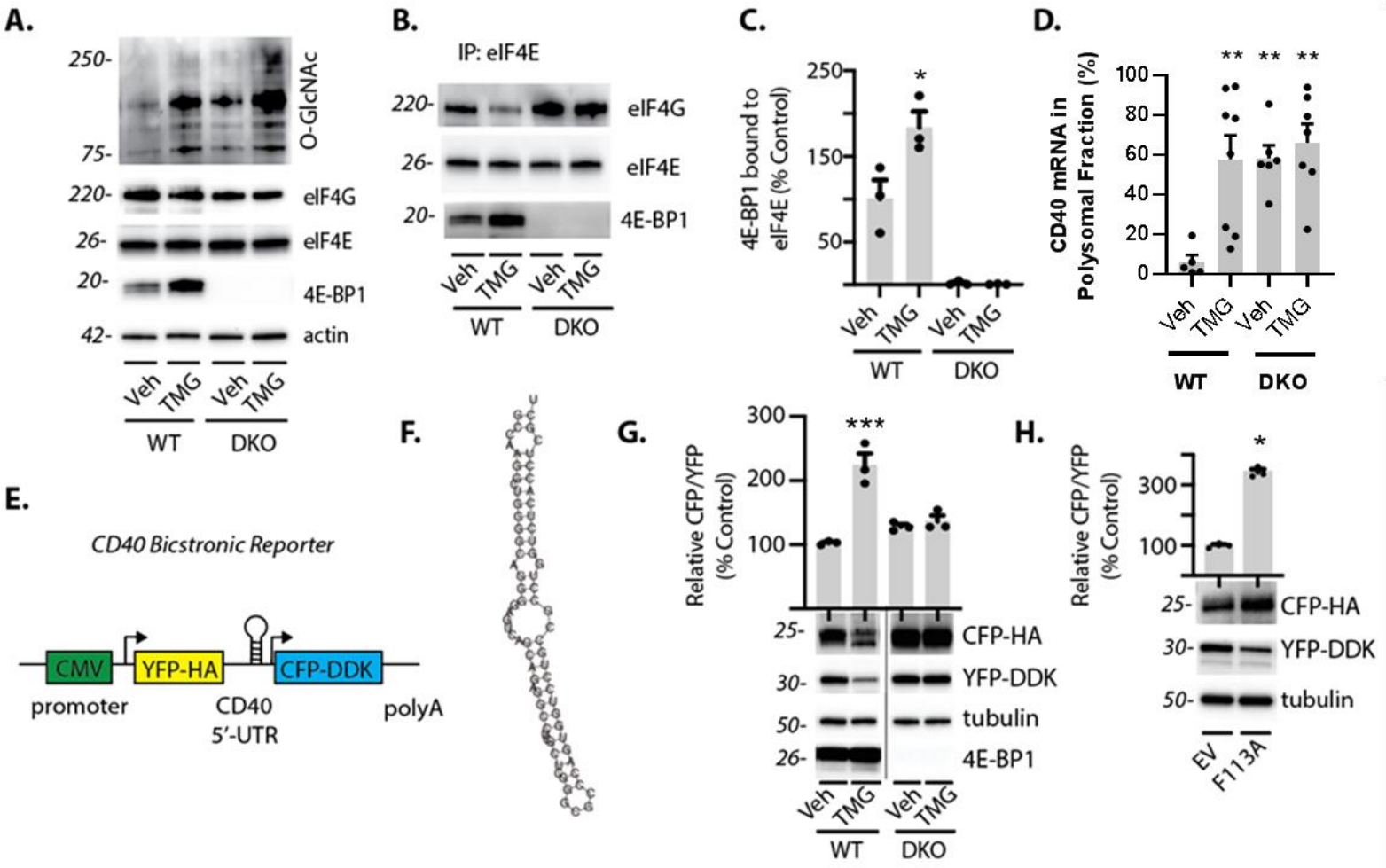

Figure 4-4. 4E-BP1 enhances cap-independent CD40 mRNA translation. *Figure Legend on next page.*

Figure 4-4. *A*, WT and 4E-BP1/2 double knockout (DKO) mouse embryonic fibroblasts were cultured in the presence of TMG or vehicle (Veh) for 24 h. Protein O-GlcNAcylation and expression of eIF4G, tubulin, eIF4E, and 4E-BP1 were assessed by Western blotting of retinal lysates. Protein molecular mass (in kilodaltons) is indicated at the left. *B*, the interaction of 4E-BP1 and eIF4G with eIF4E was examined by immunoprecipitating eIF4E from cell lysates and measuring the amount of eIF4G and 4E-BP1 in the immunoprecipitate (IP) by Western blotting. *C*, Quantification of eIF4E bound to 4E-BP1. *D*, Ribosomes were separated into either subpolysomal or polysomal fractions via sucrose density gradient centrifugation. The distribution of CD40 mRNA was assessed in each fraction via PCR. *E*, a bicistronic reporter was generated wherein a single mRNA encodes for both yellow and cyan fluorescent protein (YFP and CFP, respectively). YFP expression is mediated by cap-dependent translation, whereas cap-independent expression of CFP is under the control of the CD40 5´-untranslated region. *F*, a hairpin structure was predicted for the CD40 5´-untranslated region using the Mfold web server. *G*, WT and 4E-BP1/2 double knockout (DKO) mouse embryonic fibroblasts expressing CD40 reporter were cultured in the presence of TMG or vehicle (Veh) for 24 h. *H*, Human MIO-M1 Müller cell cultures were co-transfected with the CD40 reporter and either a plasmid that expresses an empty vector (EV) or a 4E-BP1 variant that constitutively binds eIF4E. CFP, YFP, tubulin and 4E-BP1 expression were assessed by Western blotting of cell lysates. Data in *C* were analyzed by one-way ANOVA with Tukey's post-hoc analysis. Data in *D* & *G* were analyzed via two-way ANOVA with Dunnett's post-hoc analysis. Data in *H* were analyzed via unpaired t test. Values are means + SEM. *, $p < 0.05$ *versus* WT Veh or EV; **, $p < 0.01$ *versus* WT Veh; ***, $p < 0.001$ *versus* WT Veh.

4E-BP1/2 deletion prevents diabetes-induced CD40 mRNA translation

To evaluate the role of 4E-BP1 in regulating the translation of the CD40 mRNA in the retina, diabetes was induced in WT and 4E-BP1/2 knockout mice. Blood glucose concentrations (Fig. 4-5A) and retinal protein O-GlcNAcylation (Fig. 4-5B) were significantly elevated in both WT and 4E-BP1/2-deficient diabetic mice as compared to nondiabetic mice. No significant change in total CD40 mRNA was detected by two-way ANOVA in whole retinal lysates (Fig. 4-5C). In polysome profiles, the CD40 mRNA shifted into the polysomal fraction obtained from the retina of WT diabetic mice as compared to WT nondiabetic mice, although statistical significance was not achieved via two-way ANOVA ($p=0.0918$ *versus* WT nondiabetic mice; Fig. 4-4D). However, the distribution of the CD40 mRNA in the polysomal fraction obtained from the retina of 4E-BP1/2-deficient diabetic mice was similar to that observed in 4E-BP1/2-deficient non-diabetic mice (Fig. 4-5D). There was no significant effect of either diabetes or genotype on the

distribution of the CD40 mRNA in polysomal fractions (p=0.1003 and p=0.2122, respectively). Similarly, there was no significant interaction between diabetes and genotype as determined by two-way ANOVA (p=0.1449). As a marker for retinal inflammation, inducible nitric oxide synthase 2 (NOS2) mRNA abundance was evaluated in retinal lysates. Diabetes enhanced NOS2 expression in the retina of wild-type mice; however there was no difference in NOS2 expression in the retina of diabetic and non-diabetic 4E-BP1/2-deficient mice (Fig. 4-5E). Two-way ANOVA analysis revealed there were significant effects of both diabetes and expression of 4E-BP1/2 on Nos2 expression (p=0.0117 and p=0.0062, respectively). There was also a significant interaction between diabetes and genotype on Nos2 expression (p=0.0188).

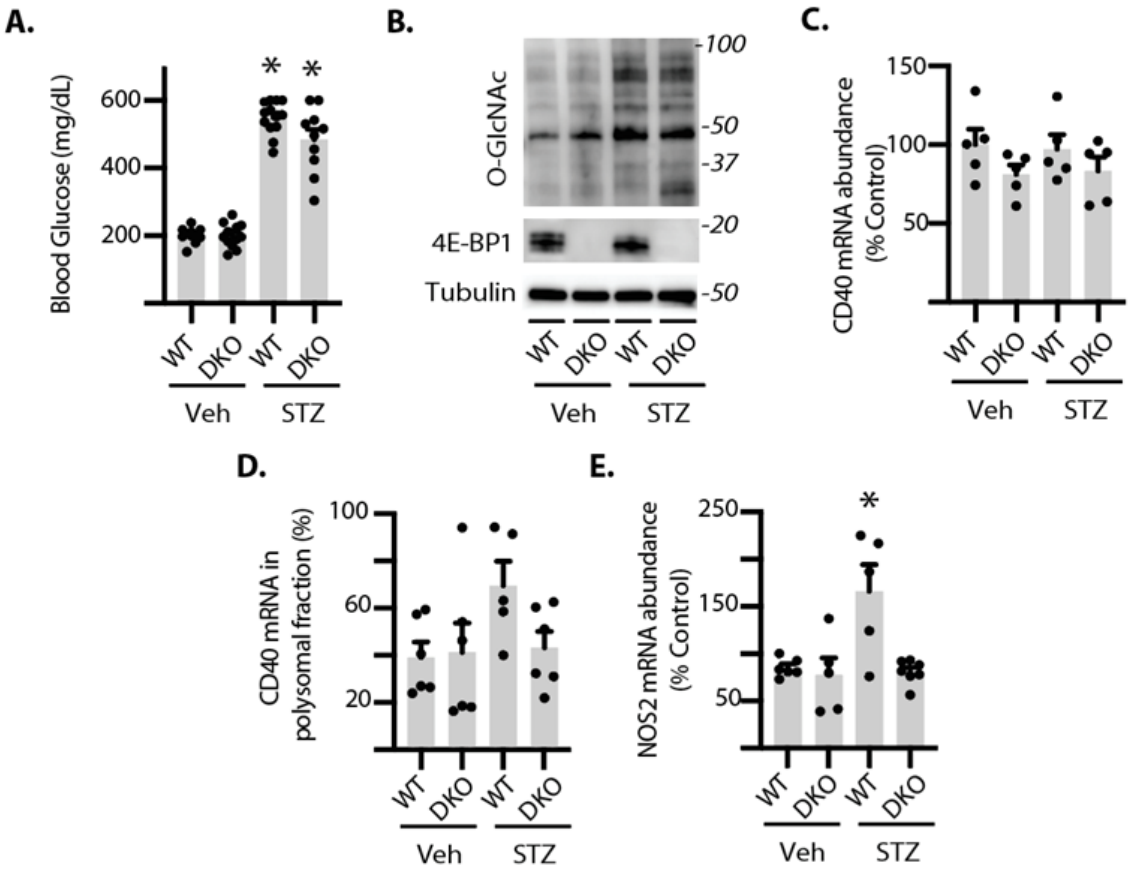

Figure 4-5. 4E-BP1/2 is necessary for diabetes-induced CD40 mRNA translation in retina.
Figure legend on next page.

Figure 4-5. Diabetes was induced in wild-type (WT) and 4E-BP1/2 double knockout (DKO) mice using streptozotocin (STZ). Nondiabetic controls were administered vehicle (Veh). Retinas were collected after 3 months of diabetes. *A*, blood glucose concentrations were evaluated. *B*, protein O-GlcNAcylation and expression of 4E-BP1 and tubulin were assessed by Western blotting of retinal lysates. Protein molecular mass (in kilodaltons) is indicated at the *right*. *C*, CD40 mRNA expression was evaluated in retinal lysates by PCR. *D*, ribosomes from retinas were separated into either subpolysomal or polysomal fractions. The distribution of the mRNA encoding CD40 was assessed in each fraction by PCR. Means were compared by unpaired t tests. *E*, NOS2 mRNA abundance was evaluated in whole retina lysates by PCR. Data in *A* & *C-E* were analyzed via two-way ANOVA with Dunnett's post-hoc analysis. Results are expressed as the relative percentage of the mRNA in the polysomal fraction. Values are means + SEM. *, $p < 0.05$ *versus* WT Veh.

Discussion

The TNF receptor superfamily member CD40 is a central mediator of inflammation in DR pathology [200, 202, 218]. In the present study, we demonstrated that in the retina of diabetic mice CD40 mRNA translation was enhanced, independent of a change in total CD40 mRNA abundance. Using a novel RiboTag mouse model, we found that diabetes enhanced CD40 mRNA translation in Müller glia. In this chapter we demonstrated the effect of diabetes on CD40 mRNA translation required eIF4E sequestration, as 4E-BP1/2 ablation prevented diabetes-induced CD40 mRNA translation in retina and normalized expression of the inflammatory marker NOS2. Retinal NOS2 expression is enhanced in both DR patients and in rodent models of the disease [219, 220]. Upregulated expression of this proinflammatory marker is critical for disease progression, as NOS2-deficient mice are resistant to diabetes-induced retinal leukostasis and capillary degeneration [221, 222]. Overall, the results here are consistent with a model wherein diabetes-induced O-GlcNAcylation enhances retinal inflammation by promoting CD40 mRNA translation.

In response to diabetes, Müller glia initiate retinal inflammation via CD40 activation, which leads to ATP release and stimulation of P2X7 purinergic receptors on

microglia/macrophages [200-202]. In the retina of diabetic CD40$^{-/-}$ mice, NOS2 expression, leukostasis, and the development of acellular capillaries are reduced as compared to diabetic WT control [200, 202]. However, Müller cell targeted add-back of CD40 to CD40$^{-/-}$ mice restores diabetes-induced retinal inflammation as assessed by inflammatory cytokine expression (e.g. NOS2) [200]. Despite the *in vivo* work pinpointing Müller cells as a critical mediator of CD40-driven inflammation in DR, *in vitro* work revealed that both human and rodent Müller glia are unable to secrete cytokines in response to CD40 ligation by its ligand CD154 [200]. This raised the possibility that CD40 signals to neighboring microglial cells to stimulate the production of pro-inflammatory cytokines. Indeed, Portillo and colleagues found that activation of CD40 on Müller glia induced pro-inflammatory responses through signaling to bystander microglia [200]. Overall, the previous findings support a model in which CD40 activation on Müller glia initiates the inflammatory response in DR. Herein, we extend on the previous studies by exploring the mechanism responsible for increased CD40 expression in retinal Müller glia of diabetic mice. In the retina of diabetic mice, we found that CD40 mRNA translation was upregulated in Müller glia concomitant with an increase in retinal protein O-GlcNAcylation. In addition, CD40 mRNA translation was enhanced in Müller glia of mice administered TMG to promote retinal protein O-GlcNAcylation.

In response to diabetes, Müller cells exhibit a range of protein expression changes that contribute to retinal inflammation, microvascular defects, and neuronal dysfunction [reviewed by Coughlin *et al* [14]]. Müller cells are uniquely sensitive to the metabolic environment in diabetes due, in part, to their exclusive expression of the high capacity/low affinity GLUT2 glucose transporter [67] and predominance of the feedback inhibition resistant glutamine-fructose-6-phosphate amidotransferase 2 (GFAT2) isoform [45]. As discussed in chapter 1, GFAT is the rate-limiting enzyme of the hexosamine biosynthetic pathway. Thus, hyperglycemia potentially has dramatic effects on protein O-GlcNAcylation in Müller cells of

diabetic patients. Diabetes causes Müller cells to become reactive and exhibit increased expression of the intermediate filament protein GFAP [223-225]. In the retina of diabetic patients, increased GFAP expression manifests prior to development of DR, suggesting an early onset of Müller glia dysfunction [226-228].

CD40 expression is generally low under basal conditions, and increased CD40 expression is a common feature of inflammatory diseases driven by the receptor [229]. CD40 protein expression is elevated in Müller glia of diabetic [200]; however, the mechanisms responsible for this increase had not been previously explored. Previous studies demonstrate that TNFα and IFN-γ from microglia activate CD40 gene transcription via cis-elements in the CD40 promoter [230]. However, cytokine-mediated CD40 transcriptional activation is not consistent with a model wherein CD40 expression in Müller glia initiates retinal inflammation [200]. Rather, transcriptional activation of CD40 through this conventional pathway would represent a model wherein retinal inflammation is initiated by the microglia. In the present study, we provide new evidence that diabetes promotes CD40 mRNA translation in Müller glia.

In chapter 3, we reported that augmented O-GlcNAcylation contributes to retinal dysfunction by dramatically altering mRNA translation, as assessed by ribosome profiling. CD40 was identified in that sequencing analysis as a gene candidate in which expression in retina was primarily altered at the level of mRNA translation. Translational control of CD40 expression is supported by a previous study demonstrating that a Graves' Disease-associated single-nucleotide polymorphism in the CD40 5′-UTR results in increased CD40 mRNA translation and protein expression [231]. As previously mentioned, CD40 was also identified in a genome-wide screen for sequence elements capable of promoting cap-independent translation [217]. In the present study we cloned the 5′-UTR of the CD40 mRNA into a reporter construct to evaluate cap-independent CD40 mRNA translation. The 5′-UTR of CD40 mRNA is not notably long at only 77 base pairs, but is particularly GC rich (72%) and predicted to form a stable stem loop

structure. It is worth noting that this sequence also contains a consensus G-quadruplex sequence (5′-…GGGCGGGGCCAAGGCTGGGGCAGGG…) [232]. When located within the 5′-UTR, GC-rich secondary structures such as these inhibit cap-dependent mRNA translation [233, 234]. However, these same highly-structured RNA elements often facilitate preferential translation when cap-dependent translation is inhibited [94, 214]. In the present study, we found that CD40 mRNA translation was enhanced by exposure to TMG. This is consistent with the activation of the CD40 5′-UTR reporter under the same conditions. Importantly, TMG failed to enhance activity of the CD40 5′-UTR in the absence of 4E-BP1/2, whereas the non-phosphorylatable 4E-BP1 F113A variant was sufficient to activate translation from the reporter. Together, these observations support a role for 4E-BP1/2-dependent translational control of CD40 expression.

Regardless of any change in expression, activation of CD40 on retinal Müller glia is dependent upon the presence of its ligand CD154. CD154 concentrations are enhanced in the blood of both diabetic patients and rodents, and plasma levels of soluble CD154 are correlated with the severity of DR [235, 236]. It remains unclear how CD154 gets into the retina prior to the development of inflammation; however, it is possible that microthrombosis in the retinal capillaries of patients with DR enables activation of platelets in the retina [237]. Activated platelets express surface CD154 that is rapidly shed upon ligation with CD40-expressing endothelial cells into the biologically active soluble CD154 [238]. Moreover, ligation of CD154-expressing platelets with CD40-expressing endothelial cells stimulates inflammatory cascades [235]. Alternatively, in advanced stages of DR when immune privilege and the blood retinal barrier are compromised, circulating immune cells (such as CD154-expressing T cells) or serum proteins (such as soluble CD154) may infiltrate the retina and contribute to inflammation-induced neurovascular retinal damage [239].

Anti-inflammatory steroids are used clinically to treat diabetic macular edema, and the implantation of the corticosteroid dexamethasone provides a therapeutic alternative for diabetic

macular edema patients refractory to the first-line anti-VEGF therapies [240]. However, long-acting dexamethasone implants are associated with an increased risk for elevations in intraocular pressure and cataract formation [240]. Therefore, there is a need to identify alternative therapies for patients who do not respond to anti-VEGF treatment. The findings here are consistent with the previous body of work indicating that CD40 activation specifically on Müller glia drives the expression of multiple cytokines and chemokines, resulting in augmentation of inflammatory signaling and ultimately chronic retinal inflammation associated with DR. We extend the previous studies by demonstrating that diabetes and enhanced O-GlcNAcylation promote CD40 mRNA translation via a 4E-BP1/2-dependent mechanism. Based on the data here, 4E-BP1/2-mediated control of CD40 expression in Müller glia may represent a novel target for therapeutic intervention to prevent retinal inflammation in DR.

Chapter 5

Angiotensin-(1-7) attenuates protein O-GlcNAcylation in the retina by EPAC/Rap1-dependent inhibition of O-GlcNAc Transferase

Introduction

Clinical evidence suggests that dysregulation of the RAS may also play an important role in the development of DR, as diabetic patients taking RAS blockers have lower risk for both incidence and progression of DR [118]. The specific signaling mechanisms that mediate the positive effects of RAS blockers in retina are not well defined, but are believed to be independent of changes in blood pressure [118]. The classic RAS is mediated by the effector peptide AngII which potentiates elevations in blood pressure via numerous mechanisms including oxidative stress, vasoconstriction, aldosterone release, and sympathetic activation. Renin, angiotensinogen, ACE, and AT_1 have all been identified in the retina of both humans and animals [241-246]. Furthermore, levels of AngII in retina are several fold higher than can be expected due to contamination from serum [247], indicating that a local ocular RAS exists independent of circulating levels of the peptide.

A reduction in AngII formation is one of the primary mediators of the beneficial cardiovascular and metabolic effects of ACEi; however, ACEi also increase the counter-regulatory axis of RAS mediated by Ang1-7, a degradation product of AngII [119-121, 248]. Ang1-7 binds to the G protein-coupled receptor Mas to produce actions that are generally opposite to those of AngII, such as vasodilation and blood pressure reduction [249]. In retina, Ang1-7 localizes to the footplates of Müller glia and extends through Müller cell processes, spanning all layers of the retina [129]. Intra-ocular administration of AAV-Ang1-7 or ACE2

reduces oxidative damage, prevents the formation of acellular capillaries, and normalizes vascular permeability in retina of STZ-induced diabetic rodents [130, 250]. Similarly, oral delivery of a probiotic expressing ACE2 reduces inflammation and prevents ganglion cell death in the retina of diabetic mice [251]. Therefore, methods to increase retinal Ang1-7 signaling may be valuable in treating DR. ACE inhibition is one such method by which retinal levels of Ang1-7 may be increased [129]. Indeed, ACE inhibitors correct electroretinogram deficits and attenuate retinal capillary degeneration and inflammation in diabetic mice [126, 252]. However, whether the beneficial actions of ACE inhibitors in retina are due to reduced AngII versus increased Ang1-7 formation remains unclear.

In the present chapter we evaluated the hypothesis that Ang1-7 attenuates retinal protein O-GlcNAcylation via regulation of the HBP. Expression and activity of the pathway's rate-limiting enzyme, GFAT represent a critical regulatory checkpoint for HBP flux. It is hypothesized hyperglycemic conditions increase flux through the HBP resulting in greater production of UDP-GlcNAc [189, 253]. In kidney, AngII transcriptionally induces expression of GFAT1 [254], indicating the RAS may regulate the rate of HBP flux. Differences in the relative tissue distribution of the GFAT isoforms, however, suggest that GFAT2, rather than GFAT1, is the primary rate-limiting step in the HBP in the retina [45, 46].

We demonstrated in Chapter 3 that aberrant O-GlcNAc cycling causes mitochondrial reprogramming and excessive generation of reactive oxygen species (ROS) in retina. As discussed in chapter 3, in diabetes, an increase in ROS plays a critical role in the development of retinal dysfunction [191, 194, 255, 256]. The aim of the present study was to investigate the impact of signaling pathways activated by Ang1-7 on retinal protein *O*-GlcNAcylation and ROS production. In the retina of mice fed a HFD, the ACEi captopril attenuated retinal protein *O*-GlcNAcylation in a manner that was dependent on Mas receptor activation. Surprisingly, the protective effects of Ang1-7 were not consistent with a change in GFAT expression or activity.

Rather, the results were consistent with a model wherein Ang1-7 repressed OGT activity by elevating production of cAMP, activating exchange protein activated by cAMP (EPAC), and increasing GTP loading of the small GTPase Ras-associated protein 1 (Rap1).

Results

ACE inhibition attenuates retinal protein O-GlcNAcylation via the Mas receptor

To evaluate the contribution of endogenous Ang1-7 to the effects of ACE inhibition on retinal *O*-GlcNAcylation, HFD-induced obese mice received chronic treatment with either the ACE inhibitor captopril in drinking water or captopril in combination with the Mas receptor antagonist A779. As expected, HFD mice treated with saline vehicle were obese (46±6 grams; Fig 5-1A) and exhibited mild hyperglycemia following a 4-hour fasting period (129±12 mg/dL; Fig 5-1B). Chronic ACE inhibition reduced body mass in HFD mice, and this effect was not reversed by the addition of A779 (Fig 5-1A). There was neither an effect of captopril alone nor captopril plus A779 on fasting blood glucose concentrations (Fig 5-1B). As expected, ACE inhibition reduced circulating AngII levels (Fig 5-1C), and increased circulating Ang1-7 levels (Fig 5-1D). We have previously demonstrated total retinal protein *O*-GlcNAcylation is increased in mice fed a HFD [45]. Global protein *O*-GlcNAcylation was attenuated in the retina of mice receiving captopril alone when compared with normal drinking water (Fig 5-1E). When mice received captopril in combination with A779, however, the decrease in retinal protein *O*-GlcNAcylation was reversed (Fig 5-1E). Thus, activation of the Mas receptor was necessary for captopril to attenuate retinal protein *O*-GlcNAcylation in HFD mice. To evaluate the effects of ACE inhibition on expression levels of genes that may directly affect the quantity of *O*-GlcNAcylated proteins, we evaluated mRNA levels of OGT, OGA, and both isoforms of GFAT

expressed in the retina. Expression of the mRNAs encoding OGT, OGA, and GFAT1/2 were not altered in mice receiving captopril alone or captopril plus A779 as compared to control mice (Fig 5-1F-I). When evaluated by Western blotting, OGT and OGA protein expression were also similar in retinal lysates (Fig 5-1J); however, we were unable to convincingly measure GFAT1 and GFAT2 protein expression by this method.

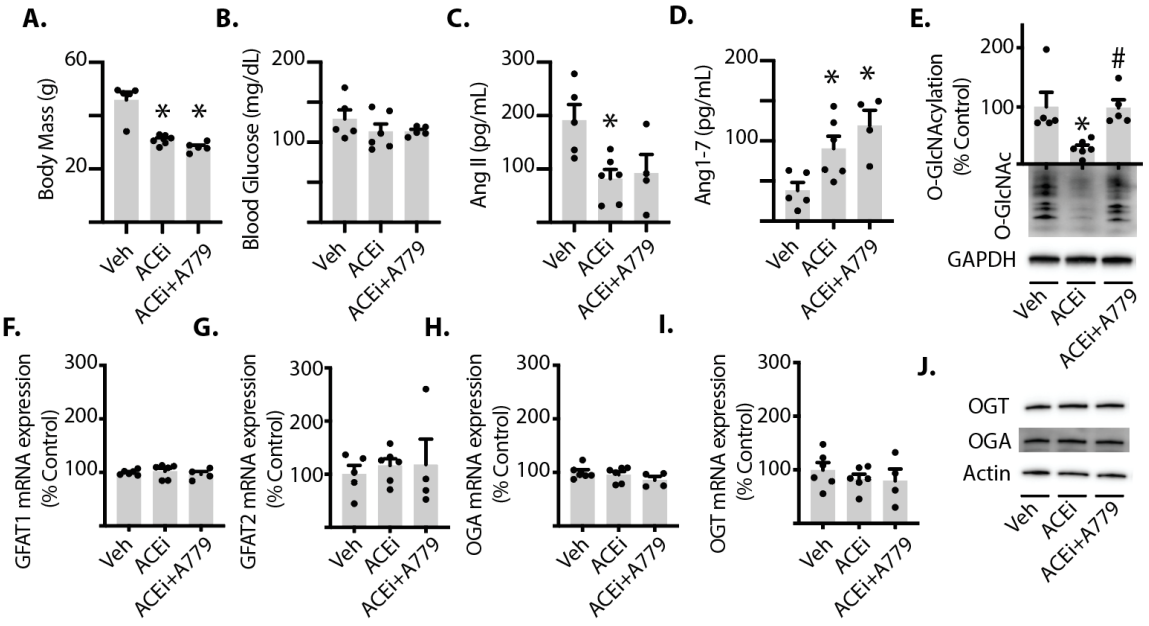

Figure 5-1. Captopril inhibits retinal protein *O*-GlcNAcylation via a Mas-dependent pathway. Mice were fed a 60% high fat diet for 11 weeks and treated chronically with saline vehicle (Veh), 50 mg/L of captopril (ACEi), or captopril plus the Ang1-7 Mas receptor antagonist A779 (400 ng/kg/min) during the last 3 weeks of diet. *A-B.* Body mass and fasting arterial blood glucose levels were evaluated. *C-D.* Plasma Ang II and Ang1-7 levels were measured by radioimmunoassay. *E.* Protein *O*-GlcNAcylation and GAPDH expression were assessed by Western blotting of retinal lysates. GFAT1 (*F.*), GFAT2 (*G.*), OGA (*H.*), and OGT (*I.*) mRNA expression in whole retina were assessed by PCR. *J.* OGT, OGA, and actin protein expression were assessed by Western blotting of retinal lysates. Data were analyzed via one-way ANOVA with Tukey's post-hoc analysis. Results are expressed as means + SEM. *p<0.05 versus Veh; #p<0.05 versus ACEi alone. Mice are a subset of those previously described [138].

Ang1-7 enhances cAMP levels and inhibits protein O-GlcNAcylation.

As Ang1-7 localizes to Müller cells in the retina [129], we used the human Müller cell line MIO-M1 to investigate direct effects of Ang1-7 on protein *O*-GlcNAcylation in retinal cells

in culture. To enhance *O*-GlcNAcylation in cell culture, we used the OGA inhibitor TMG. In MIO-M1 cells treated with both Ang1-7 and TMG, protein *O*-GlcNAcylation was significantly reduced compared to cells treated with TMG alone (Fig 5-2A-B). The Ang1-7 Mas receptor is coupled to the G_s G protein in several cell types [257-259]. To determine if Ang1-7 also activates G_s-associated signaling pathways in Müller cells, we evaluated cyclic AMP (cAMP) concentrations in cell lysates via ELISA. Ang1-7 significantly elevated cAMP levels in MIO-M1 cells (Fig 5-2C). The conversion of ATP to cAMP is catalyzed by adenylate cyclase. Therefore, activating adenylate cyclase can be used to investigate the downstream signaling pathways initiated by the second messenger cAMP. Chang *et al* previously reported that the adenylate cyclase activator Fsk reduced *O*-GlcNAc modifications of intracellular proteins in kidney epithelial cells [260]. To determine if Fsk mediated the same effect on *O*-GlcNAc modified proteins in Müller cells, cells were pre-treated with Fsk prior to inhibiting OGA. Cells exposed to both Fsk and TMG exhibited a reduction in *O*-GlcNAcylated proteins compared to cells exposed to TMG alone (Fig 5-2D). Because TMG is used to block *O*-GlcNAc removal from proteins in

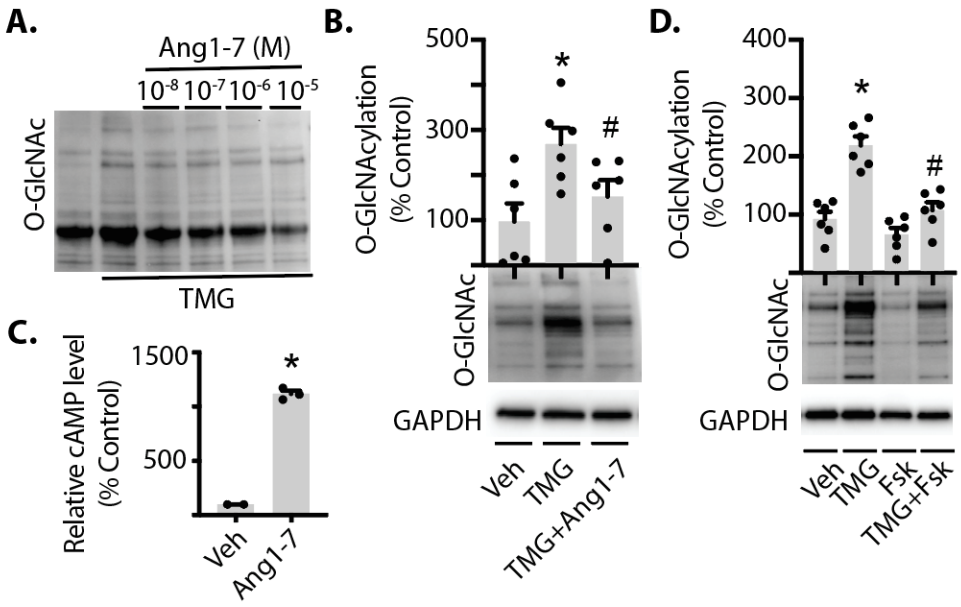

Figure 5-2. Ang1-7 inhibits *O*-GlcNAcylation and promotes cAMP levels in retinal cells in culture. *Figure legend on next page.*

Figure 5-2. MIO-M1 cells were cultured in medium containing 5 mM glucose supplemented with 10% FBS. *A.* Culture medium was supplemented with the *O*-GlcNAcase inhibitor thiamet G (TMG) in the presence or absence of Ang1-7 for 24 h. Protein O-GlcNAcylation in cell lysates was assessed by Western blotting. *B.* MIO-M1 cells were exposed to culture medium containing TMG in the presence or absence of 10^{-5} M Ang1-7 for 24 h. Protein *O*-GlcNAcylation is expressed relative to GAPDH. *C.* Relative cAMP levels were assessed in lysates from cells exposed to culture medium containing 10^{-5} M Ang1-7 for 30 min by ELISA. *D.* Cells were exposed to culture medium containing TMG in the presence or absence of the adenylate cyclase activator forskolin (Fsk). Data in *B* & *D* were analyzed by one-way ANOVA with Tukey's post-hoc analysis. Data in *C* were analyzed by unpaired t test. Results are expressed as means + SEM. *, $p<0.05$ versus Veh; #, $p<0.05$ versus TMG alone.

these studies, the data support a mechanism in which activation of pathways generating cAMP suppress the rate of *O*-GlcNAc addition.

cAMP-mediated attenuation of O-GlcNAcylation is EPAC-dependent

cAMP classically regulates cellular physiology via activation of PKA but can also activate EPAC. EPAC is involved in activation of the Ras family member Rap1 by promoting GDP/GTP exchange. To determine if these downstream effector proteins are required for cAMP-induced attenuation of *O*-GlcNAcylation, either PKA or EPAC were inhibited and cells were subsequently exposed to Fsk and TMG. In cells exposed to the PKA inhibitor H89, protein *O*-GlcNAcylation was attenuated by adenylate cyclase activation (Fig 5-3A&C). In contrast, EPAC inhibition with ESI-09 prevented the suppressive effect of adenylate cyclase activation on protein *O*-GlcNAcylation (Fig 5-3B-C). These results support a role for cAMP-dependent activation of EPAC, rather than PKA, in suppressing the rate of *O*-GlcNAc addition in Müller cells. To confirm that the effect of ESI-09 on O-GlcNAcylation was via EPAC inhibition, wild-type and constitutively active variants of the EPAC downstream effector Rap1 were expressed in MIO-M1 cells. Rap1E63 (a constitutively active Rap1 variant) expression decreased protein *O*-GlcNAcylation in response to TMG, as compared to expression of WT Rap1 (Fig 5-3D-E). Taken

together, these results support a model wherein activation of the EPAC/Rap1 signaling axis suppresses protein *O*-GlcNAcylation.

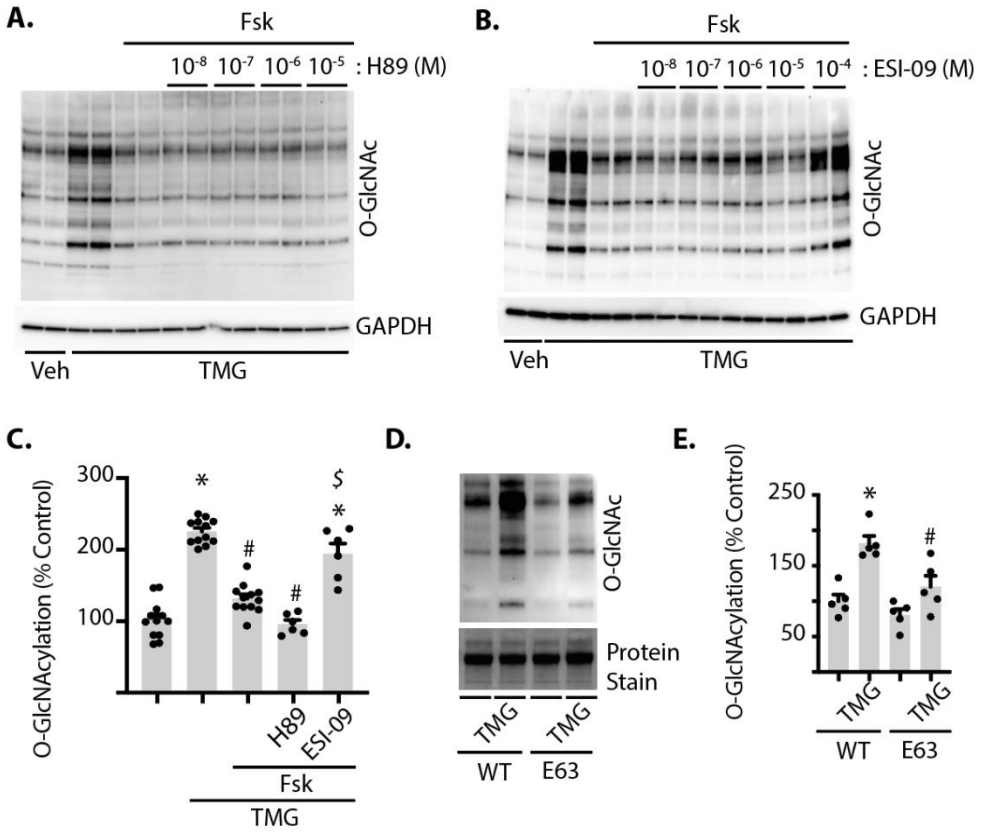

Figure 5-3. EPAC and the GTPase Rap1 inhibit *O*-GlcNAcylation in retinal cells in culture. MIO-M1 cells were cultured in medium containing 5 mM glucose supplemented with 10% FBS. TMG was added to culture medium in the presence or absence of Fsk, as well as the PKA inhibitor H89 (*A.*) or the EPAC inhibitor ESI-09 (*B.*). Protein *O*-GlcNAcylation and GAPDH expression were assessed by Western blotting. *C.* Protein *O*-GlcNAcylation in *A.* & *B.* were quantified and expressed relative to GAPDH. Quantification in *C.* is for 10^{-5} and 10^{-4} M H89 and ESI-09, respectively. Cells were transfected with plasmids for expression of either wild-type (WT) Rap1 or a constitutively active Rap1 variant (E63). Protein *O*-GlcNAcylation in *D.* was quantified in *E.* Total protein levels were evaluated by staining. Data in *C* & *E* were analyzed by one-way ANOVA with Tukey's post-hoc analysis. Results are expressed as means + SEM. *, $p<0.05$ versus Veh; #, $p<0.05$ versus TMG or WT in *C.* and *E.*, respectively; $, $p<0.05$ versus Fsk alone.

Ang1-7 acts downstream of GFAT by inhibiting OGT

The phosphorylation of glucosamine (GlcN) produces glucosamine-6-phosphate (GlcN-6-P), which may be metabolized further by enzymes in the HBP. Importantly, GlcN-6-P enters the HBP downstream of the rate-limiting enzyme GFAT. The cAMP-mediated attenuation of retinal protein *O*-GlcNAcylation is likely due to either a restricted pool of substrate (UDP-GlcNAc) available for OGT, or reduced activity of OGT itself. In cells exposed to culture medium supplemented with GlcN, protein *O*-GlcNAcylation was enhanced (Fig 5-4A). However, in cells pre-treated with Fsk prior to addition of GlcN to cell culture medium, *O*-GlcNAcylation was significantly reduced as compared to cells exposed to GlcN alone (Fig 5-4B-C). No significant change in *O*-GlcNAc modified proteins was observed in cells exposed to the osmotic control mannitol (Fig 5-4B-C). To determine if activation of EPAC could similarly attenuate GlcN-induced protein *O*-GlcNAcylation, cells were pre-treated with the EPAC activator 8-CPT. In cells pre-treated with 8-CPT prior to addition of GlcN to cell culture medium, *O*-GlcNAcylation was significantly reduced as compared to cells exposed to GlcN alone (Fig 5-4D-E). If Fsk or 8-CPT limits the pool of available UDP-GlcNAc via negative regulation of GFAT activity, it is expected that Fsk and 8-CPT would have no effect on *O*-GlcNAcylation induced by GlcN. However, the results described here support the alternate hypothesis that EPAC-specific signaling pathways negatively regulate *O*-GlcNAcylation downstream of GFAT. To determine if Ang1-7 inhibited OGT activity, HA-tagged OGT was expressed in and immunoprecipitated from cells exposed to Ang1-7. HA-tagged OGT was then assayed for glycosyltransferase activity. The

glycosyltransferase activity of OGT isolated from cells exposed to Ang1-7 was attenuated as compared to OGT from cells exposed to vehicle (Fig 5-4F).

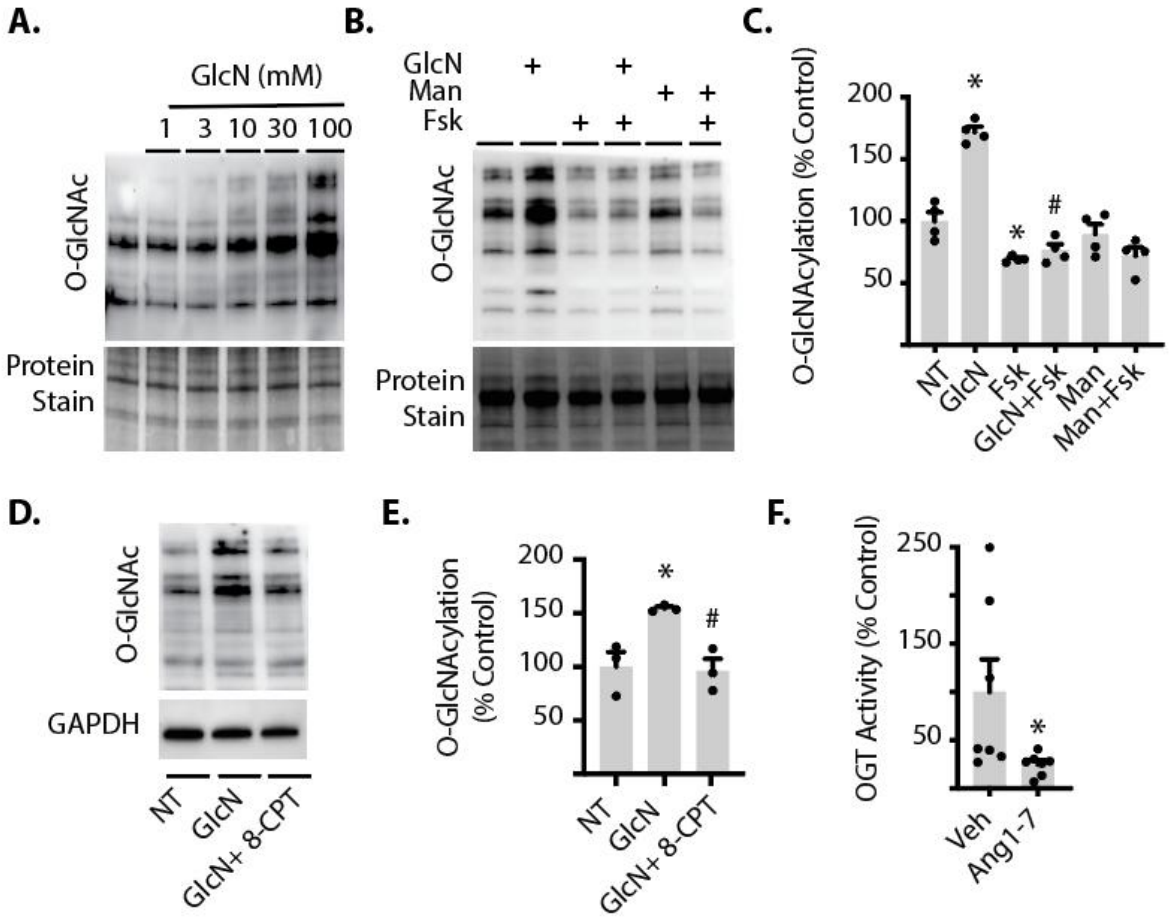

Figure 5-4. Ang1-7 inhibits OGT activity in retinal cells in culture. MIO-M1 cells were cultured in medium containing 5 mM glucose supplemented with 10% FBS. ***A*.** Cells were exposed to culture medium containing glucosamine (GlcN) for 24 h. *B-E*. Cells were exposed to culture medium containing 30 mM glucosamine (GlcN), 30 mM mannitol (Man), and/or Fsk or 8-CPT. Protein *O*-GlcNAcylation was assessed by Western blotting. Total protein levels were evaluated by staining. *O*-GlcNAcylation in *B* and *D*. was quantified in *C* and *E*. *F*. HA-tagged OGT was expressed in MIO-M1 cells in culture. 48 h after transfection, cells were exposed to Ang1-7 for 30 min, HA-tagged OGT was immunoprecipitated from cell lysates, and *in vitro* OGT activity was evaluated by glycosyltransferase assay. Data in *C* & *E* were analyzed by one-way ANOVA with Tukey's post-hoc analysis. Data in *F* were analyzed by unpaired t test. Results are expressed as means + SEM. *, $p<0.05$ versus no treatment (NT) or Veh; # $p<0.05$ versus GlcN or Veh.

Ang1-7 inhibits O-GlcNAcylation-induced mitochondrial superoxide

We recently reported that increasing retinal protein *O*-GlcNAcylation elevates levels of mitochondrial superoxide. To determine if Ang1-7 signaling could normalize the effect of O-GlcNAcylation on superoxide levels, MitoSox staining was evaluated in MIO-M1 cells. OGA inhibition increased superoxide in MIO-M1 cells; however, Ang1-7 (Fig 5-5A-B) or the Mas receptor agonist AVE 0991 (Fig 5-5C-D) reversed the TMG effect on superoxide levels. Similarly, in MIO-M1 cells exposed to hyperglycemic culture conditions, superoxide levels were found to be elevated, and Ang1-7 addition to culture medium was sufficient to normalize superoxide levels in cells exposed to hyperglycemic conditions. These results support the hypothesis that Ang1-7 signaling is sufficient to prevent increased mitochondrial superoxide production in response to stimuli that enhance *O*-GlcNAcylation.

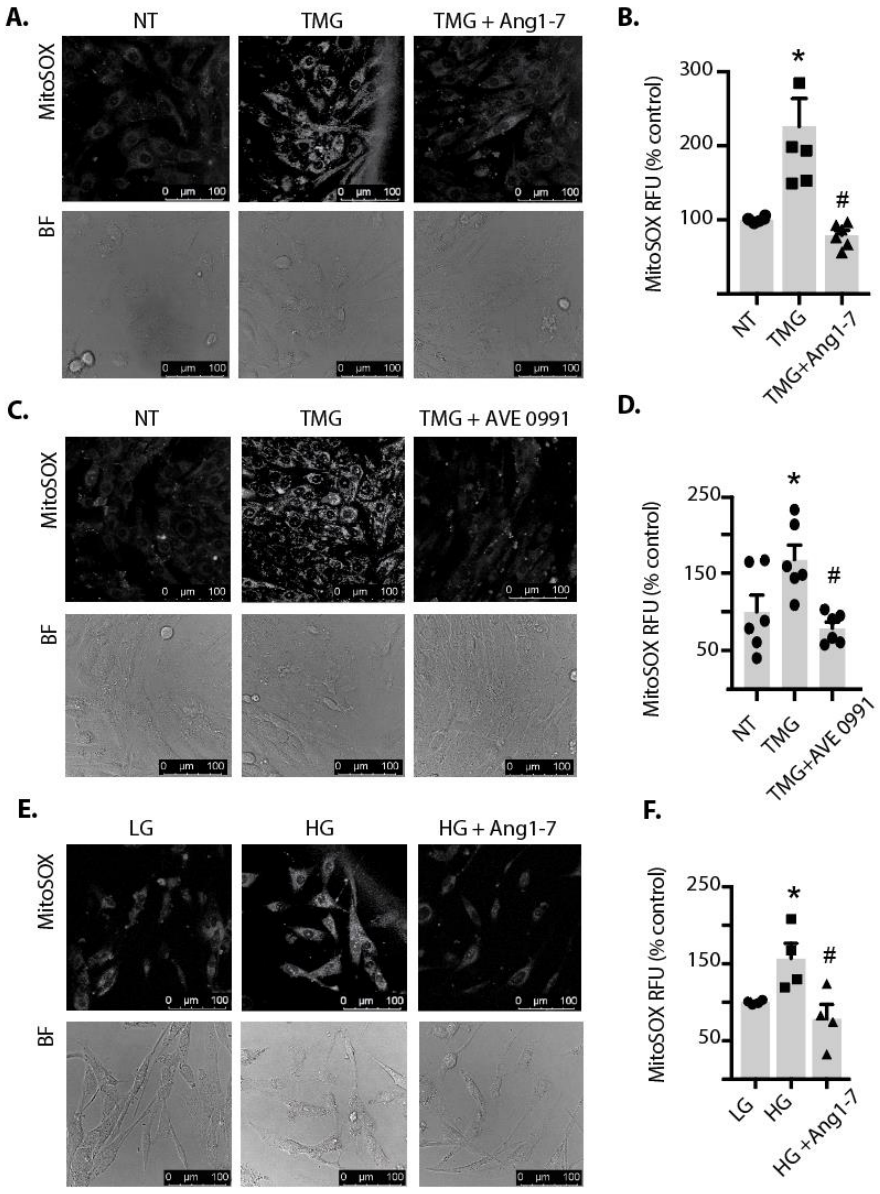

Figure 5-5. Ang1-7 inhibits *O*-GlcNAcylation-induced mitochondrial superoxide in retinal cells in culture. MIO-M1 cells were cultured in medium containing 5 mM glucose supplemented with 10% FBS. *A-D*. Cells were exposed to culture medium containing TMG in the presence or absence of Ang1-7 or the Mas receptor agonist AVE 0991. *E-F*. Cells were exposed to culture medium containing 30 mM glucose (HG) in the presence or absence of Ang1-7. Mitochondrial superoxide was assessed in live cells by MitoSox Red. MitoSox fluorescence was visualized by confocal laser microscopy (*A.*, *C.*, & *E.)* and quantified (*B.*, *D.* & *F.*, respectively). Representative MitoSox and bright-field (BF) images are shown. Data were analyzed by one-way ANOVA with Tukey's post-hoc analysis. Results are expressed as means + SEM. *, $p<0.05$ versus no treatment (NT) or low glucose (LG); #, $p<0.05$ versus TMG or HG alone. RFU, relative fluorescence units.

Discussion

In the present chapter, we evaluated the impact of pathways activated by Ang1-7 and cAMP on *O*-GlcNAcylation of retinal proteins. In this study, we found that in the retina of HFD mice, captopril attenuated retinal protein *O*-GlcNAcylation, and the effect was prevented by Mas-receptor inhibition. This finding provides mechanistic insight into the role for elevated Ang1-7 levels in the beneficial effects of ACE inhibition in retina and suggests that direct targeting of this hormone may be advantageous. Surprisingly, the repressive effect of captopril was not explained by a reduction in the expression of GFAT2, or other enzymes linked to *O*-GlcNAcylation (i.e., GFAT1, OGT, OGA). Rather, the results here are consistent with a model wherein Mas receptor activation by Ang1-7 inhibits OGT activity via activation of EPAC/Rap1 (Fig 5-6).

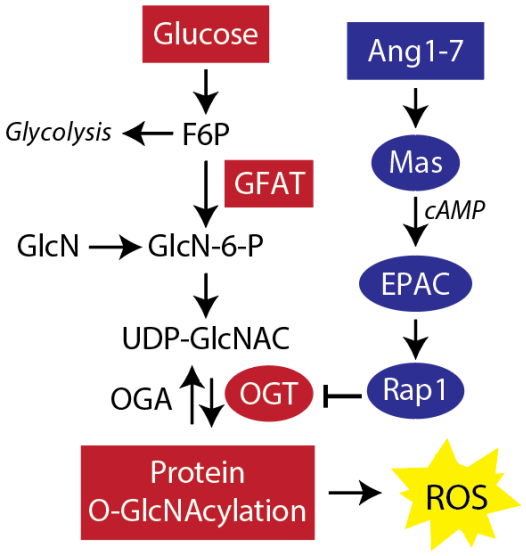

Figure 5-6. Working model for inhibition of retinal protein *O*-GlcNAcylation by Ang1-7. The results support a model wherein Ang1-7 inhibits *O*-GlcNAcylation-induced reactive oxygen species (ROS) via a novel Mas/EPAC/Rap1/OGT signaling axis. Ang1-7 activates the Mas receptor to enhance cAMP levels and activate EPAC. In turn, EPAC promotes Rap1 GDP release and GTP binding. Activation of this signaling axis suppresses protein *O*-GlcNAcylation downstream of GFAT by inhibiting OGT activity.

This study extends upon previous seminal work in the field demonstrating that retinal Müller cells are an important source of AngII and its metabolite Ang1-7, and that the ACEi captopril can cross the blood-retinal barrier to increase levels of Ang1-7 [129, 261]. The existence of an ocular RAS including components of the Ang1-7-ACE2-Mas receptor axis has been well documented [130, 241, 245, 247, 262-265], but the signaling cascades

activated downstream of the Mas receptor in retinal Müller cells are not well defined. Herein, we found cAMP levels were elevated in MIO-M1 retinal cells following exposure to culture medium containing Ang1-7. An increase in cellular cAMP concentrations following exposure to Ang1-7 has been previously described in other cell types [266] and found to be dependent on activation of the Mas receptor and adenylate cyclase [258]. Increasing intracellular cAMP concentrations via stimulation of adenylate cyclase has also been reported to decrease protein *O*-GlcNAcylation in kidney cell cultures exposed to hyperglycemic conditions [260]. Notably, a reduction in *O*-GlcNAc levels following adenylate cyclase stimulation in kidney cell cultures was overcome by supplementation with GlcN [260]. GlcN enters the HBP upon direct phosphorylation to GlcN-6-P, and thus bypasses the rate-limiting GFAT enzymes. Coupled with the finding that PKA inhibits GFAT1 by phosphorylating the enzyme on S205 *in vitro* [260], the preceding observations led us to initially hypothesize that the Ang1-7-initiated signaling cascade inhibits *O*-GlcNAcylation by repressing GFAT1 activity. However, we subsequently discovered that in both the retina of mice fed a HFD and in Müller cells in culture, GFAT2 is the predominant isoform, rather than GFAT1[45]. Unlike GFAT1, the enzymatic activity of GFAT2 is enhanced by PKA-dependent phosphorylation [267]. Thus, a repressive effect of PKA activation on *O*-GlcNAcylation, mediated by phosphorylation of the GFAT isoforms seemed unlikely. Indeed, PKA inhibition was not sufficient to prevent the repressive effect of adenylate cyclase activation on *O*-GlcNAcylation in Müller cells.

The signaling events initiated by cAMP are classically thought of as being mediated by PKA; however, EPAC is another key signaling molecule that is sensitive to this second messenger [268]. EPAC functions as the guanine nucleotide exchange factor for the small GTPase Rap1. EPAC1 and EPAC2 protein isoforms are differentially expressed in retina [269]. With immunostaining, both EPAC isoforms colocalize in Müller cell bodies within the inner nuclear layer of the retina [269]. In the present study, EPAC inhibition prevented the repressive

effect of adenylate cyclase activation on protein *O*-GlcNAcylation in Müller cells in culture. Moreover, expression of a constitutively active Rap1 variant was sufficient to repress *O*-GlcNAcylation in Müller cells following OGA inhibition. We initially suspected that cAMP/EPAC/Rap1 signaling acted to repress *O*-GlcNAcylation via a reduction in GFAT2 enzymatic activity, and thus functioned in a manner analogous to PKA-dependent GFAT1 inhibition in other cell types. However, unlike the previous observation in kidney cell cultures [260], adenylate cyclase activation was, in fact, sufficient to inhibit GlcN-induced protein *O*-GlcNAcylation in Müller cells in culture. Thus, the results are consistent with a model wherein EPAC and Rap1 act to inhibit *O*-GlcNAcylation downstream of GFAT.

In this chapter, we provided evidence that Ang1-7 exerts an inhibitory effect on OGT activity via EPAC activation. While one study has identified a novel interaction between the glycolytic enzyme pyruvate kinase and soluble adenylate cyclase that results in EPAC/Rap1 activation [270], there are currently no studies demonstrating that EPAC interacts with the metabolic enzymes of the HBP. The results here support a model wherein EPAC activation inhibits O-GlcNAcylation downstream of GFAT. Importantly, other enzymes upstream of OGT and downstream of GFAT may also be impacted. A possible mechanism by which the Ang1-7/Mas/EPAC/Rap1 axis may act to repress OGT activity is via activation of a tyrosine phosphatase. Insulin-stimulated phosphorylation of tyrosine residues on OGT enhances the enzyme's catalytic activity [271]. *In vitro*, OGT is directly phosphorylated by Src tyrosine kinase, as it contains well-over a dozen predicted Src tyrosine phosphorylation sites [271]. This is consistent with a stimulatory effect of tyrosine phosphatase inhibitors on OGT activity [271]. In proximal tubular cells, Ang1-7 acts via the Mas receptor to promote Src homology 2-containing protein-tyrosine phosphatase-1 (SHP-1) activity [272] and Rap1b-deficient cells have impaired SHP-1 activity [273]. It is therefore tempting to speculate that pathways initiating a cAMP second messenger response may suppress OGT activity by promoting EPAC/Rap1-dependent activation

of SHP-1 and OGT dephosphorylation. Unfortunately, we were unable to consistently detect OGT tyrosine phosphorylation by Western blotting following immunoprecipitation of the protein.

As discussed in chapter 3, mitochondrial dysfunction and increased ROS production are central to the development of diabetic retinopathy [191, 194, 255, 256]. As a critical regulator of mitochondrial function [179, 180], the *O*-GlcNAc modification post-translationally modifies several mitochondrial proteins directly in response to diabetes and hyperglycemic conditions [181, 182]. We recently reported that enhanced *O*-GlcNAcylation of retinal proteins promotes 4E-BP1-dependent mitochondrial dysfunction and oxidative stress. In that study, the OGA inhibitor TMG enhanced *O*-GlcNAcylation and increased reactive oxygen species in the retina. Here, Müller cells exposed to TMG exhibited an increase in mitochondrial superoxide production. However, Ang1-7 addition to culture medium was not only sufficient to prevent an increase in *O*-GlcNAcylation, but also normalized mitochondrial superoxide levels following OGA inhibition. This supports the observation that diabetes-induced oxidative stress is normalized in the retina of diabetic rodents receiving intraocular AAV-Ang1-7/ACE2 [130, 250]. The finding that Ang1-7 activates the EPAC/Rap1 signaling axis and attenuates mitochondrial superoxide production supports previous studies indicating EPAC activation suppresses ROS production [274-276]. Thus, strategies to enhance Ang1-7-mediated EPAC activation in retina could serve to prevent the increase in oxidative stress that is associated with diabetes-induced *O*-GlcNAcylation.

The present study identified a novel molecular link between Ang1-7, protein *O*-GlcNAcylation, and ROS production in retina. Ang1-7 signaling reduced protein *O*-GlcNAcylation in the retina of HFD mice. Similarly, Ang1-7 attenuated *O*-GlcNAcylation in human Müller cells by increased production of cAMP, with this effect dependent on EPAC activation. Specifically, Ang1-7 inhibited OGT activity. Thus, while further studies are needed, targeted activation of this newly identified Ang1-7/EPAC/OGT signaling axis may be beneficial

in correcting the abnormally elevated protein *O*-GlcNAcylation that is associated with diabetic retinal complications.

Chapter 6

Discussion

Summary

The pathophysiologic basis for the retina's vulnerability to hyperglycemia remains elusive despite years of clinical and laboratory investigation. Evidence supports a role for increased flux through the HBP and dysregulation of O-GlcNAc cycling in the pathogenesis of DR [277]. It was the aim of this dissertation to investigate the negative effects of enhanced retinal protein O-GlcNAcylation on mRNA translation and identify a mechanism by which it is attenuated. Many descriptive studies have identified O-GlcNAc modified transcription factors, but studies investigating the effects of this modification on protein synthesis are lacking. Therefore, O-GlcNAc-mediated control of gene expression at the level of mRNA translation is a potentially underappreciated phenomenon that could have far-reaching clinical implications. Indeed, the data presented in this thesis expand our knowledge of O-GlcNAc-mediated control of gene expression in the retina and contribute noteworthy findings to the wider field of retinal physiology. First, results from deep sequencing analysis and ribosome profiling in mice administered TMG described in Chapter 3 demonstrated that enhanced retinal protein O-GlcNAcylation primarily altered retinal gene expression at the level of mRNA translation. We confirmed this finding by validating top-scoring gene candidates from our RiboSeq dataset via sucrose density centrifugation and polysome fractionation. Furthermore, a molecular network of mitochondrial mRNAs regulated translationally via 4E-BP1 upon exposure to TMG was identified. 4E-BP1 sequestration of eIF4E was found to be necessary for O-GlcNAcylation-

induced superoxide production. Expression of a 4E-BP1 variant (F113A) that prevents phosphorylation by mTORC1 and promotes eIF4E binding enhanced mitochondrial superoxide production. However, in cells expressing a 4E-BP1 variant (Y54A) that is deficient in binding to eIF4E, TMG exposure did not enhance mitochondrial superoxide levels. Addition of WT 4E-BP1 to cells deficient in 4E-BP1/2 was sufficient to promote production of superoxide upon TMG exposure. *In vivo*, we observed both O-GlcNAcylation- and diabetes-induced ROS production that localized predominately to the photoreceptor layer in wild type mice that was not present in 4E-BP1/2 deficient mice. These results are consistent with previous work attributing induction of superoxide in diabetic rodents largely to photoreceptors, cells that use more oxygen and contain more mitochondria than other cell types found within the retina [167, 278]. Overall, the results from Chapter 3 suggest enhanced retinal protein O-GlcNAcylation promotes binding of eIF4E to 4E-BP1 to alter the pattern of mRNAs selected for translation, culminating in disruption of the dynamic function of mitochondria and subsequent generation of mitochondrial superoxide and ROS.

The second significant finding described in Chapter 4 was that translation of the mRNA encoding CD40, a critical driver of retinal inflammation and DR pathology, was enhanced by both OGA inhibition and diabetes via a 4E-BP-dependent mechanism. CD40 translation was assessed by sucrose density centrifugation and subsequent polysome fractionation. The distribution of CD40 mRNA in fractions collected from mice administered TMG showed that enhanced O-GlcNAcylation caused a shift of the CD40 mRNA into the polysomal fraction. Importantly, total CD40 mRNA abundance was not altered in whole retinal lysates from mice administered TMG. We confirmed the same increase in CD40 mRNA translation occurred independently of changes in total CD40 mRNA abundance in a model of chemically induced diabetes. Notably, the diabetes-induced translation effect was dependent upon 4E-BP. We evaluated Nos2 expression as a downstream marker of inflammation and found mRNA

expression to be upregulated in wild type diabetic mice, but not in diabetic mice lacking 4E-BP1/2. Using a novel RiboTag mouse model in which the ribosomal protein Rpl22 is HA-tagged only in Müller glia, we also discovered CD40 mRNA associated with Müller glial ribosomes is increased in both TMG treated and diabetic mice as early as 4 weeks diabetes duration. The 5'-UTR of CD40 was sufficient to drive expression of a reporter under the control of the CD40 5'-UTR in wild type cells exposed to TMG, but not in 4E-BP-deficient cells. Finally, in the human retinal Müller cell line MIO-MI, expression of the F113A 4E-BP1 variant was sufficient to similarly drive expression of the CD40 reporter under control of the CD40 5'-UTR. Consistent with previous data from our group demonstrating hyperglycemia and OGA inhibition promote binding of 4E-BP with eIF4E [93, 95] and the findings of Chapter 3, these data support a model wherein enhanced O-GlcNAcylation of 4E-BP alters the pattern of mRNAs selected for translation resulting in the promotion of oxidative stress and inflammatory signaling cascades initiated by expression of CD40 in Müller glia.

Finally, Chapter 5 describes the significant finding that Ang1-7 inhibits retinal protein O-GlcNAcylation via an EPAC/Rap1/OGT signaling axis. These data extend upon previous clinical studies indicating pharmacological blockade of the RAS improves visual outcomes in DR patients, although the mechanism responsible for mediating such effects remains unknown [118]. Our work presented here is the first to define specific molecular signaling events that may mediate the beneficial effects of Ang1-7 in retina. Specifically, we reported that retinal protein O-GlcNAcylation in mice fed a HFD and administered the ACEi captopril was significantly attenuated compared to mice fed a HFD and receiving no intervention. Notably, this attenuation was dependent upon Ang1-7 mediated signaling as administration of a Mas receptor antagonist reversed the captopril-induced attenuation of retinal protein O-GlcNAcylation. These changes were independent of changes in expression levels of OGA, OGT, or GFAT, indicating the activity rather than the level of these proteins were potentially affecting retinal protein O-GlcNAcylation

in our animal model. Exposure to Ang1-7 increased cAMP levels and similarly attenuated TMG-induced protein O-GlcNAcylation in retinal cells in culture, and we determined this effect to be mediated by EPAC rather than PKA. Given that we could not overcome cAMP-mediated suppression of protein O-GlcNAcylation with glucosamine, a metabolite that enters the HBP downstream of GFAT, we suspected activation of EPAC suppressed OGT activity. Indeed, exposure of retinal cells in culture to Ang1-7 attenuated OGT activity. We further demonstrated Ang1-7 attenuates TMG- and high glucose-induced production of mitochondrial superoxide. Collectively, these data presented in Chapters 3-5 suggest hyperglycemia-mediated disruption in O-GlcNAc cycling contributes to underlying biochemical mechanisms such as oxidative stress and chronic inflammation that are hypothesized to contribute to the deterioration of retinal function during the development and progression of DR.

Protein Synthesis in DR

Protein synthesis is an energy-intensive metabolic process and must be elegantly coordinated and integrated with the physiological and nutritional status of the whole cell. The retina is one of the most metabolically active tissues in the body. Therefore, retinal protein synthesis may be particularly susceptible to disturbances in the metabolic environment, such as occurs in diabetes. Notably, reduced protein synthesis is a characteristic feature of insulin deficiency in diabetes in insulin-sensitive tissues, such as skeletal muscle [279]. Alternatively, studies in brain have demonstrated no loss of protein occurs in brains of animals in which skeletal muscle and liver protein degradation is high [280]. In tissues such as skeletal muscle, protein synthesis is directed by mTORC1, which acts downstream of the insulin receptor/PI3K/Akt pathway [281]. Under normal metabolic conditions, the insulin receptor/PI3K/Akt pathway is highly active in the retina [282, 283]. Although the retina is

insensitive to fasting and re-feeding, unlike other insulin sensitive tissues, the activity of the insulin signaling pathway is, in fact, attenuated by diabetes [283]. Rodent models of type 1 diabetes also indicate the rates of retinal protein synthesis are reduced 39% in 12-week diabetic rats, accompanied by a 66% reduction in retinal protein degradation such that there is not net loss of retinal matter [160]. Of note, Fort and colleagues concluded type 1 diabetes did not affect 4E-BP in diabetic rodents [160]. However, this conclusion was largely based on examining levels of phosphorylated 4E-BP1 at threonine residues 37 and 46. Threonine residues 37/46 are resistant to rapamycin in some cells, and therefore are not always be used as a reliable readout of changes in mTORC1 activity. Previous work by our lab indicates hyperglycemia promotes O-GlcNAcylation of 4E-BP1 at threonine 82, thereby enhancing its stability, potentially via prevention of a competing phosphorylation event by GSK3β [95]. Therefore, while mTORC1 activity may not be attenuated in retina from diabetic rodents, O-GlcNAc modification of 4E-BP1 may contribute to alterations in retinal protein synthesis. The evidence presented in this dissertation extends upon the previous work to demonstrate 4E-BP is necessary to mediate O-GlcNAcylation-induced shifts in the pattern of mRNAs selected for translation. We have shown O-GlcNAcylation enhances the interaction between eIF4E and 4E-BP, and thereby suppresses translation of mRNAs relying on a cap-dependent mechanism. As a result, mRNAs that contain internal, highly-structured elements are more likely to recruit ribosomes when they do not have to compete with mRNAs relying on an eIF4E-mediated cap-dependent translation mechanism. Thus, O-GlcNAcylation of 4E-BP plays a critical role not in linearly regulating the rate of protein synthesis, but rather in regulating which messages get translated into retinal protein.

Müller Glia and DR

The work presented in this dissertation highlights the central role dysfunctional Müller cells play in DR pathogenesis. Via the use of a novel RiboTag mouse model in which ribosomal protein Rpl22 was HA-tagged only in Müller glia, we demonstrated the level of ribosome-associated CD40, a gene sensitive to TMG-induced alterations in mRNA translation, was enhanced in both diabetic mice and mice administered TMG. These findings are consistent with previous studies describing CD40 expression in Müller glia, rather than activated microglia, as a driver of expression of other pro-inflammatory molecules, resulting in chronic low-grade retinal inflammation that may contribute to apoptosis of neighboring retinal neurons, endothelial cells, or glial cells.

We also identify a signaling cascade in which the RAS effector peptide Ang1-7 attenuates retinal protein O-GlcNAcylation in Müller cells. Specifically, we provide evidence that Ang1-7 treatment stimulates cAMP production, and activation of cAMP-mediated signaling cascades in Müller cells selectively signals via EPAC to attenuate OGT activity. Interestingly, stimulation of β-2-adrenergic receptors in Müller cell cultures resulted in improvement in insulin receptor signaling as evidenced by increased tyrosine phosphorylation of the insulin receptor as well as increased Akt phosphorylation at serine 473 (a phosphorylation event directed by mTORC2) [284]. β-2-adrenergic receptors are G protein-coupled receptors that are coupled to G_s proteins such that when bound, adenylate cyclase is stimulated to generate cAMP. Therefore, stimulating cAMP-mediated signaling cascades improves insulin action in Müller cells. Notably, β-2-adrenergic receptor stimulation in Müller cells also reduces expression of inflammatory markers, such as TNF-α [284]. Walker and colleagues suggest stimulation of cAMP production via β-2-adrenergic receptor agonism inhibits cytokine release in retinal Müller cells exposed to hyperglycemia, resulting in a decrease of inhibitory serine phosphorylation of IRS-1 [284].

Increases in global O-GlcNAcylation promotes IRS1 serine phosphorylation, leading to attenuation of insulin signaling [56-58]. Therefore, the work presented collectively in this dissertation could provide a mechanistic explanation for the cAMP-mediated attenuation of cytokine production in Müller glia observed by Walker *et al*. That is to say, stimulating cAMP production in Müller cells could activate the EPAC/Rap1 axis to attenuate OGT activity, thereby attenuating protein O-GlcNAcylation. Attenuating retinal protein O-GlcNAcylation could prevent enhanced sequestration of eIF4E by 4E-BP1, thereby increasing competition for ribosome recruitment by mRNAs such as CD40 that may rely upon cap-independent translation as a mechanism for expression. As Portillo *et al*. demonstrated, CD40 expression in Müller glia drives expression of other pro-inflammatory cytokines, including TNF-α [200]. Therefore, increasing competition for ribosome binding to the CD40 mRNA via attenuation of protein O-GlcNAcylation may reduce CD40-mediated expression of inflammatory markers in the retina.

In the work presented in this dissertation, O-GlcNAcylation was enhanced in Müller cells via OGA inhibition or glucosamine. Attempts to induce O-GlcNAcylation in Müller cell culture via exposure to high glucose cell culture medium for 24 hours were largely unsuccessful. Müller cells are thought of as the "hardy" cells in the retina—they are relatively resistant to metabolic insults. Whether other effects of high glucose, such as cell death, occur in Müller glia has long been debated. However, work from the research group of Mohr have demonstrated diabetes leads to significant Müller cell loss at 7 months duration of chemically-induced diabetes in retinas of diabetic mice compared to non-diabetic [285]. Given the extended time required to detect Müller glial loss *in vivo*, exposure to high glucose for 24 hours *in vitro* was likely insufficient to perturb Müller cell metabolic pathways and O-GlcNAc cycling. Attempts in our lab to detect apoptotic cell death in Müller MIO-MI cells exposed to high glucose cell culture medium have also been similarly unsuccessful. However, Müller cells are reported to die via an inflammatory-driven type of cell death known as pyroptosis mediated by caspase-1 activation [14, 286]. This likely explains

why our attempts at probing for apoptotic markers of cell death (*e.g*. caspase-3 cleavage) were unfruitful. Interestingly, caspase-1 activation is a critical step in the maturation process and subsequent secretion of the cytokine IL-1β [287]. Therefore, production of pro-inflammatory molecules driven by Müller glia could contribute to pyroptosis of Müller cells, an important reservoir of neurotrophic growth factors and neuronal metabolic support.

Loss of Müller glia is accelerated when VEGF-mediated signaling is disrupted specifically in Müller cells of diabetic rodents [288]. Given that anti-VEGF therapies are the first-line treatment for DR, it is possible an unintended consequence of these drugs is accelerated Müller cell loss. The argument could be made, however, that clearance of malfunctioning Müller cells secreting inflammatory cytokines serves as a mechanism to remove detrimental signals in the retina. On the other hand, Müller cell loss has been associated with aneurysm formation, a clinical manifestation of DR [289]. More studies are necessary to determine when Müller glial responses to the diabetic milieu become maladaptive in the retina. Regardless, understanding the function of this dominant retinal cell type and finding ways to restore that function could have far-reaching clinical application.

State of Therapeutic Intervention in DR

Currently available clinical interventions for DR include intravitreal injection of anti-VEGF antibodies or pan-retinal photocoagulation. Intravitreal injections are an invasive procedure that are associated with several risks including endopthalmitis and retinal detachment. Pan-retinal photocoagulation is an inherently destructive technique aimed at ablating the proliferating blood vessels in the peripheral retina. Neither clinically available intervention is universally effective at reversing nor preventing vision loss. These therapeutic interventions for DR and associated diabetes-related ocular pathologies are targeted at consequences of the disease,

rather than underlying molecular abnormalities. As a result, there remains a significant population of patients in which these available treatments are ineffective. For example, anti-VEGF antibodies are effective in only half of diabetic macular edema patients [290]. Therefore, there is a need to better understand the early biochemical changes made in the retina in the adaptive phase during the early stages of diabetes onset.

The work presented in this dissertation identifies a novel pharmacologic strategy using Ang1-7 to stimulate cAMP production, resulting in attenuation of retinal protein O-GlcNAcylation via EPAC-mediated inhibition of OGT activity. Based on the collective findings of this work, attenuating retinal protein O-GlcNAcylation could do much to reduce oxidative stress and expression of pro-inflammatory molecules that could contribute to retinal dysfunction. Notably, a recent study supports a protective role for EPAC1-Rap1 signaling in retinal endothelial cells, as activation of the pathway not only prevents, but reverses VEGF-induced retinal vascular permeability [291]. In DR, VEGF signaling plays a causal role in the development of vascular permeability and angiogenesis [292]. VEGF acts, at least in part, by activating PKC β, which phosphorylates occludin, an integral membrane protein that is a key component of tight junctions [293],[294]. Phosphorylation of occludin by PKC at S490 prevents the interaction with other tight junction proteins [295]. Notably, S490 on occludin has also been identified as a site of O-GlcNAcylation [296]. Therefore, utilizing Ang1-7 or other EPAC activators could potentiate dual therapeutic benefit in the retina via attenuation of protein O-GlcNAcylation: 1) reducing oxidative stress and retinal inflammation and 2) improving vascular permeability. The evidence presented in this dissertation identifies novel pharmacological targets that could serve as clinical alternatives to DR patients who do not respond to limited currently available therapies, and therefore have no other option to preserve their vision.

Future Directions

Translational regulation of specific transcripts is generally achieved by RNA binding proteins that recognize cis-elements in the 5'- or 3'-UTR of an mRNA [297]. In chapter 4, we observed the 5'-UTR of CD40 was sufficient to enhance CD40 translation upon exposure to TMG. However, our studies did not address the contribution of the CD40 3'-UTR to regulating translation of the CD40 mRNA. A computational study of a large UTR database revealed the mean 3'-UTR length of human transcripts is on the order of >500 nucleotides, whereas the 5'-UTR is an average of ~150 nucleotides long [298]. Therefore, the extended length of the 3'-UTR may also significantly contribute to transcript-specific translational control. The 3'-UTR of CD40 at 741 nucleotides is notably longer than the 5'-UTR at 72 nucleotides. Additional studies utilizing a reporter containing either the CD40 3'-UTR and both the 5'-UTR and 3'-UTR could be a rigorous approach to fully elucidate what structural features of the CD40 mRNA are necessary for TMG-induced translation. Translational control of the CD40 mRNA enacted via RNA binding proteins is not well studied. In order to investigate the mechanism by which the 5'-UTR drives translation of CD40 upon TMG exposure, we created biotinylated probes containing either the CD40 5'-UTR or a scrambled sequence. Studies are underway to identify RNA binding proteins that immunoprecipitate with our biotinylated probes. Given the lack of study on translational control of CD40, understanding how expression of CD40 is regulated could be clinically beneficial as increased CD40 abundance is also associated with autoimmune disorders and cancer [231, 299, 300].

Notably in Chapter 4, the majority of the CD40 mRNA was present in the polysomal fraction collected from 4E-BP1/2-deficient MEFs which is not consistent with a model in which O-GlcNAcylation of 4E-BP1 promotes sequestration of eIF4E such that cap-independent translation of CD40 is enhanced. However, our luciferase studies (Appendix D) suggested the

expression ratio of Firefly:Renilla was decreased in 4E-BP1/2-deficient cells relative to WT cells. These results are not consistent with the results obtained from polysomal fractions collected from 4E-BP1/2-deficient MEFs. Therefore, it is possible a secondary mechanism independent of the CD40 5'-UTR regulates expression of the full length CD40 mRNA that is not captured in our reporter studies singularly evaluating the 5'-UTR. Our observations using a bicistronic reporter do support a role for TMG-induced 4E-BP1/2-mediated translational control dependent upon the CD40 5'-UTR. However, we also observe a 4E-BP1/2-dependent effect on CD40 translation that may be independent of the 5'-UTR. More studies are necessary to fully establish this unexpected dual mechanism of translational control in which 4E-BP may suppress an unknown activator of CD40 expression in MEFs. Given that lack of 4E-BP did not similarly shift the distribution of the CD40 mRNA into the polysomal fraction collected from 4E-BP1/2-deficient mice, additional studies investigating differential and cell-type specific expression of potential regulators are also needed to identify this novel secondary mechanism of regulation.

RNAs are also subject to internal chemical modifications such as methylation that act to fine-tune mRNA structure and function. N6-methyladenosine (m^6A), the most prevalent internal modification of mRNA, is mediated through "writer" and "eraser" proteins. Depletion of the m^6A writer METTL14 enhanced CD40 protein levels in B cells [301]. Interestingly, we reported METTL14 as a gene translationally repressed in retina obtained from mice administered TMG (Chapter 3). Therefore, it is possible a reduction in CD40 m^6A modification as a result of attenuated translational efficiency of METTL14 may also contribute to the O-GlcNAcylation-induced enhanced CD40 translation we reported in chapter 4.

In chapter 3, we demonstrated TMG administration in mice causes the Sod2 mRNA to shift into the subpolysomal fraction. However, in fractions collected from retina of WT diabetic mice but not in 4E-BP-deficient mice at both 4- and 12-weeks diabetes duration, the distribution of Sod2 shifts into the polysomal fraction without a concomitant increase in total Sod2 mRNA

(Appendix C). These seemingly contradictory results could be explained by the two-phase adaptive process previously described by Tan *et al* in which acute exposure to enhanced O-GlcNAcylation enhances cellular respiration and ROS production, both of which are attenuated as the length of exposure to enhanced O-GlcNAcylation lengthens [180]. Therefore, it is possible the acute 24-hour TMG treatment results in suppression of Sod2 mRNA translation and consequent increased levels of retinal ROS production while the chronic exposure to hyperglycemia in diabetic animals may mediate upregulation of Sod2 at the level of mRNA translation. The 5'-UTR of Sod2 is particularly GC rich (70%) [302] and is predicted to form a stem-loop structure (RNAfold Web Sever). Therefore, it is possible Sod2 contains a secondary structure that suppresses cap-dependent translation and thus enables cap-independent translation when O-GlcNAcylation is elevated and the interaction between 4E-BP1 and eIF4E is enhanced. However, there is also evidence to support a role for a translational enhancer element, MnSodRE (MnSod response element), in the 3'-UTR of Sod2 [303]. Furthermore, the RNA binding protein MnSodBP binds to the Sod2 3'-UTR to mediate efficient translation [304]. MnSodBP is negatively regulated by tyrosine phosphorylation [305]; therefore it is tempting to speculate a competing O-GlcNAcylation event could override tyrosine phosphorylation-mediated suppression of MnSodBP activity. However, it is not currently known if MnSodBP is O-GlcNAc modified.

Enhanced translation of Sod2 in diabetes was a surprising finding, given the role of aberrant ROS production in the pathogenesis of DR. However, enhanced Sod2 translation does not necessarily equate to increased levels of functional Sod2. While Sod2 translation may be enhanced in the retina of wild type diabetic mice, we did not evaluate Sod2 activity in our animals. Sod2 activity is suppressed in diabetic rats [194]. Furthermore, levels of acetylated Sod2 are negatively correlated with its enzymatic activity. Sirtuin 3 (SIRT3) is a de-acetylase that is stimulated by ROS to de-acetylate Sod2 and thus activate the antioxidant enzyme [306]. Notably,

O-GlcNAcylation influences SIRT3 expression [307]; however, O-GlcNAcylation of Sod2 itself could also account for the attenuated enzymatic activity previously observed in diabetic rats [194, 308]. Furthermore, it is unknown if Sod2 protein is increased in retinal mitochondria from our animals. Sod2 is a nuclear encoded gene translated in the cytosol and imported into the mitochondria via TOM and TIM complexes [309]. In chapter 3, we reported several subunits of the TOM and TIM complexes to be translationally suppressed in retina obtained from mice administered TMG. Thus, it is also possible Sod2 translation is enhanced, but the enzyme is not efficiently imported into mitochondria and thus cannot quench ROS. Regardless of the functional activity of Sod2 in retina obtained from diabetic mice, it remains to be seen how opposite trends of Sod2 mRNA translation are accounted for in the context of acute enhanced O-GlcNAcylation versus chronic hyperglycemia. Understanding the translational mechanisms at work could be a fruitful area of future study.

Concluding Remarks

The retina requires high metabolic activity and tissue stability to maintain proper visual function. Metabolic insults, such as those encountered during diabetes, cause the retina to make adaptive changes in order to function in the new metabolic environment. Early adaptive changes involve attenuation of biosynthetic pathways. However, common signaling pathways in the retina regulate both biosynthesis and cell survival [283, 310], so loss of biosynthetic activity is part of a larger disruption of retinal metabolism that results in retinal cell death when the beginning adaptive changes become maladaptive. This process most likely occurs in diabetic patients before impairments in the retinal vasculature are clinically visible. However, at this early stage of the disease, defects in the neuroretina, such as electroretinographic responses and visual field

sensitivity, become manifest [311, 312]. Therefore, there is a need to understand what mediates the early metabolic adaptations the retina undergoes, and to understand how those alterations ultimately become maladaptive.

The global re-programming of retinal metabolism could be mediated, in part, via increased flux through the HBP and consequent enhanced protein O-GlcNAcylation. The HBP exists as a means to integrate nutritional signals and fine-tune cellular responses to biological cues. The retina is particularly dependent upon such fine-tune regulation given the sophisticated coordination required of the retinal neurovascular unit that must exist to visually process the outside world. We have demonstrated in this work that enhanced retinal protein O-GlcNAcylation primarily alters gene expression at the level of mRNA translation. We further provide evidence to support the hypothesis that O-GlcNAcylation enhances the interaction between 4E-BP1 and eIF4E to disrupt mitochondrial gene expression, resulting in increased superoxide and ROS production (Fig. 6-1). The data discussed in this work also supports a model wherein CD40 expression in Müller glia in translationally upregulated in response to both diabetes and enhanced retinal protein O-GlcNAcylation (Fig.6-1). Finally, we have demonstrated O-GlcNAcylation may be attenuated via Ang1-7 or cAMP-mediated attenuation of OGT activity (Fig. 6-1). Overall, diabetes-induced retinal protein O-GlcNAcylation serves to alter the pattern of mRNAs selected for translation, resulting in oxidative and inflammatory stress that may be attenuated via Ang1-7 treatment. In conclusion, this work has identified 4E-BP-mediated production of ROS, 4E-BP-

mediated expression of CD40 in Müller glia, and activation of EPAC/Rap1 as potential new targets for therapeutic intervention in DR patients.

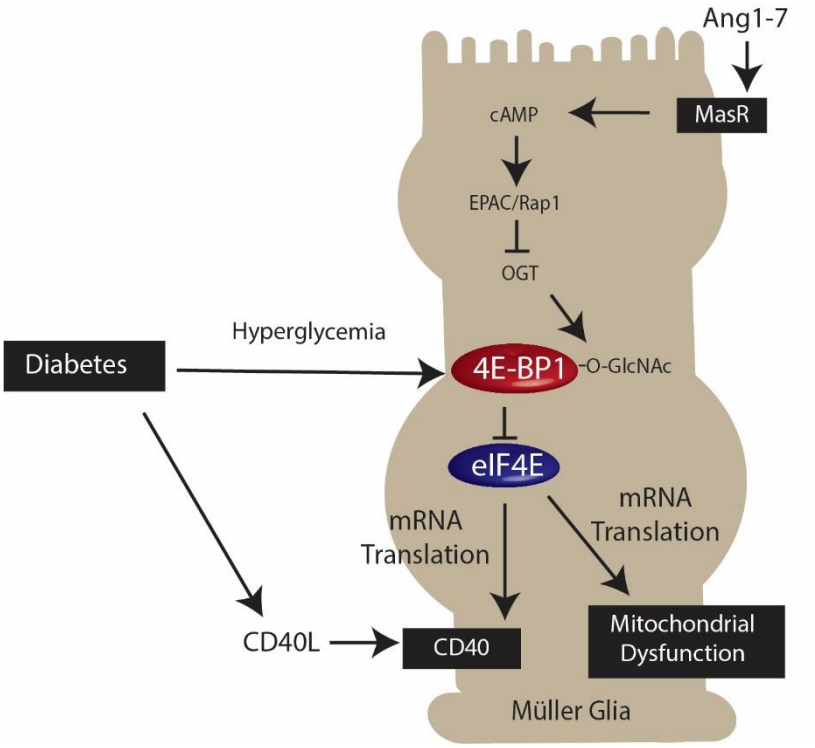

Figure 6-1. Summary Model. This dissertation provides evidence to support a model wherein Ang1-7 stimulates cAMP production to activate the EPAC/Rap1 signaling axis, thus inhibiting OGT activity. OGT facilitates protein O-GlcNAcylation. When 4E-BP is O-GlcNAcylated (such as in diabetes), eIF4E sequestration is enhanced. This alters the translation of several mRNAs encoding mitochondrial proteins, resulting in increased ROS production via a 4E-BP1 dependent mechanism. Similarly, enhanced O-GlcNAcylation promotes translation of the immune costimulatory receptor CD40 in Müller glia, which is a critical driver of retinal inflammation.

Appendix A

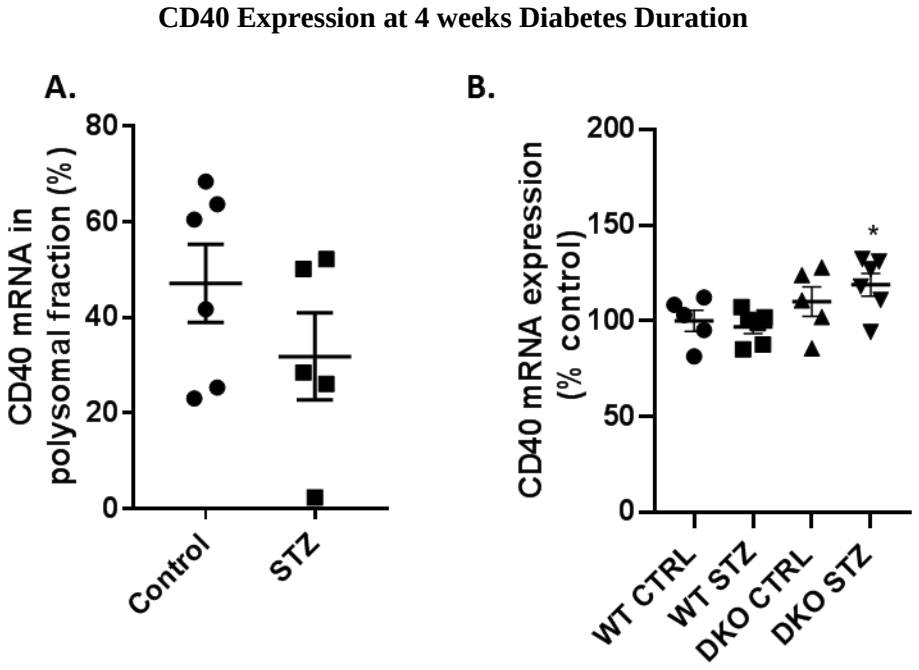

Figure A-1. CD40 translation is unchanged in STZ-induced diabetic mice at 4 weeks diabetes duration. *A.* Ribosomes were separated into either sub-polysomal (SP) or polysomal (P) fractions via sucrose density gradient centrifugation. The distribution of the mRNA CD40 was assessed in SP or P fractions via RT-PCR. Results are expressed as a relative percentage of the mRNA in the P fraction and are representative of 2 independent experiments. Values are means ± SE for three replicates assessing a pooled sample obtained from 8-10 retinas. *B.* CD40 mRNA expression in whole retina was assessed by PCR. Data were analyzed by one-way ANOVA with Tukey's post-hoc analysis *, $p<0.05$ versus WT STZ.

Appendix B

Inflammatory Gene Expression at 12 Weeks Diabetes Duration

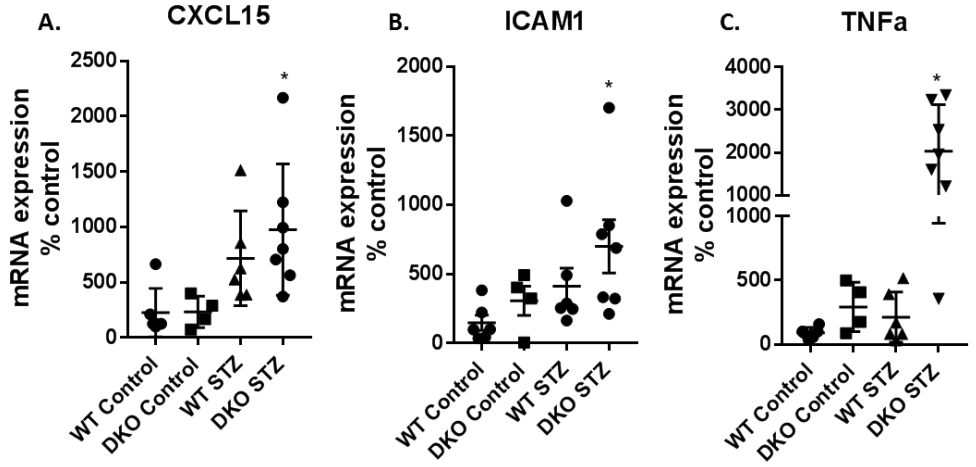

Figure B-1. 12 weeks diabetes duration enhances expression of select markers of inflammation in 4E-BP1/2 DKO mice but not in WT mice. *A-C.* CXCL15, ICAM1, and TNF-α mRNA expression in whole retina was assessed by PCR. Data were analyzed by one-way ANOVA with Tukey's post-hoc analysis. Values are means ± SE, n=4-7. *, $p<0.05$ versus WT Control.

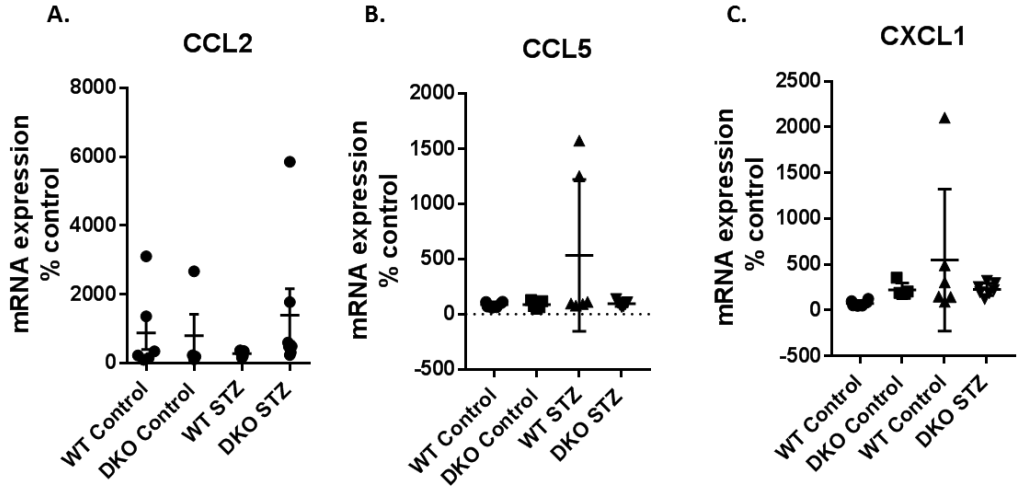

Figure B-2. 12 weeks diabetes duration does not change expression of select markers of inflammation in in WT or 4E-BP1/2 DKO mice. *A-C.* CCL2, CCL5, and CXCL1 mRNA expression in whole retina was assessed by PCR. Data were analyzed by one-way ANOVA with Tukey's post-hoc analysis. Values are means ± SE, n=4-7.

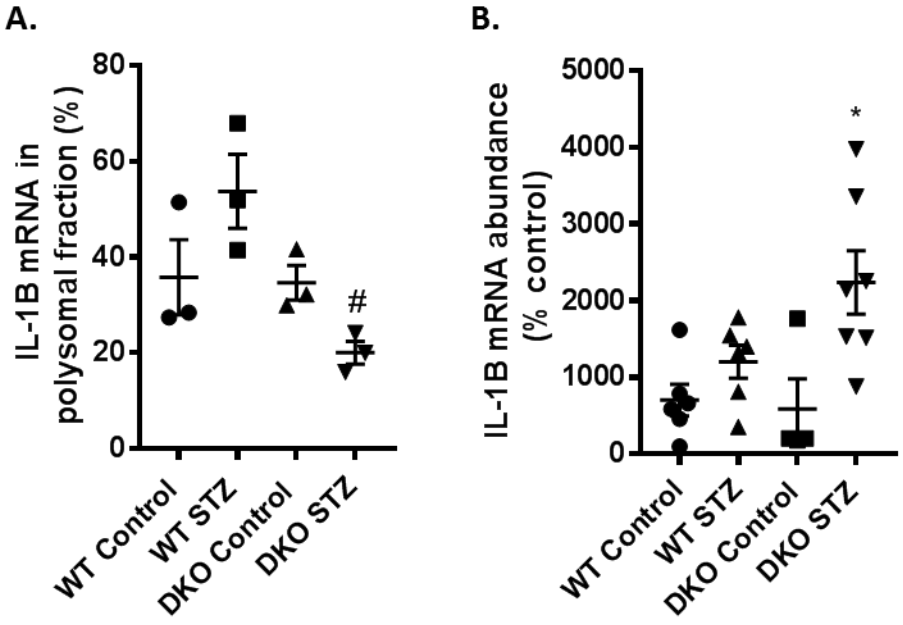

Figure B-3. IL-1β mRNA translation is suppressed while total IL-1β mRNA is increased in diabetic 4E-BP1/2 DKO mice. *A.* Ribosomes were separated into either sub-polysomal (SP) or polysomal (P) fractions via sucrose density gradient centrifugation after 12 weeks diabetes duration. The distribution of the mRNA IL-1β was assessed in SP or P fractions via RT-PCR. Results are expressed as a relative percentage of the mRNA in the P fraction. Values are means ± SE for three replicates assessing a pooled sample obtained from 8-10 retinas. *B.* IL-1β mRNA expression in whole retina was assessed by PCR after 12 weeks diabetes duration. Data were analyzed by one-way ANOVA with Tukey's post-hoc analysis. Values are means ± SE, n=4-7. *, $p<0.05$ versus WT Control. #, $p<0.05$ versus WT STZ.

Appendix C

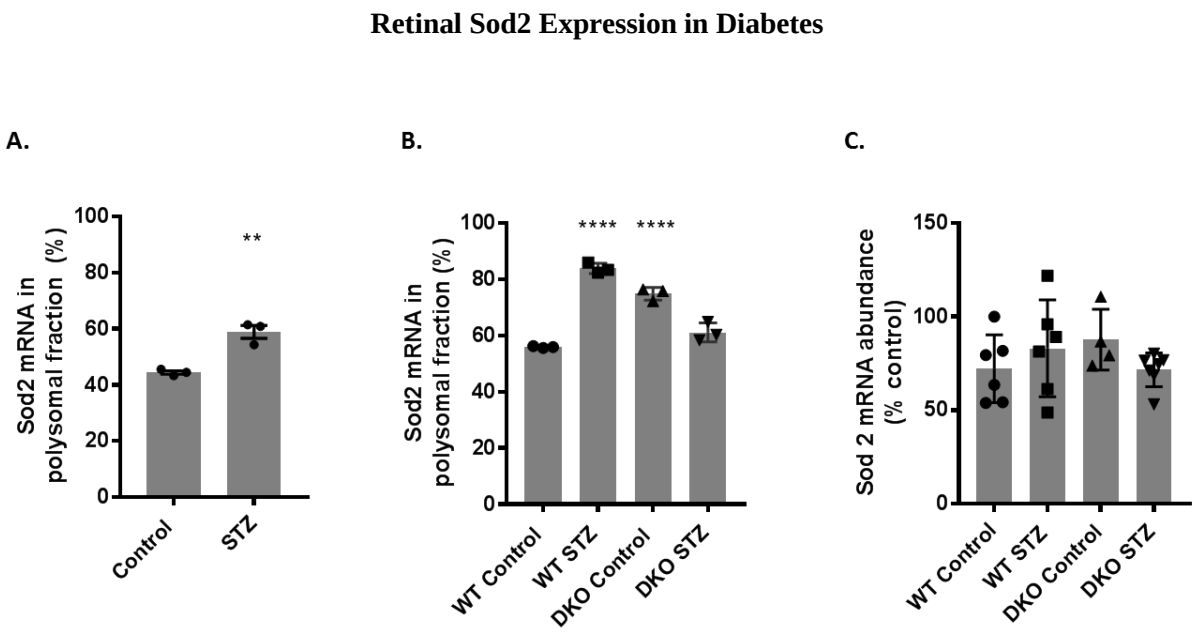

Figure C-1. Diabetes enhances Sod2 translation in WT but not 4E-BP1/2 DKO mice. *A.* Ribosomes were separated into either sub-polysomal (SP) or polysomal (P) fractions via sucrose density gradient centrifugation after 4 weeks diabetes duration. The distribution of the Sod2 mRNA was assessed in SP or P fractions via RT-PCR. Means were compared by unpaired t test. Results are expressed as a relative percentage of the mRNA in the P fraction. Values are means ± SE for three replicates assessing a pooled sample obtained from 8-10 retinas. **, $p<0.01$ versus Control. *B.* SP and P fractions were collected as described above after 12 weeks diabetes duration. Results are expressed as a relative percentage of the mRNA in the P fraction. Values are means ± SE for three replicates assessing a pooled sample obtained from 8-10 retinas. ****, $p<0.0001$ versus WT Control. *C.* Sod2 mRNA expression in whole retina was assessed by PCR after 12 weeks diabetes duration. Data were analyzed by one-way ANOVA with Tukey's post-hoc analysis. Values are means ± SE, n=4-7.

Appendix D

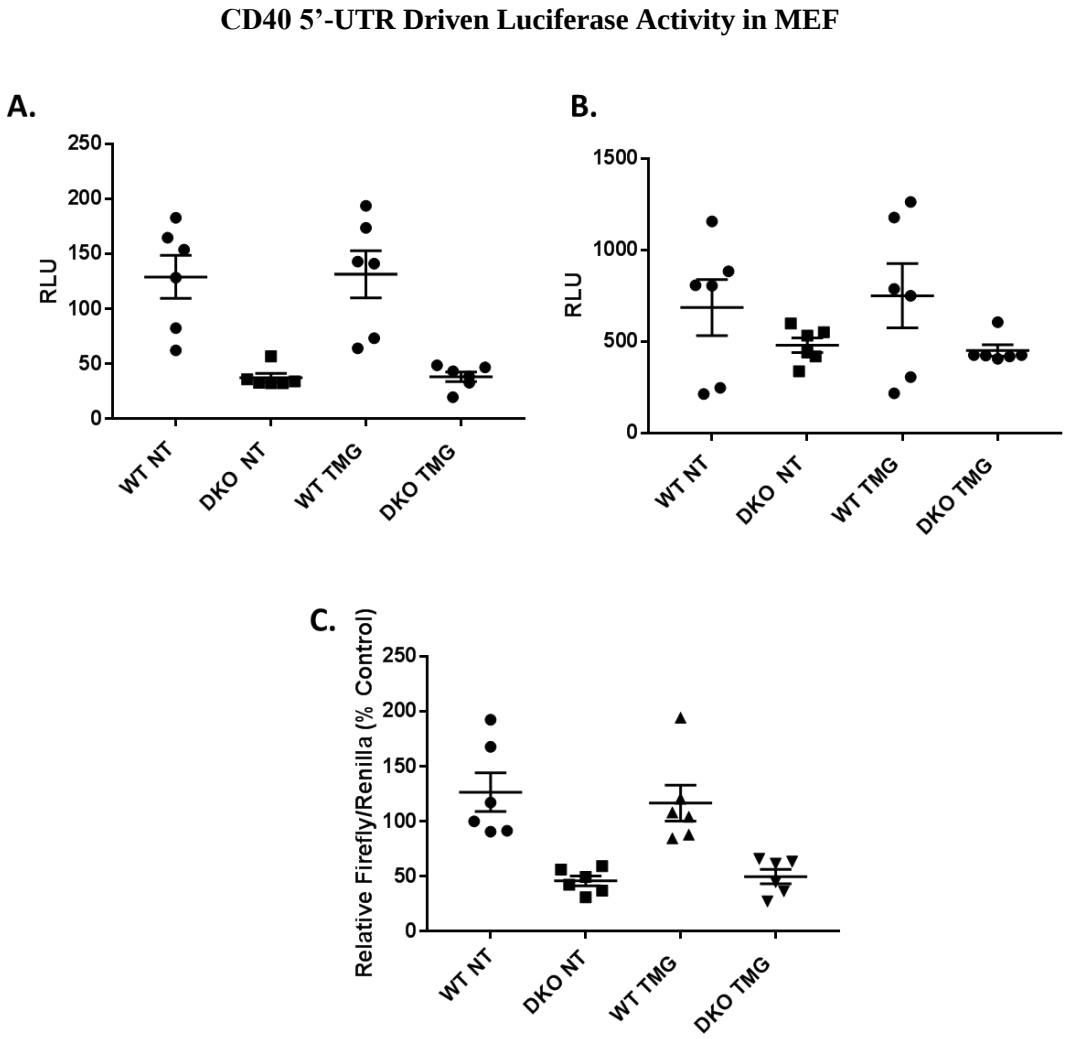

Figure D-1. 4E-BP1/2 promotes activity of CD40 5'-UTR driven luciferase reporter. Cultures of WT or 4E-BP1/2-deficient MEFs (DKO) were co-transfected with a CD40 5'-UTR-containing Firefly vector and a Renilla vector and exposed to TMG for 24 h. Luciferase activity was quantified using a dual-luciferase reporter assay system. *A.* Relative Firefly activity expressed ± SE for n=6 replicates. *B.* Relative Renilla activity activity expressed ± SE for n=6 replicates *C.* Ratio of Firefly to Renilla activities expressed ± SE for n=6 replicates.

Bibliography

1. Masland, R.H., *The fundamental plan of the retina.* Nat Neurosci, 2001. **4**(9): p. 877-86.
2. Masland, R.H., *The neuronal organization of the retina.* Neuron, 2012. **76**(2): p. 266-80.
3. Gollisch, T. and M. Meister, *Eye smarter than scientists believed: Neural computations in circuits of the retina.* Neuron, 2010. **65**(2): p. 150-64.
4. Flores-Herr, N., D.A. Protti, and H. Wässle, *Synaptic currents generating the inhibitory surround of ganglion cells in the mammalian retina.* J Neurosci, 2001. **21**(13): p. 4852-48863.
5. Bruesch, S.R. and L.B. Arey, *The number of myelinated and unmyelinated fibers in the optic nerve of vertebrates.* J Comp Neurol, 1942. **77**: p. 631.
6. Vecino E., et al., *Glia-neuron interactions in the mammalian retina.* Prog Retin Eye Res, 2016. **51**: p. 1-40.
7. Wantnabe T. and M.C. Raff, *Retinal astrocytes are immigrants from the optic nerve.* Nature, 1988. **332**(6167): p. 834-837.
8. Stone J., et al., *Development of retinal vasculature is mediated by hypoxia-induced vascular endothelial growth factor (VEGF) expression by neuroglia.* J Neurosci, 1995. **15**(7 Pt 1): p. 4738-47.
9. Ozaki H., et al., *Blockade of vascular endothelial cell growth factor feceptor signaling Is sufficient to completely prevent retinal neovascularization.* Am J Pathol, 2000. **156**(2): p. 697-707.
10. Bessis A., et al., *Microglial control of neuronal death and synaptic properties.* Glia, 2007. **55**(3).
11. Provis J.M., *Development of the primate retinal vasculature.* Prog Retin Eye Res, 2001. **20**(6).
12. Schafer D.P., et al., *Microglia sculpt postnatal neural circuits in an activity and complement-dependent manner.* Neuron, 2012. **74**(4): p. 691-705.
13. Langmann, T., *Microglia activation in retinal degeneration.* J Leukoc Biol, 2007. **81**(6): p. 1345-51.
14. Coughlin, B.A., D.J. Feenstra, and S. Mohr, *Muller cells and diabetic retinopathy.* Vision Res, 2017. **139**: p. 93-100.
15. Subirada, P.V., et al., *A journey into the retina: Muller glia commanding survival and death.* Eur J Neurosci, 2018. **47**(12): p. 1429-1443.
16. Agte, S., et al., *Muller glial cell-provided cellular light guidance through the vital guinea-pig retina.* Biophys J, 2011. **101**(11): p. 2611-9.
17. Metea, M.R. and E.A. Newman, *Signalling within the neurovascular unit in the mammalian retina.* Exp Physiol, 2007. **92**(4): p. 635-40.
18. Gardner, T.W. and J.R. Davila, *The neurovascular unit and the pathophysiologic basis of diabetic retinopathy.* Graefes Arch Clin Exp Ophthalmol, 2017. **255**(1): p. 1-6.
19. Antonetti, D.A., et al., *Diabetic retinopathy: seeing beyond glucose-induced microvascular disease.* Diabetes, 2006. **55**(9): p. 2401-11.
20. Simo, R., A.W. Stitt, and T.W. Gardner, *Neurodegeneration in diabetic retinopathy: does it really matter?* Diabetologia, 2018. **61**(9): p. 1902-1912.
21. Barber, A.J. and B. Baccouche, *Neurodegeneration in diabetic retinopathy: Potential for novel therapies.* Vision Res, 2017. **139**: p. 82-92.
22. Lind, M., et al., *The true value of HbA1c as a predictor of diabetic complications: simulations of HbA1c variables.* PLoS One, 2009. **4**(2): p. e4412.

23. Brownlee, M., *The Pathobiology of Diabetic Complications: a unifying mechanism.* Diabetes, 2005. **54**(6): p. 1615-1602.
24. Nathan, D.M., et al., *The effect of intensive treatment of diabetes on the development and progression of long-term complications in insulin-dependent diabetes mellitus.* N Engl J Med, 1993. **329**(14): p. 977-86.
25. Group, U.P.D.S., *Intensive blood-glucose control with sulphonylureas or insulin compared with conventional treatment and risk of complications in patients with type 2 diabetes (UKPDS 33).* The Lancet, 1998. **352**(9131): p. 837-853.
26. Kempen, J.H., et al., *The prevalence of diabetic retinopathy among adults in the United States.* Arch Ophthalmol, 2004. **122**(4): p. 552-63.
27. Roy, M.S., et al., *The prevalence of diabetic retinopathy among adult type 1 diabetic persons in the United States.* Arch Ophthalmol, 2004. **122**(4): p. 546-51.
28. Aiello, L.P., *Angiogenic pathways in diabetic retinopathy.* N Engl J Med, 2005. **353**(8): p. 839-41.
29. Adamis, A.P., et al., *Increased vascular endothelial growth factor levels in the vitreous of eyes with proliferative diabetic retinopathy.* Am J Ophthalmol, 1994. **118**(4): p. 445-50.
30. Aiello, L.P., et al., *Vascular endothelial growth factor in ocular fluid of patients with diabetic retinopathy and other retinal disorders.* N Engl J Med, 1994. **331**(22): p. 1480-7.
31. Pusparajah, P., L.H. Lee, and K. Abdul Kadir, *Molecular markers of diabetic retinopathy: potential screening tool of the future?* Front Physiol, 2016. **7**.
32. Behl, T., I. Kaur, and A. Kotwani, *Implication of oxidative stress in progression of diabetic retinopathy.* Surv Ophthalmol, 2016. **61**(2): p. 187-96.
33. Semeraro, F., et al., *Diabetic Retinopathy: vascular and inflammatory disease.* J Diabetes Res, 2015. **2015**: p. 582060.
34. Brownlee, M., *Biochemistry and molecular cell biology of diabetic complications.* Nature, 2001. **414**(6865): p. 813-820.
35. Kaiser, N., et al., *Differential regulation of glucose transport and transporters by glucose in vascular endothelial and smooth muscle cells.* Diabetes, 1993. **42**(1): p. 80-89.
36. Heilig, C.W., et al., *Overexpression of glucose transporters in rat mesangial cells cultured in a normal glucose milieu mimics the diabetic phenotype.* J Clin Invest, 1995. **96**(4): p. 1802-14.
37. Korshunov, S.S., V.P. Skulachev, and A.A. Starkov, *High protonic potential actuates a mechanism of production of reactive oxygen species in mitochondria.* FEBS Lett, 1997. **416**(1): p. 15-8.
38. Geraldes, P. and G.L. King, *Activation of protein kinase C isoforms and its impact on diabetic complications.* Circ Res, 2010. **106**(8): p. 1319-31.
39. Lee, A.Y. and S.S. Chung, *Contributions of polyol pathway to oxidative stress in diabetic cataract.* Faseb j, 1999. **13**(1): p. 23-30.
40. Wells, L. and G.W. Hart, *O-GlcNAc turns twenty: functional implications for post-translational modification of nuclear and cytosolic proteins with a sugar.* FEBS Lett, 2003. **546**(1): p. 154-8.
41. Torres, C.R. and G.W. Hart, *Topography and polypeptide distribution of terminal N-acetylglucosamine residues on the surfaces of intact lymphocytes. Evidence for O-linked GlcNAc.* J Biol Chem, 1984. **259**(5): p. 3308-17.
42. Copeland, R.J., J.W. Bullen, and G.W. Hart, *Cross-talk between GlcNAcylation and phosphorylation: roles in insulin resistance and glucose toxicity.* Am J Physiol Endocrinol Metab, 2008. **295**(1): p. E17-28.
43. Zachara, N.E. and G.W. Hart, *Cell signaling, the essential role of O-GlcNAc!* Biochim Biophys Acta, 2006. **1761**(5-6): p. 599-617.

44. Buse, M.G., *Hexosamines, insulin resistance, and the complications of diabetes: current status.* Am J Physiol Endocrinol Metab, 2006. **290**(1): p. E1-E8.
45. Dai, W., et al., *Consumption of a high fat diet promotes protein O-GlcNAcylation in mouse retina via NR4A1-dependent GFAT2 expression.* Biochim Biophys Acta Mol Basis Dis, 2018. **1864**(12): p. 3568-3576.
46. Oki, T., et al., *cDNA cloning and mapping of a novel subtype of glutamine:fructose-6-phosphate amidotransferase (GFAT2) in human and mouse.* Genomics, 1999. **57**(2): p. 227-34.
47. Clark, R.J., et al., *Diabetes and the accompanying hyperglycemia impairs cardiomyocyte calcium cycling through increased nuclear O-GlcNAcylation.* J Biol Chem, 2003. **278**(45): p. 44230-7.
48. Konrad, R.J. and J.E. Kudlow, *The role of O-linked protein glycosylation in beta-cell dysfunction.* Int J Mol Med, 2002. **10**(5): p. 535-9.
49. Walgren, J.L., et al., *High glucose and insulin promote O-GlcNAc modification of proteins, including alpha-tubulin.* Am J Physiol Endocrinol Metab, 2003. **284**(2): p. E424-34.
50. Kim, S.J., et al., *Increased O-GlcNAcylation of NF-kappaB enhances retinal ganglion cell death in streptozotocin-induced diabetic retinopathy.* Curr Eye Res, 2016. **41**(2): p. 249-57.
51. Gurel, Z., et al., *Retinal O-linked N-acetylglucosamine protein modifications: implications for postnatal retinal vascularization and the pathogenesis of diabetic retinopathy.* Mol Vis, 2013. **19**: p. 1047-59.
52. Xu, C., et al., *O-GlcNAcylation under hypoxic conditions and its effects on the blood-retinal barrier in diabetic retinopathy.* Int J Mol Med, 2014. **33**(3): p. 624-32.
53. Xu, C., et al., *Identification of O-GlcNAcylation modification in diabetic retinopathy and crosstalk with phosphorylation of Stat3 in retina vascular endothelium cells.* Cell Physiol Biochem, 2018. **49**(4): p. 1389-1402.
54. Yki-Jarvinen, H., et al., *Increased glutamine:fructose-6-phosphate amidotransferase activity in skeletal muscle of patients with NIDDM.* Diabetes, 1996. **45**(3): p. 302-7.
55. Vosseller, K., et al., *Elevated nucleocytoplasmic glycosylation by O-GlcNAc results in insulin resistance associated with defects in Akt activation in 3T3-L1 adipocytes.* Proc Nat Acad Sci, 2002. **99**(8): p. 5313-5318.
56. Andreozzi, F., et al., *Activation of the hexosamine pathway leads to phosphorylation of insulin receptor substrate-1 on Ser307 and Ser612 and impairs the phosphatidylinositol 3-kinase/Akt/mammalian target of rapamycin insulin biosynthetic pathway in RIN pancreatic beta-cells.* Endocrinology, 2004. **145**(6): p. 2845-57.
57. Yang, X., et al., *Phosphoinositide signalling links O-GlcNAc transferase to insulin resistance.* Nature, 2008. **451**(7181): p. 964-9.
58. Whelan, S.A., et al., R*egulation of insulin receptor substrate 1 (IRS-1)/Akt kinase-mediated insulin signaling by O-linked β-N-acetylglucosamine in 3T3-l1 adipocytes.* J Biol Chem, 2010. **285**(8): p. 5204-11.
59. Patti, M.E., et al., *Activation of the hexosamine pathway by glucosamine in vivo induces insulin resistance of early postreceptor insulin signaling events in skeletal muscle.* Diabetes, 1999. **48**(8): p. 1562-71.
60. D'Alessandris, C., et al., *Increased O-glycosylation of insulin signaling proteins results in their impaired activation and enhanced susceptibility to apoptosis in pancreatic beta-cells.* FASEB J, 2004. **18**(9): p. 959-61.
61. Barber, A.J., et al., *Neural apoptosis in the retina during experimental and human diabetes. Early onset and effect of insulin.* J Clin Invest, 1998. **102**(4): p. 783-91.

62. Gurel, Z., et al., *Identification of O-GlcNAc modification targets in mouse retinal pericytes: implication of p53 in pathogenesis of diabetic retinopathy.* PLoS One, 2014. **9**(5): p. e95561.
63. Huang, Q. and N. Sheibani, *High glucose promotes retinal endothelial cell migration through activation of Src, PI3K/Akt1/eNOS, and ERKs.* Am J Physiol Cell Physiol, 2008. **295**(6): p. C1647-57.
64. Donovan, K., et al., *O-GlcNAc modification of transcription factor Sp1 mediates hyperglycemia-induced VEGF-A upregulation in retinal cells.* Invest Ophthalmol Vis Sci, 2014. **55**(12): p. 7862-73.
65. Matthews, J.A., et al., *Glucosamine-induced increase in Akt phosphorylation corresponds to increased endoplasmic reticulum stress in astroglial cells.* Mol Cell Biochem, 2007. **298**(1-2): p. 109-23.
66. Mao, X., et al., *O-GlcNAc glycosylation of p27(kip1) promotes astrocyte migration and functional recovery after spinal cord contusion.* Exp Cell Res, 2015. **339**(2): p. 197-205.
67. Watanabe, T., et al., *GLUT2 expression in the rat retina: localization at the apical ends of Muller cells.* Brain Res, 1994. **655**(1-2): p. 128-34.
68. Dai, W., et al., *Deletion of the stress-response protein REDD1 promotes ceramide-induced retinal cell death and JNK activation.* Faseb j, 2018: p. fj201800413RR.
69. Wang, J., et al., *A nutrient-sensing pathway regulates leptin gene expression in muscle and fat.* Nature, 1998. **393**(6686): p. 684-8.
70. Zachara, N.E., *The roles of O-linked beta-N-acetylglucosamine in cardiovascular physiology and disease.* Am J Physiol Heart Circ Physiol, 2012. **302**(10): p. H1905-18.
71. Comer, F.I. and G.W. Hart, *O-GlcNAc and the control of gene expression.* Biochim Biophys Acta, 1999. **1473**(1): p. 161-71.
72. Issad, T. and M. Kuo, *O-GlcNAc modification of transcription factors, glucose sensing and glucotoxicity.* Trends Endocrinol Metab, 2008. **19**(10): p. 380-9.
73. Nagel, A.K. and L.E. Ball, *Intracellular protein O-GlcNAc modification integrates nutrient status with transcriptional and metabolic regulation.* Adv Cancer Res, 2015. **126**: p. 137-66.
74. Hart, G.W., *Nutrient regulation of signaling and transcription.* J Biol Chem, 2019. **294**(7): p. 2211-2231.
75. Ranuncolo, S.M., et al., *Evidence of the involvement of O-GlcNAc-modified human RNA polymerase II CTD in transcription in vitro and in vivo.* J Biol Chem, 2012. **287**(28): p. 23549-61.
76. Lewis, B.A., A.L. Burlingame, and S.A. Myers, *Human RNA Polymerase II Promoter Recruitment in Vitro Is Regulated by O-Linked N-Acetylglucosaminyltransferase (OGT).* J Biol Chem, 2016. **291**(27): p. 14056-61.
77. Resto, M., et al., *O-GlcNAcase is an RNA polymerase ii elongation factor coupled to pausing factors SPT5 and TIF1beta.* J Biol Chem, 2016. **291**(43): p. 22703-22713.
78. Wang, P., et al., *OGT mediated histone H2B S112 GlcNAcylation regulates DNA damage response.* J Genet Genomics, 2015. **42**(9): p. 467-75.
79. Leturcq, M., T. Lefebvre, and A.S. Vercoutter-Edouart, *O-GlcNAcylation and chromatin remodeling in mammals: an up-to-date overview.* Biochem Soc Trans, 2017. **45**(2): p. 323-338.
80. Fujiki, R., et al., *GlcNAcylation of histone H2B facilitates its monoubiquitination.* Nature, 2011. **480**(7378): p. 557-60.
81. Zhang, Y., et al., *O-GlcNAc modification of Sp1 mediates hyperglycaemia-induced ICAM-1 up-regulation in endothelial cells.* Biochem Biophys Res Commun, 2017. **484**(1): p. 79-84.

82. Al-Shabrawey, M., et al., *Role of NADPH oxidase and Stat3 in statin-mediated protection against diabetic retinopathy.* Invest Ophthalmol Vis Sci, 2008. **49**(7): p. 3231-8.
83. Yun, J.H., et al., *Endothelial Stat3 activation increases vascular leakage through downregulating tight junction proteins: implications for diabetic retinopathy*. J Cell Physiol, 2017. **232**(5): p. 1123-1134.
84. Baltimore, D., *NF-kappaB is 25.* Nat Immunol, 2011. **12**(8): p. 683-5.
85. Zhao, Y., et al., *NF-kappaB in type 1 diabetes.* Inflamm Allergy Drug Targets, 2011. **10**(3): p. 208-17.
86. Powers, E.T., *Translation: An O-GlcNAc stamp of approval.* Nat Chem Biol, 2015. **11**(5): p. 307-8.
87. Zeidan, Q., et al., *O-GlcNAc cycling enzymes associate with the translational machinery and modify core ribosomal proteins.* Mol Biol Cell, 2010. **21**(12): p. 1922-36.
88. Pestova, T.V., et al., *Molecular mechanisms of translation initiation in eukaryotes.* Proc Natl Acad Sci U S A, 2001. **98**(13): p. 7029-36.
89. Lopez-Lastra, M., A. Rivas, and M.I. Barria, *Protein synthesis in eukaryotes: the growing biological relevance of cap-independent translation initiation.* Biol Res, 2005. **38**(2-3): p. 121-46.
90. Pestova, T.V., C.U. Hellen, and I.N. Shatsky, *Canonical eukaryotic initiation factors determine initiation of translation by internal ribosomal entry.* Mol Cell Biol, 1996. **16**(12): p. 6859-69.
91. Svitkin, Y.V., et al., *Eukaryotic translation initiation factor 4E availability controls the switch between cap-dependent and internal ribosomal entry site-mediated translation.* Mol Cell Biol, 2005. **25**(23): p. 10556-65.
92. Kimball, S.R., et al., *Insulin and diabetes cause reciprocal changes in the association of eIF-4E and PHAS-I in rat skeletal muscle.* Am J Physiol, 1996. **270**(2 Pt 1): p. C705-9.
93. Dennis, M.D., et al., *Hyperglycemia-induced O-GlcNAcylation and truncation of 4E-BP1 protein in liver of a mouse model of type 1 diabetes.* J Biol Chem, 2011. **286**(39): p. 34286-97.
94. Dennis, M.D., et al., *Hyperglycemia mediates a shift from cap-dependent to cap-independent translation via a 4E-BP1-dependent mechanism.* Diabetes, 2013. **62**(7): p. 2204-14.
95. Miller, W.P., et al., *The translational repressor 4e-bp1 contributes to diabetes-induced visual dysfunction.* Invest Ophthalmol Vis Sci, 2016. **57**(3): p. 1327-37.
96. Dennis, M.D., et al., *Regulated in development and DNA damage 1 is necessary for hyperglycemia-induced vascular endothelial growth factor expression in the retina of diabetic rodents.* J Biol Chem, 2015. **290**(6): p. 3865-74.
97. Schrufer, T.L., et al., *Ablation of 4E-BP1/2 prevents hyperglycemia-mediated induction of VEGF expression in the rodent retina and in Muller cells in culture.* Diabetes, 2010. **59**(9): p. 2107-16.
98. Rechsteiner, M. and S.W. Rogers, *PEST sequences and regulation by proteolysis.* Trends Biochem Sci, 1996. **21**(7): p. 267-71.
99. Jang, I., et al., *O-GlcNAcylation of eIF2alpha regulates the phospho-eIF2alpha-mediated ER stress response.* Biochim Biophys Acta, 2015. **1853**(8): p. 1860-9.
100. Jo, S., A. Lockridge, and E.U. Alejandro, *eIF4G1 and carboxypeptidase E axis dysregulation in O-GlcNAc transferase-deficient pancreatic beta-cells contributes to hyperproinsulinemia in mice.* J Biol Chem, 2019. **294**(35): p. 13040-13050.
101. Li, X., et al., *O-GlcNAcylation of core components of the translation initiation machinery regulates protein synthesis.* Proc Natl Acad Sci U S A, 2019. **116**(16): p. 7857-7866.

102. Gallie, D.R., *The cap and poly(A) tail function synergistically to regulate mRNA translational efficiency.* Genes Dev, 1991. **5**(11): p. 2108-16.
103. Richter, K., M. Haslbeck, and J. Buchner, *The heat shock response: life on the verge of death.* Mol Cell, 2010. **40**(2): p. 253-66.
104. Zhang, X., X.E. Shu, and S.B. Qian, *O-GlcNAc modification of eIF4GI acts as a translational switch in heat shock response.* Nat Chem Biol, 2018. **14**(10): p. 909-916.
105. Hart, G.W., et al., *Cross talk between O-GlcNAcylation and phosphorylation: roles in signaling, transcription, and chronic disease.* Annu Rev Biochem, 2011. **80**: p. 825-58.
106. Wang, Z., A. Pandey, and G.W. Hart, *Dynamic interplay between O-linked N-acetylglucosaminylation and glycogen synthase kinase-3-dependent phosphorylation.* Mol Cell Proteomics, 2007. **6**(8): p. 1365-79.
107. Wang, Z., M. Gucek, and G.W. Hart, *Cross-talk between GlcNAcylation and phosphorylation: site-specific phosphorylation dynamics in response to globally elevated O-GlcNAc.* Proc Natl Acad Sci U S A, 2008. **105**(37): p. 13793-8.
108. Ong, Q., W. Han, and X. Yang, *O-GlcNAc as an Integrator of Signaling Pathways.* Front Endocrinol (Lausanne), 2018. **9**: p. 599.
109. Erickson, J.R., et al., *Diabetic hyperglycaemia activates CaMKII and arrhythmias by O-linked glycosylation.* Nature, 2013. **502**(7471): p. 372-6.
110. Xie, S., et al., *O-GlcNAcylation of protein kinase A catalytic subunits enhances its activity: a mechanism linked to learning and memory deficits in Alzheimer's disease.* Aging Cell, 2016. **15**(3): p. 455-64.
111. Lee, Y., et al., *Sleep deprivation impairs learning and memory by decreasing protein O-GlcNAcylation in the brain of adult zebrafish.* Faseb j, 2020. **34**(1): p. 853-864.
112. Li, J., et al., *Potential antidepressant and resilience mechanism revealed by metabolomic study on peripheral blood mononuclear cells of stress resilient rats.* Behav Brain Res, 2017. **320**: p. 12-20.
113. Phipps, J.A., et al., *The renin-angiotensin system and the retinal neurovascular unit: A role in vascular regulation and disease.* Exp Eye Res, 2019. **187**: p. 107753.
114. Choudhary, R., et al., *Therapeutic targets of renin-angiotensin system in ocular disorders.* J Curr Ophthalmol, 2017. **29**(1): p. 7-16.
115. Culman, J., et al., *Angiotensin as neuromodulator/neurotransmitter in central control of body fluid and electrolyte homeostasis.* Clin Exp Hypertens, 1995. **17**(1-2): p. 281-93.
116. Chung, O., et al., *Physiological and pharmacological implications of AT1 versus AT2 receptors.* Kidney Int Suppl, 1998. **67**: p. S95-9.
117. Fletcher, E.L., et al., *The renin-angiotensin system in retinal health and disease: Its influence on neurons, glia and the vasculature.* Prog Retin Eye Res, 2010. **29**(4): p. 284-311.
118. Wang, B., et al., *Effects of RAS inhibitors on diabetic retinopathy: a systematic review and meta-analysis.* Lancet Diabetes Endocrinol, 2015. **3**(4): p. 263-74.
119. Campbell, D.J., et al., *Differential regulation of angiotensin peptide levels in plasma and kidney of the rat.* Hypertension, 1991. **18**(6): p. 763-73.
120. Kohara, K., K.B. Brosnihan, and C.M. Ferrario, *Angiotensin(1-7) in the spontaneously hypertensive rat.* Peptides, 1993. **14**(5): p. 883-91.
121. Kucharewicz, I., et al., *Antithrombotic effect of captopril and losartan is mediated by angiotensin-(1-7).* Hypertension, 2002. **40**(5): p. 774-9.
122. Chappell, M.C., et al., *Metabolism of angiotensin-(1-7) by angiotensin-converting enzyme.* Hypertension, 1998. **31**(1 Pt 2): p. 362-7.
123. Roks, A.J., et al., *Angiotensin-(1-7) is a modulator of the human renin-angiotensin system.* Hypertension, 1999. **34**(2): p. 296-301.

124. Guimaraes, P.S., et al., *Increasing angiotensin-(1-7) levels in the brain attenuates metabolic syndrome-related risks in fructose-fed rats.* Hypertension, 2014. **63**(5): p. 1078-85.
125. Williams, I.M., et al., *Chronic angiotensin-(1-7) improves insulin sensitivity in high-fat fed mice independent of blood pressure.* Hypertension, 2016. **67**(5): p. 983-91.
126. Bui, B.V., et al., *ACE inhibition salvages the visual loss caused by diabetes.* Diabetologia, 2003. **46**(3): p. 401-8.
127. Gilbert, R.E., et al., *Angiotensin converting enzyme inhibition reduces retinal overexpression of vascular endothelial growth factor and hyperpermeability in experimental diabetes.* Diabetologia, 2000. **43**(11): p. 1360-7.
128. Funatsu, H., et al., *Risk evaluation of outcome of vitreous surgery for proliferative diabetic retinopathy based on vitreous level of vascular endothelial growth factor and angiotensin II.* Br J Ophthalmol, 2004. **88**(8): p. 1064-8.
129. Senanayake, P.D., et al., *Retinal angiotensin II and angiotensin-(1-7) response to hyperglycemia and an intervention with captopril.* J Renin Angiotensin Aldosterone Syst, 2018. **19**(3): p. 1470320318789323.
130. Verma, A., et al., *ACE2 and ang-(1-7) confer protection against development of diabetic retinopathy.* Mol Ther, 2012. **20**(1): p. 28-36.
131. Gellai, R., et al., *Role of O-linked N-acetylglucosamine modification in diabetic nephropathy.* Am J Physiol Renal Physiol, 2016. **311**(6): p. F1172-f1181.
132. Singh, R., et al., *Mechanism of increased angiotensin II levels in glomerular mesangial cells cultured in high glucose.* J Am Soc Nephrol, 2003. **14**(4): p. 873-80.
133. Hsieh, T.J., et al., *High glucose stimulates angiotensinogen gene expression and cell hypertrophy via activation of the hexosamine biosynthesis pathway in rat kidney proximal tubular cells.* Endocrinology, 2003. **144**(10): p. 4338-49.
134. Vidotti, D.B., et al., *High glucose concentration stimulates intracellular renin activity and angiotensin II generation in rat mesangial cells.* Am J Physiol Renal Physiol, 2004. **286**(6): p. F1039-45.
135. Marsh, S.A., L.J. Dell'Italia, and J.C. Chatham, *Activation of the hexosamine biosynthesis pathway and protein O-GlcNAcylation modulate hypertrophic and cell signaling pathways in cardiomyocytes from diabetic mice.* Amino Acids, 2011. **40**(3): p. 819-28.
136. Tanaka, T., et al., *Thiamine attenuates the hypertension and metabolic abnormalities in CD36-defective SHR: uncoupling of glucose oxidation from cellular entry accompanied with enhanced protein O-GlcNAcylation in CD36 deficiency.* Mol Cell Biochem, 2007. **299**(1-2): p. 23-35.
137. Einstein, F.H., et al., *Enhanced activation of a "nutrient-sensing" pathway with age contributes to insulin resistance.* Faseb j, 2008. **22**(10): p. 3450-7.
138. Loloi, J., et al., *Angiotensin-(1-7) contributes to insulin-sensitizing effects of angiotensin-converting enzyme inhibition in obese mice.* Am J Physiol Endocrinol Metab, 2018. **315**(6): p. E1204-e1211.
139. Premaratna, S.D., et al., *Angiotensin-converting enzyme inhibition reverses diet-induced obesity, insulin resistance and inflammation in C57BL/6J mice.* Int J Obes (Lond), 2012. **36**(2): p. 233-43.
140. Kimball, S.R., et al., *Insulin stimulates protein synthesis in skeletal muscle by enhancing the association of eIF-4E and eIF-4G.* Am J Physiol, 1997. **272**(2 Pt 1): p. C754-9.
141. Kimball, S.R., R.L. Horetsky, and L.S. Jefferson, *Implication of eIF2B rather than eIF4E in the regulation of global protein synthesis by amino acids in L6 myoblasts.* J Biol Chem, 1998. **273**(47): p. 30945-53.

142. Dennis, M.D., et al., *Hyperglycemia mediates a shift from cap-dependent to cap-independent translation via a 4e-bp1 dependent mechanism.* Diabetes, 2013.
143. Livak, K.J. and T.D. Schmittgen, *Analysis of relative gene expression data using real-time quantitative PCR and the 2(-Delta Delta C(T)) Method.* Methods, 2001. **25**(4): p. 402-8.
144. Rodriguez, J.M., et al., *APPRIS: annotation of principal and alternative splice isoforms.* Nucleic Acids Res, 2013. **41**(Database issue): p. D110-7.
145. Bray, N.L., et al., *Near-optimal probabilistic RNA-seq quantification.* Nat Biotechnol, 2016. **34**(5): p. 525-7.
146. Love, M.I., W. Huber, and S. Anders, *Moderated estimation of fold change and dispersion for RNA-seq data with DESeq2.* Genome Biol, 2014. **15**(12): p. 550.
147. Li, W., et al., *Riborex: fast and flexible identification of differential translation from Ribo-seq data.* Bioinformatics, 2017. **33**(11): p. 1735-1737.
148. *The effect of intensive treatment of diabetes on the development and progression of long-term complications in insulin-dependent diabetes mellitus. The Diabetes Control and Complications Trial Research Group.* The New England journal of medicine, 1993. **329**(14): p. 977-86.
149. Duverger, E., A.C. Roche, and M. Monsigny, *N-acetylglucosamine-dependent nuclear import of neoglycoproteins.* Glycobiology, 1996. **6**(4): p. 381-6.
150. Roos, M.D., et al., *O glycosylation of an Sp1-derived peptide blocks known Sp1 protein interactions.* Molecular and cellular biology, 1997. **17**(11): p. 6472-80.
151. Gao, Y., J. Miyazaki, and G.W. Hart, *The transcription factor PDX-1 is post-translationally modified by O-linked N-acetylglucosamine and this modification is correlated with its DNA binding activity and insulin secretion in min6 beta-cells.* Archives of biochemistry and biophysics, 2003. **415**(2): p. 155-63.
152. Soesanto, Y.A., et al., *Regulation of Akt signaling by O-GlcNAc in euglycemia.* American journal of physiology. Endocrinology and metabolism, 2008. **295**(4): p. E974-80.
153. Han, I. and J.E. Kudlow, *Reduced O glycosylation of Sp1 is associated with increased proteasome susceptibility.* Molecular and cellular biology, 1997. **17**(5): p. 2550-8.
154. Zeidan, Q., et al., *O-GlcNAc cycling enzymes associate with the translational machinery and modify core ribosomal proteins.* Molecular biology of the cell, 2010. **21**(12): p. 1922-36.
155. Nandi, A., et al., *Global identification of O-GlcNAc-modified proteins.* Analytical chemistry, 2006. **78**(2): p. 452-8.
156. Teo, C.F., et al., *Glycopeptide-specific monoclonal antibodies suggest new roles for O-GlcNAc.* Nature chemical biology, 2010. **6**(5): p. 338-43.
157. Wells, L., et al., *Mapping sites of O-GlcNAc modification using affinity tags for serine and threonine post-translational modifications.* Mol Cell Proteomics, 2002. **1**(10): p. 791-804.
158. Khidekel, N., et al., *Probing the dynamics of O-GlcNAc glycosylation in the brain using quantitative proteomics.* Nat Chem Biol, 2007. **3**(6): p. 339-48.
159. Dennis, M.D., et al., *Hyperglycemia-induced o-glcnacylation and truncation of 4e-bp1 protein in liver of a mouse model of type 1 diabetes*. The Journal of biological chemistry, 2011. **286**(39): p. 34286-97.
160. Fort, P.E., et al., *mTORC1-independent reduction of retinal protein synthesis in type 1 diabetes.* Diabetes, 2014. **63**(9): p. 3077-90.
161. Ptushkina, M., et al., *Repressor binding to a dorsal regulatory site traps human eIF4E in a high cap-affinity state*. EMBO J, 1999. **18**(14): p. 4068-75.

162. von der Haar, T., et al., *The mRNA cap-binding protein eIF4E in post-transcriptional gene expression.* Nature Structural and Molecular Biology, 2004. **11**(6): p. 503-511.
163. Dierschke, S.K., et al., *O-GlcNAcylation alters the selection of mRNAs for translation and promotes 4E-BP1-dependent mitochondrial dysfunction in the retina.* J Biol Chem, 2019. **294**(14): p. 5508-5520.
164. Morita, M., et al., *mTORC1 controls mitochondrial activity and biogenesis through 4E-BP-dependent translational regulation.* Cell Metab, 2013. **18**(5): p. 698-711.
165. Mader, S., et al., *The translation initiation factor eIF-4E binds to a common motif shared by the translation factor eIF-4 gamma and the translational repressors 4E-binding proteins.* Mol Cell Biol, 1995. **15**(9): p. 4990-7.
166. Schalm, S.S., et al., *TOS motif-mediated raptor binding regulates 4E-BP1 multisite phosphorylation and function.* Curr Biol, 2003. **13**(10): p. 797-806.
167. Du, Y., et al., *Photoreceptor cells are major contributors to diabetes-induced oxidative stress and local inflammation in the retina.* Proc Natl Acad Sci U S A, 2013. **110**(41): p. 16586-91.
168. Komili, S. and P.A. Silver, *Coupling and coordination in gene expression processes: a systems biology view.* Nat Rev Genet, 2008. **9**(1): p. 38-48.
169. Maier, T., M. Guell, and L. Serrano, *Correlation of mRNA and protein in complex biological samples.* FEBS Lett, 2009. **583**(24): p. 3966-73.
170. Schwanhausser, B., et al., *Global quantification of mammalian gene expression control.* Nature, 2011. **473**(7347): p. 337-42.
171. Jovanovic, M., et al., *Immunogenetics. Dynamic profiling of the protein life cycle in response to pathogens.* Science, 2015. **347**(6226): p. 1259038.
172. Holcik, M. and N. Sonenberg, *Translational control in stress and apoptosis.* Nat Rev Mol Cell Biol, 2005. **6**(4): p. 318-27.
173. Spriggs, K.A., M. Bushell, and A.E. Willis, *Translational regulation of gene expression during conditions of cell stress.* Mol Cell, 2010. **40**(2): p. 228-37.
174. Ozcan, S., S.S. Andrali, and J.E. Cantrell, *Modulation of transcription factor function by O-GlcNAc modification.* Biochim Biophys Acta, 2010. **1799**(5-6): p. 353-64.
175. Schuller, A.P., et al., *eIF5A Functions Globally in Translation Elongation and Termination.* Mol Cell, 2017. **66**(2): p. 194-205 e5.
176. Zid, B.M., et al., *4E-BP extends lifespan upon dietary restriction by enhancing mitochondrial activity in Drosophila.* Cell, 2009. **139**(1): p. 149-60.
177. Couvillion, M.T., et al., *Synchronized mitochondrial and cytosolic translation programs.* Nature, 2016. **533**(7604): p. 499-503.
178. Van Haute, L., et al., *Mitochondrial transcript maturation and its disorders.* J Inherit Metab Dis, 2015. **38**(4): p. 655-80.
179. Tan, E.P., et al., *Altering O-linked beta-N-acetylglucosamine cycling disrupts mitochondrial function.* J Biol Chem, 2014. **289**(21): p. 14719-30.
180. Tan, E.P., et al., *Sustained O-GlcNAcylation reprograms mitochondrial function to regulate energy metabolism.* J Biol Chem, 2017. **292**(36): p. 14940-14962.
181. Ma, J., et al., *O-GlcNAcomic Profiling identifies widespread O-linked beta-N-Acetylglucosamine modification (O-GlcNAcylation) in oxidative phosphorylation system regulating cardiac mitochondrial function.* J Biol Chem, 2015. **290**(49): p. 29141-53.
182. Ma, J., et al., *Comparative proteomics reveals dysregulated mitochondrial o-glcnacylation in diabetic hearts.* J Proteome Res, 2016. **15**(7): p. 2254-64.
183. Banerjee, P.S., J. Ma, and G.W. Hart, *Diabetes-associated dysregulation of O-GlcNAcylation in rat cardiac mitochondria.* Proc Natl Acad Sci U S A, 2015. **112**(19): p. 6050-5.

184. Madsen-Bouterse, S.A., et al., *Role of mitochondrial DNA damage in the development of diabetic retinopathy, and the metabolic memory phenomenon associated with its progression.* Antioxid Redox Signal, 2010. **13**(6): p. 797-805.
185. Kern, T.S., et al., *Response of capillary cell death to aminoguanidine predicts the development of retinopathy: comparison of diabetes and galactosemia.* Invest Ophthalmol Vis Sci, 2000. **41**(12): p. 3972-8.
186. Benard, G. and R. Rossignol, *Ultrastructure of the mitochondrion and its bearing on function and bioenergetics.* Antioxid Redox Signal, 2008. **10**(8): p. 1313-42.
187. Zhong, Q. and R.A. Kowluru, *Diabetic retinopathy and damage to mitochondrial structure and transport machinery.* Invest Ophthalmol Vis Sci, 2011. **52**(12): p. 8739-46.
188. Du, X.L., et al., *Hyperglycemia inhibits endothelial nitric oxide synthase activity by posttranslational modification at the Akt site.* J Clin Invest, 2001. **108**(9): p. 1341-8.
189. Brownlee, M., *Biochemistry and molecular cell biology of diabetic complications.* Nature, 2001. **414**(6865): p. 813-20.
190. Young, T.A., C.C. Cunningham, and S.M. Bailey, *Reactive oxygen species production by the mitochondrial respiratory chain in isolated rat hepatocytes and liver mitochondria: studies using myxothiazol.* Arch Biochem Biophys, 2002. **405**(1): p. 65-72.
191. Kanwar, M., et al., *Oxidative damage in the retinal mitochondria of diabetic mice: possible protection by superoxide dismutase.* Invest Ophthalmol Vis Sci, 2007. **48**(8): p. 3805-11.
192. Kowluru, R.A., L. Atasi, and Y.S. Ho, *Role of mitochondrial superoxide dismutase in the development of diabetic retinopathy.* Invest Ophthalmol Vis Sci, 2006. **47**(4): p. 1594-9.
193. Kowluru, R.A., J. Tang, and T.S. Kern, *Abnormalities of retinal metabolism in diabetes and experimental galactosemia. VII. Effect of long-term administration of antioxidants on the development of retinopathy.* Diabetes, 2001. **50**(8): p. 1938-42.
194. Kowluru, R.A., et al., *Overexpression of mitochondrial superoxide dismutase in mice protects the retina from diabetes-induced oxidative stress.* Free Radic Biol Med, 2006. **41**(8): p. 1191-6.
195. Rubsam, A., S. Parikh, and P.E. Fort, *Role of Inflammation in Diabetic Retinopathy.* Int J Mol Sci, 2018. **19**(4).
196. Semeraro, F., et al., *Diabetic retinopathy, a vascular and inflammatory disease: Therapeutic implications.* Diabetes Metab, 2019. **45**(6): p. 517-527.
197. Tang, J. and T.S. Kern, *Inflammation in diabetic retinopathy.* Prog Retin Eye Res, 2011. **30**(5): p. 343-58.
198. Wang, M. and W.T. Wong, *Microglia-Muller cell interactions in the retina.* Adv Exp Med Biol, 2014. **801**: p. 333-8.
199. Wang, M., et al., *Adaptive Muller cell responses to microglial activation mediate neuroprotection and coordinate inflammation in the retina.* J Neuroinflammation, 2011. **8**: p. 173.
200. Portillo, J.A.C., et al., *CD40 in retinal müller cells induces P2X7-dependent cytokine expression in macrophages/microglia in diabetic mice and development of early experimental diabetic retinopathy.* Diabetes, 2017. **66**(2): p. 483-93.
201. Portillo, J.A., et al., *Proinflammatory responses induced by CD40 in retinal endothelial and Muller cells are inhibited by blocking CD40-Traf2,3 or CD40-Traf6 signaling.* Invest Ophthalmol Vis Sci, 2014. **55**(12): p. 8590-7.
202. Portillo, J.A., et al., *CD40 promotes the development of early diabetic retinopathy in mice.* Diabetologia, 2014. **57**(10): p. 2222-31.
203. Li, Y., et al., *O-GlcNAcylation in immunity and inflammation: An intricate system (Review).* Int J Mol Med, 2019. **44**(2): p. 363-374.

204. Swamy, M., et al., *Glucose and glutamine fuel protein O-GlcNAcylation to control T cell self-renewal and malignancy.* Nat Immunol, 2016. **17**(6): p. 712-20.
205. Lund, P.J., J.E. Elias, and M.M. Davis, *Global analysis of O-GlcNAc glycoproteins in activated human t cells.* J Immunol, 2016. **197**(8): p. 3086-3098.
206. Wu, J.L., et al., *O-GlcNAcylation is required for B cell homeostasis and antibody responses.* Nat Commun, 2017. **8**(1): p. 1854.
207. Kneass, Z.T. and R.B. Marchase, *Protein O-GlcNAc modulates motility-associated signaling intermediates in neutrophils.* J Biol Chem, 2005. **280**(15): p. 14579-85.
208. Krick, S., et al., *FGF23 induction of O-Linked N-Acetylglucosamine regulates IL-6 secretion in human bronchial epithelial cells.* Front Endocrinol (Lausanne), 2018. **9**: p. 708.
209. James, L.R., et al., *Flux through the hexosamine pathway is a determinant of nuclear factor kappaB- dependent promoter activation.* Diabetes, 2002. **51**(4): p. 1146-56.
210. Dela Justina, V., et al., *Increased O-Linked N-Acetylglucosamine modification of NF-KappaB and augmented cytokine production in the placentas from hyperglycemic rats.* Inflammation, 2017. **40**(5): p. 1773-1781.
211. Mazumder, B., X. Li, and S. Barik, *Translation control: a multifaceted regulator of inflammatory response.* J Immunol, 2010. **184**(7): p. 3311-9.
212. Nandi, A., et al., *Global identification of O-GlcNAc-modified proteins.* Anal Chem, 2006. **78**(2): p. 452-8.
213. Teo, C.F., et al., *Glycopeptide-specific monoclonal antibodies suggest new roles for O-GlcNAc.* Nat Chem Biol, 2010. **6**(5): p. 338-43.
214. Holcik, M., N. Sonenberg, and R.G. Korneluk, *Internal ribosome initiation of translation and the control of cell death.* Trends Genet, 2000. **16**(10): p. 469-73.
215. Sanz, E., et al., *Cell-type-specific isolation of ribosome-associated mRNA from complex tissues.* Proc Natl Acad Sci U S A, 2009. **106**(33): p. 13939-44.
216. Roesch, K., et al., *The transcriptome of retinal Muller glial cells.* J Comp Neurol, 2008. **509**(2): p. 225-38.
217. Weingarten-Gabbay, S., et al., *Comparative genetics. Systematic discovery of cap-independent translation sequences in human and viral genomes.* Science, 2016. **351**(6270).
218. Portillo, J.A., et al., *CD40 mediates retinal inflammation and neurovascular degeneration.* J Immunol, 2008. **181**(12): p. 8719-26.
219. Abu El-Asrar, A.M., et al., *Expression of the inducible isoform of nitric oxide synthase in the retinas of human subjects with diabetes mellitus.* Am J Ophthalmol, 2001. **132**(4): p. 551-6.
220. Du, Y., et al., *Diabetes-induced nitrative stress in the retina, and correction by aminoguanidine.* J Neurochem, 2002. **80**(5): p. 771-9.
221. Zheng, L., et al., *Critical role of inducible nitric oxide synthase in degeneration of retinal capillaries in mice with streptozotocin-induced diabetes.* Diabetologia, 2007. **50**(9): p. 1987-1996.
222. Leal, E.C., et al., *Inducible nitric oxide synthase isoform is a key mediator of leukostasis and blood-retinal barrier breakdown in diabetic retinopathy.* Invest Ophthalmol Vis Sci, 2007. **48**(11): p. 5257-65.
223. Lieth, E., et al., *Glial reactivity and impaired glutamate metabolism in short-term experimental diabetic retinopathy. Penn State Retina Research Group.* Diabetes, 1998. **47**(5): p. 815-20.

224. Barber, A.J., D.A. Antonetti, and T.W. Gardner, *Altered expression of retinal occludin and glial fibrillary acidic protein in experimental diabetes. The Penn State Retina Research Group.* Invest Ophthalmol Vis Sci, 2000. **41**(11): p. 3561-8.
225. Rungger-Brandle, E., A.A. Dosso, and P.M. Leuenberger, *Glial reactivity, an early feature of diabetic retinopathy.* Invest Ophthalmol Vis Sci, 2000. **41**(7): p. 1971-80.
226. Sundstrom, J.M., et al., *Proteomic Analysis of Early Diabetic Retinopathy Reveals Mediators of Neurodegenerative Brain Diseases.* Invest Ophthalmol Vis Sci, 2018. **59**(6): p. 2264-2274.
227. Vujosevic, S., et al., *Proteome analysis of retinal glia cells-related inflammatory cytokines in the aqueous humour of diabetic patients.* Acta Ophthalmol, 2016. **94**(1): p. 56-64.
228. Vujosevic, S., et al., *Aqueous Humor Biomarkers of Muller Cell Activation in Diabetic Eyes.* Invest Ophthalmol Vis Sci, 2015. **56**(6): p. 3913-8.
229. Yellin, M.J., et al., *Immunohistologic analysis of renal CD40 and CD40L expression in lupus nephritis and other glomerulonephritides.* Arthritis Rheum, 1997. **40**(1): p. 124-34.
230. Benveniste, E.N., V.T. Nguyen, and D.R. Wesemann, *Molecular regulation of CD40 gene expression in macrophages and microglia.* Brain Behav Immun, 2004. **18**(1): p. 7-12.
231. Jacobson, E.M., et al., *A Graves' disease-associated Kozak sequence single-nucleotide polymorphism enhances the efficiency of CD40 gene translation: a case for translational pathophysiology.* Endocrinology, 2005. **146**(6): p. 2684-91.
232. Kwok, C.K., G. Marsico, and S. Balasubramanian, *Detecting RNA G-quadruplexes (rG4s) in the transcriptome.* Cold Spring Harb Perspect Biol, 2018. **10**(7).
233. Pelletier, J. and N. Sonenberg, *Insertion mutagenesis to increase secondary structure within the 5' noncoding region of a eukaryotic mRNA reduces translational efficiency.* Cell, 1985. **40**(3): p. 515-26.
234. Kozak, M., *Circumstances and mechanisms of inhibition of translation by secondary structure in eucaryotic mRNAs.* Mol Cell Biol, 1989. **9**(11): p. 5134-42.
235. Cipollone, F., et al., *Enhanced soluble CD40 ligand contributes to endothelial cell dysfunction in vitro and monocyte activation in patients with diabetes mellitus: effect of improved metabolic control.* Diabetologia, 2005. **48**(6): p. 1216-24.
236. Lamine, L.B., et al., *Elevation in circulating soluble CD40 ligand concentrations in type 2 diabetic retinopathy and association with its severity.* Exp Clin Endocrinol Diabetes, 2018.
237. Boeri, D., M. Maiello, and M. Lorenzi, *Increased prevalence of microthromboses in retinal capillaries of diabetic individuals.* Diabetes, 2001. **50**(6): p. 1432-9.
238. Henn, V., et al., *The inflammatory action of CD40 ligand (CD154) expressed on activated human platelets is temporally limited by coexpressed CD40.* Blood, 2001. **98**(4): p. 1047-54.
239. Xu, H. and M. Chen, *Diabetic retinopathy and dysregulated innate immunity.* Vision Res, 2017. **139**: p. 39-46.
240. Urbancic, M. and I. Gardasevic Topcic, *Dexamethasone implant in the management of diabetic macular edema from clinician's perspective.* Clin Ophthalmol, 2019. **13**: p. 829-840.
241. Danser, A.H., et al., *Renin, prorenin, and immunoreactive renin in vitreous fluid from eyes with and without diabetic retinopathy.* J Clin Endocrinol Metab, 1989. **68**(1): p. 160-7.
242. Deinum, J., et al., *Identification and quantification of renin and prorenin in the bovine eye.* Endocrinology, 1990. **126**(3): p. 1673-82.

243. Sramek, S.J., et al., *An ocular renin-angiotensin system. Immunohistochemistry of angiotensinogen.* Invest Ophthalmol Vis Sci, 1992. **33**(5): p. 1627-32.
244. Feman, S.S., et al., *Serum angiotensin converting enzyme in diabetic patients.* Am J Med Sci, 1993. **305**(5): p. 280-4.
245. Wagner, J., et al., *Demonstration of renin mRNA, angiotensinogen mRNA, and angiotensin converting enzyme mRNA expression in the human eye: evidence for an intraocular renin-angiotensin system.* Br J Ophthalmol, 1996. **80**(2): p. 159-63.
246. Murata, M., M. Nakagawa, and S. Takahashi, *Expression and localization of angiotensin II type 1 receptor mRNA in rat ocular tissues.* Ophthalmologica, 1997. **211**(6): p. 384-6.
247. Danser, A.H., et al., *Angiotensin levels in the eye.* Invest Ophthalmol Vis Sci, 1994. **35**(3): p. 1008-18.
248. Ishiyama, Y., et al., *Upregulation of angiotensin-converting enzyme 2 after myocardial infarction by blockade of angiotensin II receptors.* Hypertension, 2004. **43**(5): p. 970-6.
249. Santos, R.A., et al., *Angiotensin-(1-7) is an endogenous ligand for the G protein-coupled receptor Mas.* Proc Natl Acad Sci U S A, 2003. **100**(14): p. 8258-63.
250. Dominguez, J.M., et al., *Adeno-associated virus overexpression of angiotensin-converting enzyme-2 reverses diabetic retinopathy in type 1 diabetes in mice.* Am J Pathol, 2016. **186**(6): p. 1688-700.
251. Verma, A., et al., *Expression of human ACE2 in lactobacillus and beneficial effects in diabetic retinopathy in mice.* Mol Ther Methods Clin Dev, 2019. **14**: p. 161-70.
252. Zhang, J.Z., et al., *Captopril inhibits capillary degeneration in the early stages of diabetic retinopathy.* Curr Eye Res, 2007. **32**(10): p. 883-9.
253. McClain, D.A., *Hexosamines as mediators of nutrient sensing and regulation in diabetes.* J Diabetes Complications, 2002. **16**(1): p. 72-80.
254. James, L.R., et al., *Angiotensin II activates the GFAT promoter in mesangial cells.* Renal Physiology, 2001. **281**(1): p. F151-F162.
255. Kowluru, R.A., et al., *Abnormalities of retinal metabolism in diabetes or experimental galactosemia. III. Effects of antioxidants.* Diabetes, 1996. **45**(9): p. 1233-7.
256. Nishikawa, T., et al., *Normalizing mitochondrial superoxide production blocks three pathways of hyperglycaemic damage.* Nature, 2000. **404**(6779): p. 787-90.
257. Sahr, A., et al., *The Angiotensin-(1-7)/Mas axis improves pancreatic beta-cell function in vitro and in vivo.* Endocrinology, 2016. **157**(12): p. 4677-4690.
258. Tetzner, A., et al., *G-protein-coupled receptor MrgD is a receptor for angiotensin-(1-7) involving adenylyl cyclase, camp, and phosphokinase a.* Hypertension, 2016. **68**(1): p. 185-94.
259. Liu, G.C., et al., *Angiotensin-(1-7)-induced activation of ERK1/2 is cAMP/protein kinase A-dependent in glomerular mesangial cells.* Am J Physiol Renal Physiol, 2012. **302**(6): p. F784-90.
260. Chang, Q., et al., *Phosphorylation of human glutamine:fructose-6-phosphate amidotransferase by cAMP-dependent protein kinase at serine 205 blocks the enzyme activity.* J Biol Chem, 2000. **275**(29): p. 21981-7.
261. Senanayake, P., et al., *Angiotensin II and its receptor subtypes in the human retina.* Invest Ophthalmol Vis Sci, 2007. **48**(7): p. 3301-11.
262. Berka, J.L., et al., *Renin-containing Muller cells of the retina display endocrine features.* Invest Ophthalmol Vis Sci, 1995. **36**(7): p. 1450-8.
263. Brandt, C.R., et al., *Renin mRNA is synthesized locally in rat ocular tissues.* Curr Eye Res, 1994. **13**(10): p. 755-63.
264. Kida, T., et al., *Renin-angiotensin system in proliferative diabetic retinopathy and its gene expression in cultured human muller cells.* Jpn J Ophthalmol, 2003. **47**(1): p. 36-41.

265. Foureaux, G., et al., *Activation of endogenous angiotensin converting enzyme 2 prevents early injuries induced by hyperglycemia in rat retina.* Braz J Med Biol Res, 2015. **48**(12): p. 1109-14.
266. Tallant, E.A. and M.A. Clark, *Molecular mechanisms of inhibition of vascular growth by angiotensin-(1-7).* Hypertension, 2003. **42**(4): p. 574-9.
267. Hu, Y., et al., *Phosphorylation of mouse glutamine-fructose-6-phosphate amidotransferase 2 (GFAT2) by cAMP-dependent protein kinase increases the enzyme activity.* J Biol Chem, 2004. **279**(29): p. 29988-93.
268. de Rooij, J., et al., *Epac is a Rap1 guanine-nucleotide-exchange factor directly activated by cyclic AMP.* Nature, 1998. **396**(6710): p. 474-7.
269. Whitaker, C.M. and N.G. Cooper, *Differential distribution of exchange proteins directly activated by cyclic AMP within the adult rat retina.* Neuroscience, 2010. **165**(3): p. 955-67.
270. Onodera, Y., J.M. Nam, and M.J. Bissell, *Increased sugar uptake promotes oncogenesis via EPAC/RAP1 and O-GlcNAc pathways.* J Clin Invest, 2014. **124**(1): p. 367-84.
271. Whelan, S.A., M.D. Lane, and G.W. Hart, *Regulation of the O-linked beta-N-acetylglucosamine transferase by insulin signaling.* J Biol Chem, 2008. **283**(31): p. 21411-7.
272. Gava, E., et al., *Angiotensin-(1-7) activates a tyrosine phosphatase and inhibits glucose-induced signalling in proximal tubular cells.* Nephrol Dial Transplant, 2009. **24**(6): p. 1766-73.
273. Kumar, S., et al., *The small GTPase Rap1b negatively regulates neutrophil chemotaxis and transcellular diapedesis by inhibiting Akt activation.* J Exp Med, 2014. **211**(9): p. 1741-58.
274. Yang, Z., et al., *Epac2-Rap1 signaling regulates reactive oxygen species production and susceptibility to cardiac arrhythmias.* Antioxid Redox Signal, 2017. **27**(3): p. 117-132.
275. Mukai, E., et al., *Exendin-4 suppresses SRC activation and reactive oxygen species production in diabetic Goto-Kakizaki rat islets in an Epac-dependent manner.* Diabetes, 2011. **60**(1): p. 218-26.
276. Stokman, G., et al., *Epac-Rap signaling reduces oxidative stress in the tubular epithelium.* J Am Soc Nephrol, 2014. **25**(7): p. 1474-85.
277. Semba, R.D., et al., *The role of O-GlcNAc signaling in the pathogenesis of diabetic retinopathy.* Proteomics Clin Appl, 2014. **8**(0): p. 218-31.
278. Prunty, M.C., et al., *In vivo imaging of retinal oxidative stress using a reactive oxygen species-activated fluorescent probe.* Invest Ophthalmol Vis Sci, 2015. **56**(10): p. 5862-70.
279. Pain, V.M. and P.J. Garlick, *Effect of streptozotocin diabetes and insulin treatment on the rate of protein synthesis in tissues of the rat in vivo.* J Biol Chem, 1974. **249**(14): p. 4510-4.
280. Dice, J.F., et al., *General characteristics of protein degradation in diabetes and starvation.* Proc Natl Acad Sci U S A, 1978. **75**(5): p. 2093-7.
281. Rapley, J., et al., *The mechanism of insulin-stimulated 4E-BP protein binding to mammalian target of rapamycin (mTOR) complex 1 and its contribution to mTOR complex 1 signaling.* J Biol Chem, 2011. **286**(44): p. 38043-53.
282. Reiter, C.E., et al., *Characterization of insulin signaling in rat retina in vivo and ex vivo.* Am J Physiol Endocrinol Metab, 2003. **285**(4): p. E763-74.
283. Reiter, C.E., et al., *Diabetes reduces basal retinal insulin receptor signaling: reversal with systemic and local insulin.* Diabetes, 2006. **55**(4): p. 1148-56.

284. Walker, R.J., et al., *Role of beta-adrenergic receptor regulation of TNF-alpha and insulin signaling in retinal Muller cells.* Invest Ophthalmol Vis Sci, 2011. **52**(13): p. 9527-33.
285. Feenstra, D.J., E.C. Yego, and S. Mohr, *Modes of retinal cell death in diabetic retinopathy.* J Clin Exp Ophthalmol, 2013. **4**(5): p. 298.
286. Trueblood, K.E., S. Mohr, and G.R. Dubyak, *Purinergic regulation of high-glucose-induced caspase-1 activation in the rat retinal Muller cell line rMC-1.* Am J Physiol Cell Physiol, 2011. **301**(5): p. C1213-23.
287. Denes, A., G. Lopez-Castejon, and D. Brough, *Caspase-1: is IL-1 just the tip of the ICEberg?* Cell Death Dis, 2012. **3**: p. e338.
288. Fu, S., et al., *Muller glia are a major cellular source of survival signals for retinal neurons in diabetes.* Diabetes, 2015. **64**(10): p. 3554-63.
289. Hori, S. and N. Mukai, *Ultrastructural lesions of retinal pericapillary Muller cells in streptozotocin-induced diabetic rats.* Albrecht Von Graefes Arch Klin Exp Ophthalmol, 1980. **213**(1): p. 1-9.
290. Simo, R., J.M. Sundstrom, and D.A. Antonetti, *Ocular Anti-VEGF therapy for diabetic retinopathy: the role of VEGF in the pathogenesis of diabetic retinopathy.* Diabetes Care, 2014. **37**(4): p. 893-9.
291. Ramos, C.J., et al., *The EPAC-Rap1 pathway prevents and reverses cytokine-induced retinal vascular permeability.* J Biol Chem, 2018. **293**(2): p. 717-730.
292. Wang, J., et al., *Muller cell-derived VEGF is essential for diabetes-induced retinal inflammation and vascular leakage.* Diabetes, 2010. **59**(9): p. 2297-305.
293. Harhaj, N.S., et al., *VEGF activation of protein kinase C stimulates occludin phosphorylation and contributes to endothelial permeability.* Invest Ophthalmol Vis Sci, 2006. **47**(11): p. 5106-15.
294. Murakami, T., E.A. Felinski, and D.A. Antonetti, *Occludin phosphorylation and ubiquitination regulate tight junction trafficking and vascular endothelial growth factor-induced permeability.* J Biol Chem, 2009. **284**(31): p. 21036-46.
295. Sundstrom, J.M., et al., *Identification and analysis of occludin phosphosites: a combined mass spectrometry and bioinformatics approach.* J Proteome Res, 2009. **8**(2): p. 808-17.
296. Butt, A.M., et al., *Computational identification of interplay between phosphorylation and O-beta-glycosylation of human occludin as potential mechanism to impair hepatitis C virus entry.* Infect Genet Evol, 2012. **12**(6): p. 1235-45.
297. Mazumder, B., V. Seshadri, and P.L. Fox, *Translational control by the 3'-UTR: the ends specify the means.* Trends Biochem Sci, 2003. **28**(2): p. 91-8.
298. Pesole, G., et al., *UTRdb and UTRsite: specialized databases of sequences and functional elements of 5' and 3' untranslated regions of eukaryotic mRNAs. Update 2002.* Nucleic Acids Res, 2002. **30**(1): p. 335-40.
299. Raychaudhuri, S., et al., *Common variants at CD40 and other loci confer risk of rheumatoid arthritis.* Nat Genet, 2008. **40**(10): p. 1216-23.
300. Nieters, A., et al., *A functional TNFRSF5 polymorphism and risk of non-Hodgkin lymphoma, a pooled analysis.* Int J Cancer, 2011. **128**(6): p. 1481-5.
301. Jiang, C., et al., *CRISPR/Cas9 Screens Reveal Multiple Layers of B cell CD40 Regulation.* Cell Rep, 2019. **28**(5): p. 1307-1322.e8.
302. Wispe, J.R., et al., *Synthesis and processing of the precursor for human manganо-superoxide dismutase.* Biochim Biophys Acta, 1989. **994**(1): p. 30-6.
303. Knirsch, L. and L.B. Clerch, *A region in the 3' UTR of MnSOD RNA enhances translation of a heterologous RNA.* Biochem Biophys Res Commun, 2000. **272**(1): p. 164-8.

304. Chung, D.J., A.E. Wright, and L.B. Clerch, *The 3' untranslated region of manganese superoxide dismutase RNA contains a translational enhancer element.* Biochemistry, 1998. **37**(46): p. 16298-306.
305. Knirsch, L. and L.B. Clerch, *Tyrosine phosphorylation regulates manganese superoxide dismutase (MnSOD) RNA-binding protein activity and MnSOD protein expression.* Biochemistry, 2001. **40**(26): p. 7890-5.
306. Bause, A.S. and M.C. Haigis, *SIRT3 regulation of mitochondrial oxidative stress.* Exp Gerontol, 2013. **48**(7): p. 634-9.
307. Tan, E.P., et al., *Interplay between O-GlcNAc and acetylation regulates mitochondrial function (756.7).* FASEB J, 2014. **28**.
308. Dinic, S., et al., *Decreased O-GlcNAcylation of the key proteins in kinase and redox signalling pathways is a novel mechanism of the beneficial effect of alpha-lipoic acid in diabetic liver.* Br J Nutr, 2013. **110**(3): p. 401-12.
309. Candas, D. and J.J. Li, *MnSOD in oxidative stress response-potential regulation via mitochondrial protein influx.* Antioxid Redox Signal, 2014. **20**(10): p. 1599-617.
310. Nakamura, M., et al., *Excessive hexosamines block the neuroprotective effect of insulin and induce apoptosis in retinal neurons.* J Biol Chem, 2001. **276**(47): p. 43748-55.
311. Jackson, G.R., et al., *Inner retinal visual dysfunction is a sensitive marker of non-proliferative diabetic retinopathy.* Br J Ophthalmol, 2012. **96**(5): p. 699-703.
312. Bearse, M.A., Jr., et al., *A multifocal electroretinogram model predicting the development of diabetic retinopathy.* Prog Retin Eye Res, 2006. **25**(5): p. 425-48.

VITA

Sadie K. Dierschke

Education

2015-2020 PhD Biomedical Science and Clinical and Translational Science, Pennsylvania State University College of Medicine, Hershey, PA

2011-2015 BS Food Science, *summa cum laude*, with Honors, Texas Tech University, Lubbock, TX

Publications

Dierschke SK, Toro AL, Miller WP, Dennis MD. Diabetes enhances translation of the mRNA encoding CD40 in retinal Müller glia via a 4E-BP1/2-dependent mechanism. *In preparation*.

Dierschke SK, Toro AL, Barber AJ, Arnold AC, Dennis MD. Angiotensin-(1-7) attenuates protein O-GlcNAcylation in the retina by EPAC/Rap1-dependent inhibition of O-GlcNAc Transferase. *Invest Ophthalmol Vis Science*. IOVS-19-28572R1. *In press*.

Dierschke SK, Miller WP, Favate JS, Shah P, Imamura Kawasawa Y, Salzberg AC, Kimball SR, Jefferson LS, Dennis MD. O-GlcNAcylation alters the selection of mRNAs for translation and promotes 4E-BP1-dependent mitochondrial dysfunction in the retina. *J Biol Chem*. 2019 Apr 5;294(14):5508-5520.

Dai W, **Dierschke SK**, Toro AL, Dennis MD. Consumption of a high fat diet promotes protein O-GlcNAcylation in mouse retina via NR4A-1 dependent GFAT2 expression. *Biochim Biophys Acta Mol Basis Dis*. 2018 Sep 11;1864(12):3568-3576.

Dai W, Miller WP, Toro AL, Black AJ, **Dierschke SK**, Feehan RP, Kimball SR, Dennis MD. Deletion of the stress-response protein REDD1 promotes ceramide-induced retinal cell death and JNK activation. *Faseb J*. 2018 Jun 19:fj201800413RR.

Selected Presentations

2019 "Diabetes enhances translation of the mRNA encoding CD40 in Müller glia to promote retinal inflammation." Poster Presentation, American Diabetes Association 79th Scientific Sessions, San Diego, CA.

2019 "O-GlcNAcylation alters the selection of mRNAs for translation and promotes 4E-BP1-dependent mitochondrial dysfunction in retina." Oral Presentation, Graduate School Forum. Hershey, PA.

2018 "Regulation of Retinal Protein O-GlcNAcylation by Angiotensin-(1-7) and cAMP." Oral Presentation, Translational Science 2018. Washington, D.C.

2018 "Angiotensin-(1-7) attenuates retinal protein O-GlcNAcylation in mice fed a high fat diet." Moderated poster discussion, American Diabetes Association 78th Scientific Sessions, Orlando, FL.